

**STUDY OF COMPRESSIBILITY AND PERMEABILITY CHARACTERISTICS OF
GRANULATED BENTONITE PERMEATED WITH DIFFERENT PORE FLUIDS**



A dissertation submitted in

Partial fulfilment of the requirements for the award of the degree of

MASTER OF TECHNOLOGY

In

CIVIL ENGINEERING

(With specialization in Geotechnical Engineering)

Under

ASSAM SCIENCE AND TECHNOLOGY UNIVERSITY

SESSION: 2022-2024



Submitted by:

SUSHMITA HAZARIKA

M.TECH 4th Semester

Roll No: PG/C/22/19

ASTU Registration No:247906118

Under the guidance of:

DR.(MRS.) BINU SHARMA

Professor, Assam Engineering College

Department of Civil Engineering

ASSAM ENGINEERING COLLEGEJALUKBARI,

GUWAHATI-13, ASSAM

DECLARATION

I hereby declare that the work presented in this report entitled " **STUDY OF COMPRESSIBILITY AND PERMEABILITY CHARACTERISTICS OF GRANULATED BENTONITE PERMEATED WITH DIFFERENT PORE FLUIDS** " in partial fulfilment of the requirement for the award of the degree of Master of Technology in Civil Engineering with specialization in Geotechnical engineering submitted to the Department of Civil Engineering, Assam Engineering College, Jalukbari, Guwahati-13 under Assam Science and Technology University, is an authentic record of my own work carried out in the said college for twelve months under the supervision and guidance of Dr. Binu Sharma, Professor, Department of Civil Engineering, Assam Engineering College, Jalukbari, Guwahati-13, Assam.

Do hereby declare that this project report is solemnly done by me and is my effort and that no part of it has been plagiarized without citation.'

Date:

Place:

Name: SUSHMITA HAZARIKA

M.Tech 4th Semester

College Roll No: PG/C/22/19

ASTU Roll No: 220620062018

ASTU Registration No: 247906118

Department of Civil Engineering

Assam Engineering College

Jalukbari, Guwahati- 781013

CERTIFICATE

This is to certify that the work presented in this report entitled — **“STUDY OF COMPRESSIBILITY AND PERMEABILITY CHARACTERISTICS OF GRANULATED BENTONITE PERMEATED WITH DIFFERENT PORE FLUIDS”** is submitted by Sushmita Hazarika, Roll No: PG/C/22/19, a student of M.Tech 4th semester, Department of Civil Engineering, Assam Engineering College, under my guidance and supervision and submitted in the partial fulfilment of the requirement for the award of the Degree of Master of Technology in Civil Engineering with specialization in Geotechnical Engineering under Assam Science and Technology University.

Date:

Place:

DR. (MRS.) BINU SHARMA

B.E. (Gau), M.E. (U.O.R), Ph.D. (Gau)

Professor

Department of Civil Engineering,

Assam Engineering College,

Jalukbari, Guwahati-781013

Certificate from the Head of the Department

This is to certify that the following student of M.Tech 4th semester of Civil Engineering Department (Geotechnical Engineering), Assam Engineering College, has submitted her project on — **“STUDY OF COMPRESSIBILITY AND PERMEABILITY CHARACTERISTICS OF GRANULATED BENTONITE PERMEATED WITH DIFFERENT PORE FLUIDS”** in partial fulfilment of the requirement for the award of the Degree of Master of Technology in Civil Engineering with specialization in Geotechnical Engineering under Assam Science and Technology University.

Name: SUSHMITA HAZARIKA

College Roll No: PG-C-22/19

ASTU Roll No: 220620062018

ASTU Registration No: 247906118

Date:

Place:

DR. JAYANTA PATHAK

Professor & Head of Department

Department of Civil Engineering Assam

Engineering College Jalukbari, Guwahati- 781013

ACKNOWLEDGEMENT

I would like to extend my sincere appreciation to Dr. (Mrs.) Binu Sharma, Professor in the Department of Civil Engineering at Assam Engineering College, for her extensive support and encouragement throughout the project. Her guidance, constant supervision and provision of necessary information were invaluable to me. Working under her was an inspiring and great experience, and I am highly indebted to her.

This project would not have been possible without the help of my seniors Priyanka Das and Bhaskar Medhi ; laboratory assistants and staffs, for their guidance in various ways. Without their guidance and support it would have not been possible for me to prepare and complete this study.

I am also grateful to Dr. Jayanta Pathak, Professor and Head of the Department of Civil Engineering at Assam Engineering College as well as the entire community of the Department of Civil Engineering at Assam Engineering College for providing us with the necessary infrastructure and comfort throughout the course, particularly during my project.

Date:

Place:

Name: SUSHMITA HAZARIKA

M.Tech 4th Semester

Department of Civil Engineering

Assam Engineering College

Jalukbari, Guwahati- 781013

Abstract

Bentonite, a swelling clay, is the key component of Geo synthetic clay liners due to its ability to swell when hydrated, creating an impermeable barrier. Geo synthetic clay liners have a thin layer of unhydrated granulated bentonite or powdered bentonite. The behaviour of granulated bentonite after exposure to landfill leachates is receiving importance.

In this research work one-dimensional consolidation tests was performed on granulated bentonite to study the compressibility and permeability behaviour, swelling and swelling pressure of granulated bentonite permeated with different pore fluids. Pore fluids consisted of distilled water, 20% ethanol/methanol-80% distilled water, 40% ethanol/methanol 60% distilled water, 60% ethanol/methanol -40% distilled water, 80% ethanol/methanol -20% distilled water. The granulated bentonite was being placed in the consolidation cell in unhydrated loose condition. The addition of organic pore fluids decreased both swelling percentage and swelling pressure. As organic pore fluid concentration increased, the compressibility of the granulated bentonites increases. The coefficient of consolidation increases with increase in concentration of the organic pore fluid content. Again it was observed that the sample had to be kept for around 48 hours to allow the sample to consolidate till there is little or no further compression. Permeability characteristics were also assessed, revealing that permeability was lowest with 100% distilled water and increased with organic pore fluid concentration. This observations suggest organic fluids influence granulated bentonite's compressibility, permeability and swelling behaviour, possibly affecting its long-term stability within GCL.

List of Table

Table No	Description	Page No.
Table 2.1	Equations referred by Yousry, M. M. and Gunther, E. B. (1985) to predict the swelling pressure for expansive soils	12
Table 2.2	Equations referred by Zumrawi, M. M. E. (2012) to predict the swelling pressure for expansive soils	14
Table 2.3	Equations referred by Zumrawi, M. M. E. (2013) to predict the swelling pressure for expansive soils	17
Table 4.1	Swelling Index of Granulated Bentonite	27
Table 4.2	Swell Percentage and swelling pressures of Granulated bentonite for distilled water and ethanol as pore fluids	36
Table 4.3	Swell Percentage and swelling pressures of Granulated Bentonite for distilled water and methanol as pore fluids	37
Table 5.1	Compression Index of the granulated bentonite with ethanol distilled water	46
Table 5.2	Consolidation and permeability properties of granulated bentonite mixed with 100% Distilled water & ethanol solution	63
Table 5.3	Consolidation and permeability properties of granulated bentonite mixed with 20% Ethanol & 80% Distilled water	63
Table 5.4	Consolidation and permeability properties of granulated bentonite mixed with 40% Ethanol & 60% Distilled water	64
Table 5.5	Consolidation and permeability properties of granulated bentonite mixed with 60% Ethanol & 40% Distilled water	64
Table 5.6	Consolidation and permeability properties of granulated bentonite mixed with 80% Ethanol & 20% Distilled water	65
Table 5.7	Consolidation and permeability properties of granulated bentonite mixed with 20% Methanol & 80% Distilled water	65
Table 5.8	Consolidation and permeability properties of granulated bentonite mixed with 40% Methanol & 60% Distilled water	66
Table 5.9	Specimen height and void ratio calculation for 100% Distilled water sample	79

Table 5.10	Specimen height and void ratio calculation for 20%Ethanol & 80% Distilled water sample	79
Table 5.11	Specimen height and void ratio calculation for 40%Ethanol & 60% Distilled water sample	80
Table 5.12	Specimen height and void ratio calculation for 60%Ethanol & 40% Distilled water sample	80
Table 5.13	Specimen height and void ratio calculation for 80%Ethanol & 20% Distilled water sample	81
Table 5.14	Specimen height and void ratio calculation for 20%Methanol & 80% Distilled water sample	81
Table 5.15	Specimen height and void ratio calculation for 40%Methanol & 60% Distilled water sample	82

List of Figures

Figure	Title	Page No
Fig. 3.1	Consolidation setup	24
Fig. 4.1	Free Swell Index of Ethanol Distilled water content	28
Fig. 4.2	Modified Free Swell Index of Ethanol Distilled water content	28
Fig. 4.3	Free Swell Ratio of Ethanol Distilled water content	29
Fig. 4.4	Free Swell Index of Methanol Distilled water content	29
Fig. 4.5	Modified Free Swell Index of Methanol Distilled water content	30
Fig. 4.6	Free Swell Ratio of Methanol Distilled water content	30
Fig. 4.7	Time vs. swell % relationship of Granulated bentonite for 100% distilled water mixture as pore fluid	32
Fig. 4.8	Time vs. swell % relationship of Granulated bentonite for 20% Ethanol+80% distilled water mixture as pore fluid	32
Fig. 4.9	Time vs. swell % relationship of Granulated bentonite for 40% Ethanol+60% distilled water mixture as pore fluid	33
Fig. 4.10	Time vs. swell % relationship of Granulated bentonite for 60% Ethanol+80% distilled water mixture as pore fluid	33
Fig. 4.11	Time vs. swell % relationship of Granulated bentonite for 80% Ethanol+20% distilled water mixture as pore fluid	34
Fig. 4.12	Time vs. swell % relationship of Granulated bentonite for 20% Methanol+80% distilled water mixture as pore fluid	34
Fig. 4.13	Time vs. swell % relationship of Granulated bentonite for 40% Methanol+60% distilled water mixture as pore fluid	35
Fig. 4.14	Combine graph for the Time vs. swell % relationship of Granulated bentonite with Ethanol distilled water content	35
Fig. 4.15	Plot between Odometric swell vs Free swell index for ethanol-distilled water solution	37
Fig. 4.16	Plot between oedometric swell vs. modified free swell index for ethanol-distilled water solution	38

Fig. 4.17	Combine graph of Time vs. time/% swell relationship for various pore fluids	39
Fig. 5.1	Relationship between void ratio vs effective stress of Granulated bentonite for 100% distilled water as pore fluid	41
Fig. 5.2	Relationship between void ratio vs effective stress of Granulated bentonite for 20%Ethanol+ 80% Distilled water as pore fluid	42
Fig. 5.3	Relationship between void ratio vs effective stress of Granulated bentonite for 40%Ethanol+ 60% Distilled water as pore fluid	42
Fig. 5.4	Relationship between void ratio vs effective stress of Granulated bentonite for 60%Ethanol+ 40% Distilled water as pore fluid	43
Fig. 5.5	Relationship between void ratio vs effective stress of Granulated bentonite for 80%Ethanol+ 20% Distilled water as pore fluid	43
Fig. 5.6	Combination of Relationship between void ratio vs effective stress of Granulated bentonite for Ethanol distilled water mixuture	44
Fig. 5.7	Relationship between void ratio vs effective stress of Granulated bentonite for 20%Methanol+ 80% Distilled water as pore fluid	44
Fig. 5.8	Relationship between void ratio vs effective stress of Granulated bentonite for 40%Methanol+ 60% Distilled water as pore fluid	45
Fig. 5.9	Void ratio versus log effective stress	46
Fig. 5.10	Relationship between Ethanol-distilled water and compression index.	47
Fig. 5.11	Time-consolidation curve of sample 1 for 100% Distilled water as pore fluid at 80- 160kPa	48
Fig. 5.12	Time-consolidation curve of sample 1 for 100% Distilled water as pore fluid at 160- 320kPa	49
Fig.5.13	Time-consolidation curve of sample 1 for 100% Distilled water as pore fluid at 560- 600kPa	49
Fig.5.14	Time-consolidation curve of sample 2 for 20% Ethanol as pore fluid at 40- 80kPa	50
Fig.5.15	Time-consolidation curve of sample 2 for 20% Ethanol as pore fluid at 80- 160kPa	50
Fig.5.16	Time-consolidation curve of sample 1 for 20% Ethanol as pore fluid at 160- 320kPa	51

Fig.5.17	Time-consolidation curve of sample 2 for 20% Ethanol as pore fluid at 320-480kPa	51
Fig.5.18	Time-consolidation curve of sample 3 for 40%Ethanol+60% Distilled water as pore fluid at 20- 40kPa	52
Fig.5.19	Time-consolidation curve of sample 3 for 40%Ethanol+60% Distilled water as pore fluid at 40- 80kPa	52
Fig.5.20	Time-consolidation curve of sample 3 for 40%Ethanol+60% Distilled water as pore fluid at 80- 160kPa	53
Fig.5.21	Time-consolidation curve of sample 3 for 40%Ethanol+60% Distilled water as pore fluid at 320- 480kPa	53
Fig.5.22	Time-consolidation curve of sample 3 for 40%Ethanol+60% Distilled water as pore fluid at 540- 640kPa	54
Fig.5.23	Time-consolidation curve of sample 4 for 60%Ethanol+40% Distilled water as pore fluid at 20- 40kPa	54
Fig.5.24	Time-consolidation curve of sample 4 for 60%Ethanol+40% Distilled water as pore fluid at 40- 80kPa	55
Fig.5.25	Time-consolidation curve of sample 4 for 60%Ethanol+40% Distilled water as pore fluid at 160- 240kPa	55
Fig.5.26	Time-consolidation curve of sample 4 for 60%Ethanol+40% Distilled water as pore fluid at 240- 320kPa	56
Fig.5.27	Time-consolidation curve of sample 4 for 60%Ethanol+40% Distilled water as pore fluid at 540- 640kPa	56
Fig.5.28	Time-consolidation curve of sample 5 for 80%Ethanol+20% Distilled water as pore fluid at 40- 80kPa	57
Fig.5.29	Time-consolidation curve of sample 5 for 80%Ethanol+20% Distilled water as pore fluid at 80- 160kPa	57
Fig.5.30	Time-consolidation curve of sample 5 for 80%Ethanol+20% Distilled water as pore fluid at 240- 320kPa	58
Fig.5.31	Time-consolidation curve of sample 6 for 20%Methanol+80% Distilled water as pore fluid at 40- 80kPa	58
Fig.5.32	Time-consolidation curve of sample 6 for 20%Methanol+80% Distilled water as pore fluid at 80- 160kPa	59
Fig.5.33	Time-consolidation curve of sample 6 for 20%Methanol+80% Distilled water as pore fluid at 160- 320kPa	59

Fig. 5.34	Time-consolidation curve of sample 6 for 20%Methanol+80% Distilled water as pore fluid at 600- 640kPa	60
Fig. 5.35	Time-consolidation curve of sample 7 for 40%Methanol+60% Distilled water as pore fluid at 40- 80kPa	60
Fig. 5.36	Time-consolidation curve of sample 7 for 40%Methanol+60% Distilled water as pore fluid at 80- 160kPa	61
Fig. 5.37	Time-consolidation curve of sample 7 for 40%Methanol+60% Distilled water as pore fluid at 160- 320kPa	61
Fig. 5.38	Time-consolidation curve of sample 7 for 40%Methanol+60% Distilled water as pore fluid at 600- 640kPa	62
Fig. 6.1	Coefficient of permeability vs. void ratio relationship for 100% Distilled water	69
Fig. 6.2	Coefficient of permeability vs. void ratio relationship for 20% Ethanol+ 80% Distilled water	69
Fig. 6.3	Coefficient of permeability vs. void ratio relationship for 40% Ethanol+ 60% Distilled water	70
Fig. 6.4	Coefficient of permeability vs. void ratio relationship for 60% Ethanol+ 40% Distilled water	70
Fig. 6.5	Coefficient of permeability vs. void ratio relationship for 80% Ethanol+ 20% Distilled water	71
Fig. 6.6	Combination of Relationship between Coefficient of permeability vs. void ratio of Granulated bentonite for Ethanol-distilled water	71
Fig. 6.7	Coefficient of permeability vs. void ratio relationship for 20% Methanol+ 80% Distilled water	72
Fig. 6.8	Coefficient of permeability vs. void ratio relationship for 40% Methanol+ 60% Distilled water	72
Fig. 6.9	Coefficient of permeability vs %ethanol distilled water content of pore fluid relationship at void ratio, $e=2.5$ & $e=3$	73

TABLE OF CONTENTS

CONTENTS	Page No
Declaration	ii
Certificate	iii
Certificate from the head of the department	iv
Acknowledgement	v
Abstract	vi
List of Tables	vii-viii
List of Figures	ix-xii
Chapter 1 : Introduction	
1.1 Introduction	1
1.2 Granulated Bentonite	2
1.3 Pore fluids	2
1.4 Objective of the study	3
Chapter 2 : Background and Literature	
2.1 General	4
2.2 Literature Review	4-21
Chapter 3 : Materials and Methodology	
3.1 General	22
3.2 Material	22
3.2.1 Granulated Bentonite	22
3.2.2 Pore fluids	22
3.3 Testing Methods	22
3.3.1 Atterberg limits	22
3.3.2 Free swelling test	23
3.3.3 Oedometric swell and Swelling pressure	23
3.3.4 Consolidation test	23
3.3.5 Permeability test	24
Chapter 4: Analysis of Swelling behaviour of Granulated bentonite	
4.1 Introduction	25
4.2 Analysis of Free swelling behaviour of Granulated bentonite	25
4.2.1 Effect of Granulated bentonite on free swelling	25
4.3 Analysis of Oedometric swelling and swelling pressure of Granulate bentonite	31
4.3.1 Effect of Granulated bentonite on oedometric swelling	31
4.3.2 Comparison of the swelling curves with distilled water and ethanol solution	35
4.3.3 Relation between free swell and oedometric swelling of Granulated	37

bentonite	
4.4 Representation of oedometric swelling in the form of a rectangular hyperbola	38
Chapter 5 : Analysis of Compressibility behaviour of Granulated bentonite	
5.1 Introduction	40
5.2 Analysis of Compressibility behaviour of Granulated bentonite in presence of organic pore fluid	40
5.3 Determination of Compression index (C_c)	45
5.4 Determination of Coefficient of consolidation (C_v)	47
5.4.1 Comparison of the C_v values	48
Chapter 6: Analysis of Permeability behaviour of Granulated bentonite	
6.1 Introduction	67
6.2 Determination of coefficient of permeability (k)	67
6.3 Analysis of Permeability behaviour of granulated bentonite in presence of organic pore fluid	68
6.3.1 Variation of the permeability with void ratio	68
6.4 Variation of the permeability with %ethanol distilled water content of pore fluids	73
Chapter 7: Conclusion and Scope for Further Study	
7.1 Conclusion	75
7.2 Scope for further study	75
References	77-78
Appendix I	79-82

CHAPTER 1

Introduction

1.1 Introduction

Geosynthetic Clay Liners (GCLs) have played a very important role in modern civil engineering and environmental practices. A Geosynthetic Clay Liner (GCL) is a specialized geotechnical barrier engineered to control fluid migration in various construction and environmental applications. GCLs are thin (7–10 mm) engineered barriers used to control the flow of liquids and the migration of contaminants in waste containment systems and other hydraulic structures. GCLs typically consist of a thin layer of granular or powdered sodium bentonite sandwiched between two geotextiles that are bonded by needle punching or stitching. The sodium bentonite (NaB) in GCLs is in the form of particulate granules comprised of montmorillonite clusters with a small fraction of accessory minerals (e.g., quartz, calcite, etc.), as shown illustratively. Bentonite is a type of absorbent clay that is often used in geotechnical and environmental applications. Granulated bentonite refers to bentonite that has been processed into small granules. This form of bentonite is often used for ease of handling, spreading, and mixing in various applications. The geotextiles serve both as a mechanical support for the clay and as a filter to prevent the migration of fine-grained soil particles. In most of these previous studies the initial condition of the soil sample is considered at optimum moisture content and maximum dry density. But the geo synthetic clay liner bentonites (powder/granulated) remain un-hydrated after placement during exposure to the landfill leachates. Thus, the chemical compatibility of un-hydrated GCL, bentonites is receiving significant interest currently (Jo et al., 2001; Scalia et al., 2010; Wang et al., 2019; Das and Bharat, 2021). Therefore, in this present study, efforts are given to investigate the various geotechnical and engineering properties of granulated bentonite in presence of different proportions of organic pore fluids. To study the compressibility and permeability behaviour, swelling and swelling pressure of granulated bentonite permeated with different pore fluids in unhydrated/dry state is studied which is the need of the hour. To observe the behaviour of granulated bentonite, nine different organic pore fluids consisted of distilled water, 20% ethanol/methanol-80% distilled water, 40% ethanol/methanol 60% distilled water, 60% ethanol/methanol -40% distilled water, 80% ethanol/methanol -20% distilled water were selected and mixed at various proportions to simulate the contaminants that is predominantly organic in nature and that has a wide variation in the dielectric constants. GCLs are ideal for

applications where high strength and puncture resistance is required, such as: Landfills, Lagoons, Ponds, Irrigation conservation, Natural pool liners, Effluent ponds. GCLs are nearly impervious and can be used as an alternative to conventional compacted clay liners. They offer equivalent or lower rates of release of fluids and chemicals than Compacted Clay Liners (CCLs). Key objectives include enhancing landfill liner systems, controlling erosion, stabilizing slopes, and facilitating ease of installation. GCLs contribute to long-term performance, compatibility with other geosynthetics, and reduced environmental impact, making them a versatile solution for diverse engineering projects.

1.2 Granulated Bentonite

Granulated bentonite is a processed form of bentonite clay, renowned for its high absorbency and swelling properties. Composed mainly of the mineral montmorillonite, it is ground and formed into small granules for diverse industrial applications. In agriculture, it improves soil structure and water retention, while in construction, it is used in geosynthetic clay liners for landfill containment. The foundry industry utilizes it as a binder in moulding sands, and it serves as a crucial component in drilling muds for the oil and gas sector. Additionally, granulated bentonite is used in water treatment for purifying liquids. Bentonites used in geosynthetic clay liners typically have montmorillonite contents ranging from 65 to 90% (Shackelford et al. 2000). In case of waste disposal liner systems, 15%-100% bentonites are used to reduce leakage of pollutants to the sub soil and ground water table (Pusch, 2015). Bentonite is primarily composed of montmorillonite mineral, having high specific surface area, high cation exchange capacity (CEC), high charge density and ability to interlayer swelling.

1.3 Pore fluids

The pore fluid chemistry plays a very important role on behaviour of soils. Various past studies showed that the factors like pore fluid concentration, viscosity, dielectric constant etc. influence the behaviour of soils (Kinsky et. al, 1971; Muniram et. al, 1990; Kaya and Fang, 2000; Sentenac et. al, 2007; Olgun and Yıldız, 2010; Sheela et. al, 2010; Spagnoli et. al, 2011; Mishra et.al, 2005, 2015; Schanz et. al, 2018). Distilled water, ethanol, methanol and their mixes at various proportions were used as the pore-fluids to study the behaviour of the granulated bentonite upon permeation with organic pore fluids. The ethanol and methanol were mixed at an increment of 20% by volume with distilled water to prepare organic pore fluid of different

proportions. The various proportion of organic pore fluids obtained after mixing are 100% distilled water, 20% ethanol/methanol-80% distilled water, 40% ethanol/methanol-60% distilled water, 60% ethanol/methanol-40% distilled water,80% ethanol/methanol -20% distilled water.

1.4 Objective of the study

Granulated bentonite serves multiple crucial objectives in Geosynthetic Clay Liners (GCLs). Its primary function is to create a low-permeability barrier by swelling upon contact with water, effectively preventing fluid migration. This property is essential for environmental containment applications such as landfills and mining operations, where stopping leachate seepage and contamination is critical. Additionally, the granulated form of bentonite ensures ease of handling and uniform distribution during installation, enhancing the reliability and performance of GCLs. The granules also contribute to the mechanical stability of the liner by maintaining consistent coverage and minimizing potential weak spots, which is vital for ensuring long-term durability and effectiveness under diverse environmental conditions.

The objectives of this study can be summarised as follows:

- i) Study the free swelling and oedometric swelling behaviour of granulated bentonite permeated with ethanol- distilled water and methanol- distilled water.
- ii) Study the consolidation characteristics of granulated bentonite permeated with ethanol-distilled water and methanol- distilled water mixtures.
- iii) Study and evaluate the permeability characteristics of granulated bentonite permeated with ethanol-distilled water and methanol- distilled water mixtures.

CHAPTER 2

Background and Literature review

2.1 General

The municipal solid wastes after decomposition mix with ground water in the form of leachate and can cause serious health issue. As a modern day solution, generally clay - sand mixtures are used as landfill liners or barriers to restrict the movements of these contaminants into deep soil and groundwater (Lundgren, 1981; Chapuis, 1981, 1990; Abeeel, 1986; Sallfores et.al., 1986; Kenney et.al., 1992; Mollins et.al., 1996). Clays particularly bentonite is used with sand for liner or barrier constructions due to its high swelling and low permeability behaviour (Komine and Ogata, 1994, 1999; Sivapullaiah et.al., 2000; Gates et.al. 2009). In the presence of water as pore fluid, bentonite forms a diffuse double layer due to its high swelling character and reduces permeability (Shackelford, 1997; Komine, 2008). But it has been noticed that the permeability behaviour of bentonite changes when the pore fluid changes from water to other organic/inorganic fluids (Mesri and Olson, 1971; Gilligan and Clemence, 1984; Anderson et.al. 1985; Uppot and Stephenson, 1989). Considerable increase in permeability in granulated bentonite has been observed, when permeated with organic pore fluids having dielectric constants lesser than water (Mitchell and Madsen, 1987; Bowders and Daniel, 1987; Fernandez and Quigley, 1988; Shackelford, 1994). Hence for efficient design and working of landfill liners, it is very important to study the behaviour of the granulated bentonite in presence of different chemicals. This chapter provides the background and comprehensive literature review on the granulated bentonite clay as liner material and their behaviour with the interaction of different types of chemicals.

2.2 Literature Review

Arasan S. (2010) reviewed various papers on the geotechnical properties such as consistency limits, hydraulic conductivity, shear strength, swelling and compressibility of clay liners using organic and inorganic chemicals acting as leachate. The author found that due to low permeability, a clay liner is the main material used in solid waste disposal landfills and it is affected due to various chemical, biological and physical events caused by the leachate. After studying various papers the author concluded that the behavior of the low plasticity clays (CL and kaolinite clay) is different from the high plasticity clay (CH and bentonite clay). The author

found that the liquid limit and swelling decreases with increasing chemical concentration for high plasticity clay but the liquid limit and swelling increases with increasing chemical concentration for low plasticity clay. The author found that the hydraulic conductivity increases with increasing chemical concentration for high plasticity clay but the hydraulic conductivity decreases with increasing chemical concentration for low plasticity clay. The author found limited information regarding shear strength of clay and clay liners interacted with chemicals but concluded that the shear strength of clay increases with increase in chemical concentration. The author found that the effect of chemicals on the geotechnical properties may be explained by Diffuse Double Layer (DDL) and Gouy-Chapman theories. According to these theories the chemical solutions tended to reduce the thickness of the DDL and flocculate the clay particles, resulting in reduction of liquid limit, reduction of swelling and increasing of hydraulic conductivity of high plasticity clays but the chemical solutions tended to increase the thickness of the DDL and disperse the clay particles, resulting in increasing of liquid limit, increasing of swelling and reduction of hydraulic conductivity of low plasticity clays.

Baille et al. (2010) studied the swelling pressures and one-dimensional compressibility behavior of several compacted saturated bentonite specimens using oedometer and distilled water as pore fluid. The author used newly developed high pressure oedometer to measure the swelling pressure of initially unsaturated compacted bentonite specimen and increasing the loading up to 25MPa. The author prepared the compacted bentonite specimens at several dry densities and different water contents. The author compared the void ratio-swelling pressure data and the compression– decompression paths of the compacted saturated specimens with the compression–decompression path of an initially saturated bentonite specimen subjected to a maximum vertical pressure of 21 MPa. From the experiments The author concluded that at the same water content, the swelling pressure increased with an increase in the dry density and also at the same dry density, the swelling pressure was found to decrease with an increase in the water content indicating that the influence of molding water on the fabric of the clay can be quite significant. The author found that the void ratio-swelling pressure data and the corresponding compression paths of the compacted saturated bentonite specimens remained distinctly below that of the void ratio–vertical pressure compression path of the initially saturated specimen even at very large pressures. The author found that the C_c values of the compacted saturated specimens were found to decrease from 0.53 to 0.32 with an increase in the initial dry density from 1.17 Mg/m³ to 1.70 Mg/m³ but the initial compaction conditions marginally affected the decompression index that remained between 0.19 and 0.26 indicating

that the influence of initial compaction conditions on the fabric and structure of bentonite was very nearly eliminated at large pressures. The author found that with an increase in the applied pressure or a decrease in the void ratio, C_v was found to decrease for both initially saturated specimen and compacted saturated specimens but at large pressures, C_v increased for the initially saturated specimen, whereas it remained nearly constant for the compacted saturated specimen. The author also found that the variation of coefficient of permeability with the void ratio to be distinctly bilinear for the initially saturated bentonite specimen, whereas for the compacted saturated specimens the relationship was found to be nearly linear and remained within a narrow band.

Sharma and Deka (2016) studied the compressibility, swelling and permeability behaviour of bentonite- sand mixture by performing one dimensional consolidation tests on six different mixtures of bentonite with sand. The bentonite- sand mixtures were formed by varying sand content in bentonite in increments of 5% from 5% to 25% by dry weight. Dry bentonite-sand mixtures were placed initially in the consolidation cell at their loosest dry state and then allowed to saturate. Swelling characteristics and swelling pressures of the bentonite-sand mixtures were also evaluated. The author found that the liquid limit and plastic limit decreased with addition of sand to bentonite content. Coefficient of consolidation (C_v) showed a small increase with increase in sand content for low stress ranges whereas for high stress range of 320kN/m², it is found to remain constant and the Compression index (C_c) decreased with increase in sand content. Addition of sand also decreased the swelling pressure. The coefficient of permeability for pure bentonite is least and increases with addition of sand to bentonite.

Sharma et al. (2017) studied the one dimensional compressibility behavior of six bentonite sand mixtures having a dry unit weight of 12kN/m³. The permeability of the samples was evaluated at different stress ranges by falling head permeability test. The swelling and swelling pressure were maximum for 100% bentonite and it decreased with the addition of sand. The author found that the samples with higher unit weight had higher values of both swelling percentage and swelling pressure. With the addition of sand to bentonite an increase in permeability trend has been observed but the values are found to lie within a narrow range.

Cantillo et al. (2017) have developed a correlation equation to estimate the swell pressure of clays found in the city of Barranquilla, Colombia using laboratory tests. The author selected the soil of Barranquilla as it has presented large landslides and slopes instability problems due to swell behavior of underlying clays. The author used the constant volume

method (Sridharan, 2009) to determine swell pressure values implemented to develop the correlations equations. The author collected a total of 38 samples and for each samples the water content, liquid limit, plastic limit, and void ratio were measured. The author used Logarithmic models ($y = a + b \ln x$), and exponential models ($\ln y = a + bx$) to model the swell pressure (dependent variable) as a function of the selected properties. The correlation equations found were-

$$SP(\text{kPa}) = 1460.79 - 397.30 \ln(w(\%))$$

2.1

$$\ln(SP(\text{kPa})) = 7.97 - 0.12 w(\%)$$

2.2

$$\ln(SP(\text{kPa})) = 7.77 - 0.12 w(\%) + 0.0054 PI(\%)$$

2.3

Where, SP = swell pressure in kPa

w = water content in %

PI = plasticity index in %.

Among equation 2.1 and 2.2, the author found that the best fit and correlation equation to predict swell pressure is equation 2.2. The author found that the Atterberg limits i.e. plasticity index used in equation 2.3 was not statistically significant and concluded that the Atterberg limits does not have a major impact in the estimation of swell pressure for the studied soil samples.

Estabragh et al.(2014) studied the effect of pore fluid and stress history on the consolidation behavior of two clay soils with low and high plasticity. The author prepared the soil samples using slurry method with water and different concentrations (10, 25 and 40%) of two organic fluids (glycerol and ethanol). The author performed Consolidation tests on two types of samples (a-slurry samples, b- slurry samples compressed under a pre-defined load to represent the effect of stress history) in an odometer apparatus. The author found that the compression index C_c was increased

with increasing the concentration of ethanol but for the glycerol it was not considerable in the case of normally consolidated slurry samples but the value of C_c decreases with increasing concentration in the case of stress history samples. The author found that the pre-consolidation pressure of the sample with stress history is dependent on the type of soil and organic fluid and it increases with increasing concentration of organic fluid.

Estabragh et al. (2015) studied the effect of pore fluid contamination on the shear strength and stress–strain behavior of a clay soil. The author performed a series of one-dimensional consolidation and (consolidated undrained) triaxial tests on samples with pore fluid as water and organic materials (glycerol and ethanol with concentrations of 10, 25 and 40%). The author found that the consolidation and shear strength behavior of soil is dependent on the dielectric constant of pore fluid and by decreasing the dielectric constant, the compressibility of the soil was decreased and stiffness of the soil was increased. The author found that the friction angles in terms of effective and total stresses increases for soils with organic pore fluid, and this increase was a function of type of pore fluid and its concentration. The author found that the slope of critical state line was changed with organic pore fluid, and the critical state condition was a function of the structure that was produced by organic fluids during the procedure of sample preparation.

Evangelina and John (2010) studied the effect of leachate on calcium bentonite and four types of sodium activated bentonites. The author used acetic acid and calcium chloride to represent the components of leachate. The author studied the variations of properties like Atterberg's limits, swell index, percentage of swell and hydraulic conductivity with various concentrations of the chemicals. After conducting laboratory tests on various samples The author found that liquid limit, plasticity index, free swell and percentage swelling of all types of bentonite reduced due to the effect of acetic acid and calcium chloride solutions. The author found that the hydraulic conductivity increases with increase in concentration of acetic acids. The author found that for all types of bentonites the variation in liquid limit, plasticity index, free swell, percentage swelling and hydraulic conductivity were comparatively high with calcium chloride than to acetic acid solution.

Sridharan et al. (1986) studied the swelling pressure of clays using the conventional consolidation test method, method of equilibrium void ratio for different consolidation pressure and constant volume method. The author found that the conventional consolidation test gives an upper bound value, the method of equilibrium void ratio for different consolidation pressure gives the least value and test by the constant volume method gives the intermediate values. Black cotton soils were used to determine the swelling pressure by all the three methods. Constant volume method was quick and only one specimen was required, however it is sensitive to load increment and rate of loading. Even consolidation test method requires only one specimen but it is time consuming. Method of equilibrium void ratio required three specimens. The author found that the swelling pressure of black cotton soil was primarily

dependent upon the initial dry unit weight or void ratio. The effect of initial moisture content was relatively less. A rectangular hyperbola was obtained from the time versus swelling and time versus pressure curves. The author concluded that the amount of swelling or swelling pressure could be easily estimated by the following findings.

Sridharan et al. (1996) studied the swelling behaviour of mixtures of bentonite clay and non swelling coarser fractions of different sizes and shapes. The author observed that swelling occurs only after the voids of the non swelling particles are filled up with swollen clay particles. The author found that the swelling of soils occurs in three distinct phases- intervoid swelling, primary swelling and secondary swelling. The intervoid swelling is due to swelling of finer expansive clay within the voids created by coarser non swelling particles and does not contribute to volume increase. Primary swelling constitutes about 80% of the total swelling. It was found that the time-swell curves follow a rectangular hyperbolic relationship during the primary and secondary swelling and hence it can be used to predict the magnitude of maximum swelling. The author also found that the total swell is not proportional to the swelling clay content, and it has been found for the same percent of expansive clay, the total swelling decreases significantly with the increase in the size of the non swelling fraction.

Sridharan and Gurtug (2003) studied the swelling behaviour of three compacted Cyprus soils varying significantly in their physical properties. The study was made with variation in compaction energies from standard Proctor to modified Proctor. A comparative study was made with kaolinite and highly plastic montmorillonite clay. A unique relationship was developed between percent swell and the swelling pressure irrespective of soil type and the level of compaction energy. It was found that the percent swell and swelling pressure increases linearly with increase in compaction energy. The time versus percent swell has the shape of a rectangular hyperbola and the time over percent swell versus time showed a good linear relationship. The ultimate percent swell could be obtained from the initial readings.

Singh and Prasad (2007) investigated the effect of inorganic & organic chemical on bentonite soil. Two chemicals- Aluminium hydroxide and Acetic acid that are generally found in municipal solid waste were selected. The effect of these chemicals on bentonite soil has been studied in a controlled condition in the laboratory. The engineering properties such as Differential Free Swell, Hydraulic Conductivity and Swelling Pressure were found out. The author found that acetic acid upon contact with bentonite soil leads to the formation of flocs and reduces the hydraulic conductivity by 17% but when Aluminum hydroxide is in contact

with bentonite soil, flocs reduced in size. The author found that the XRD diffractogram of bentonite with Aluminum hydroxide and Acetic acid does not show any marked departure in peaks when compared with XRD diffractogram of bentonite soil alone. Hence, the author concluded that the mineral phases remain same, i.e. mainly montmorillonite and quartz. The author found that the IR spectra of bentonite with Aluminium hydroxide and Acetic acid do not show any marked change in fundamental vibrational modes of the constituents units. However in case of bentonite + acetic acid the peak at 1026 cm^{-1} was found missing by the author and concluded that this happened due to formation of some new bond. The author found that the cation exchange capacity decreases in case of bentonite + Acetic acid by 21.5% as compared to bentonite alone but increased by 0.38% in case of bentonite + Aluminium hydroxide. The author found that the optimum moisture content and maximum dry density reduced in case of acetic acid as compared to bentonite alone but in case of aluminium hydroxide, maximum dry density reduced but optimum moisture content showed an increase by 5%. The author when compared the strength parameter 'c' with bentonite found that it decreased by 50% and 43% upon addition of aluminium hydroxide and acetic acid respectively. The author when compared the differential free swell with bentonite found that it decreased by 49% and 47% upon addition of aluminium hydroxide and acetic acid respectively. The author when compared the hydraulic conductivity with bentonite found that it reduced by 12% and 17% with addition of aluminium hydroxide and acetic acid respectively.

Sharma et al. (2021) investigated the behaviour of different bentonite sand mixtures through one-dimensional consolidation using ethanol water solution mixed in the ratio of 20:80 by volume, as the permeating fluid. The same series of experiments were performed with pure water also as the permeating liquid to get a good comparison of the change in properties. The bentonite - sand mixture were mixed in the following proportion by percentage of dry weight as B:S = 100:0, 90:10, 80:20, 70:30, 60:40 and 50:50 (B: bentonite , S: sand). Dry bentonite - sand mixtures were placed initially in the consolidation cell at their loosest dry state and then allowed to saturate. It was found that the Atterberg limits decreased with the addition of sand to bentonite and the values were directly proportional to the percentage of bentonite present in the samples. The swelling percentage was highest for the sample with 100% bentonite irrespective of the pore fluid used and the total swelling percentages were higher for all the samples with pure water as pore fluid as compared to ethanol-water solution. The swelling pressure decreased with the addition of sand to bentonite for both the conditions. The compression index decreased with the increase in sand content and it had higher values for the

samples with ethanol-water solution as the pore fluid. The co-efficient of permeability of the samples increased with the increasing sand content. The co-efficient of permeability of the samples with ethanol-water solution were low in comparison to the ones with pure water.

Vipulanandan and Leung (1991) studied the effects of methanol and seepage control in permeable kaolinite soil. In this study the effect of water and methanol on the behaviour of kaolinite clay and clay sand mixture were observed. Moreover bentonites (sodium based), Portland cement and sodium silicates were used as additives and grouting materials to study the seepage control measures in clay and clay sand mixtures. Sedimentation analysis was performed for different concentrations of methanol (0, 25%, 50%, 75% and 100%). Sedimentation was significant when methanol concentration were more than 75%. Pure methanol caused the soil particles to flocculate and settle out in just a few minutes and hence had the potential to affect the hydraulic conductivity. The reason for the flocculation was suggested to the low dielectric constant of methanol, which reduced the diffuse double layer in clay particles

Mowafy and Bauer (1985) tried to deduce a semi empirical equation to determine the value of swelling pressure in terms of initial dry density, initial water content, and clay content of the soil. From literature, the author found that side friction and non uniform distribution of moisture over the soil specimen were the main source of error in laboratory studies while investigating the swelling properties of soil. The author used three methods-conventional method, filter paper method and rubber membrane method to investigate the effect of side friction on the swelling properties of the soils and evaluated each of the methods. The author found that frictional stresses, mobilized between a soil specimen and a rigid confining ring during swelling of the soil cannot be eliminated completely. The author also found that side frictional effects can be reduced considerably during swelling by lining the oedometer ring with filter papers or with a thin rubber membrane and recommended one of the two methods to determine the swelling properties of expansive soils using an oedometer ring.

Before establishing an empirical equation to predict the swelling pressure for expansive soils, the author referred many literatures and found the following equations-

Table 2.1

Equations referred by Yousry, M. M. and Gunther, E. B. (1985)

Relationship	References
$P_s = 1.2 \gamma_d/w_s$	A. H. El-Ramli (1965)
$\text{Log } P_s = 2.132 + 0.0208 w_L + 0.000665 \gamma_d - 0.0269 w_n$	A. Komornik and D. David (1969)
$P_s = a (SI) + b (w_L - w^*) + C (SI) (1/S_r)$	G. Zacharias and B. V. Ranganatham (1972)
$\text{Log } P_s = 2.55 \gamma_d/\gamma_w - 1.705$ $\text{Log } P_s = 0.0294 C - 1.923$	G. Dedier (1975)

$\text{Log } P_s = 2.55 \gamma_d/\gamma_w - 1.705$ $\text{Log } P_s = 0.0294 C - 1.923$	G. Dedier (1975)
$\text{Log } P_s = 2.17 (\gamma_d + 0.084 C) - 3.91$ (for sandy-clay soils) $\text{Log } P_s = 2.5 (\gamma_d + 0.06 C) - 4$ (for silty-clay soils)	S. Rabba (1978)

Where, P_s is swelling pressure; γ_d is dry density; w_s is shrinkage limit; w_L is liquid limit; w_n is natural water content; SI is shrinkage index; S_r is degree of saturation of specimen before start of test; w^* is water content at $S_r = 100\%$; $a = -225/6.4$; $b = 290/6.4$ and $c = 1.2/6.4$.

The author tested 28 specimens having various clay, silt and sand contents and different dry densities and initial water contents in an oedometer apparatus. The author proposed a general equation for the swelling pressure as follows-

$$\text{Log } P_s = A \gamma_d + B c - D w_n - E$$

2.7

Where P_s = swelling pressure in MPa,

γ_d = dry unit weight in kN/m³,

c = clay content in percent,

w_n = initial water content in percent.

A, B, D and E are constants determined experimentally

The author performed multiple regression analysis using the least square method to determine the constants A, B, D and E as follows-

$$A = 1.366$$

$$B = 8.951 \times 10^{-3}$$

$$D = 2.179 \times 10^{-2}$$

$$E = 2.840$$

$$\text{Coefficient of correlation, } R = \sqrt{R^2} = 0.71$$

$$\text{Coefficient of determination, } R^2 = 0.50$$

$$\text{Standard deviation, } \sigma^2 = 0.071$$

$$\text{Standard error or regression, } \sigma = 0.27$$

After substituting the values for the constants A, B, D, and E in the general relationship the following equation for the swelling pressure was generated-

$$\log P_s = 1.366 \gamma_d + 8.951 (10^{-3}) c - 2.179 (10^{-2}) w_n - 2.840$$

2.8

The author found that the initial water content has a marked effect on both the resulting swelling pressure and on the amount of swell for the soils investigated. The author noted that most equations from literature to predict the swelling pressure are linear in nature and partly empirical, only the equation proposed by Komornik and David taken the initial water content into consideration.

The author concluded that the proposed relationship can be used in design problems to estimate the expected swelling pressures for the expansive soil found in Nasr City but it should be tested, however, for other expansive soils before a universal application.

Zumrawi M. M. E. (2012) predicted correlation equations using the results of a laboratory investigation for the swelling characteristics, namely, swell percent at a certain surcharge pressure (S_p) and swelling pressure (SP). The author measured the S_p and the SP for four expansive soils compacted at different water contents and dry densities. Before establishing an

empirical equation to predict the swelling pressure for expansive soils, the author referred many literatures and found the following equations-

Table 2.2

Equations referred by Zumrawi, M. M. E. (2012)

Relationship	References
$S = K (A^{2.44}) (C^{3.44})$ Where, K: is a constant for all types of clay mineral ($K \approx 3.6 \times 10^{-5}$). $S = K (M) (PI^{2.44})$ Where, M: is a constant ($M = 60$ for natural soils and 100 for artificial soils).	Seed, H. B., Woodward, R.J., and Lundgren, R. (1962)
$S = m_t (SI)^{2.67}$ Where, m_t : is a constant equals 41.13 for natural soils.	Ranganatham, B. V. and Satyanarayan, B. (1965)
$\text{Log (SP)} = -2.132 + 0.0208 (LL) + 0.000665 (\gamma_d) - 0.0269 (w)$	Komornik, A. and D. David, (1969)
$\text{Log (SP)} = -5.020 + 0.01383 (PI) + 2.356 (\gamma_d)$	Erzin, Y. and Erol, O. (2004)

Where, S is swell percent of soil; A is activity; C is clay content; PI is plasticity index; SI is shrinkage index as a percentage; SP is swelling pressure; LL is liquid limit; γ_d is dry density of soil sample and w is the water content (%).

The author measured the swell percent in the conventional oedometer cells for 48 compacted soil samples by applying four different surcharge pressures 2.5kPa, 7kPa, 25kPa and 40kPa and also measured the swelling pressure of the compacted soil samples. The soil samples were compacted at different water contents and dry densities. The author observed that the measured swell percent and swelling pressure were influenced by the initial dry density and water content as well as the clay content, plasticity index and the surcharge load under which the sample was tested.

After performing the regression analysis on the experimental data the author found that it was possible to combine the initial state parameters in a way reflecting the influence of each

of them on the swell percent or swelling pressure and came up with a new concept called Initial State Factor (F_i). The concept of the initial state factor was first developed by Mohamed, A. E .M. (1986). The initial state factor (F_i) is defined as a combination of the soil initial state parameters such as dry density (ρ_d), water content (ω) and void ratio (e) and can be expressed

$$F_i = \frac{\rho_d}{\rho_w} \times \frac{1}{\omega \cdot e}$$

2.9

Where, ρ_w is the water density.

The author carried out statistical (regression) analysis to correlate the measured swell percent or swelling pressure to the initial state factor as a combination of initial water content, initial dry density and void ratio. The author found a direct linear relationship between the swell percent or swelling pressure and the initial state factor for all the analysed data and proposed the following equations-

$$\text{Swell percent} = M \times (F_i - F_0)$$

2.10

$$\text{Swell pressure} = M \times (F_i - F_0)$$

2.11

Where, F_0 is the value of F_i at zero swells percent or swelling pressure; M is the gradient of the straight line.

For the swell percent, the author found that increasing the surcharge load will increase F_0 and decrease M values, while increase in clay content and plasticity index will increase F_0 and M values and found that following equations-

$$F_0 = 7.1 \times (P)^{0.22} \times (PI \times C)^{0.78}$$

2.12

$$M = 245(P)^{-0.26} \times (PI \times C)^{1.26}$$

2.13

For the swell pressure, the author found that increasing in clay content and plasticity index will increase M and decrease F_0 values and found the following equations-

$$F_0 = 0.84 \times (PI \times C)^{-0.96}$$

2.14

$$M = 245(P)^{-0.26} \times (PI \times C)^{1.26}$$

2.15

Substituting the values in general equation 2.10 and 2.11, the author expressed the following equations-

$$\text{Swell Percent} = 24.5 \times P^{-0.26} \times (PI \times C)^{1.26} [F_i - 7.1 \times P^{0.22} \times (PI \times C)^{0.78}]$$

2.16

$$\text{Swelling Pressure} = 249 \times (PI \times C)^{1.18} [F_i - 0.84 \times (PI \times C)^{-0.96}]$$

2.17

Where: F_i : is the initial state factor

P : is the surcharge pressure (KPa)

PI : is the plasticity index

C : is the clay content.

The author compared the data obtained from the proposed equations with the experimental data and found a good agreement between the measured and predicted swell percent and swelling pressure values. The author concluded that swell percent or swelling pressure can be defined as a function of initial soil state factor and the surcharge pressure, clay content and plasticity index.

Zumrawi M. M. E. (2013) tried to predict the swelling pressure in compacted clay from given soil index parameters such as dry density, water content, void ratio, clay content and plasticity index. . Before establishing an empirical equation to predict the swelling pressure for expansive soils, the author referred many literatures and found the following equations-

Table 2.3**Equations referred by Zumrawi, M. M. E. (2013)**

Relationship	References
$\text{Log}(P_s) = -2.132 + 0.0208(w_L) + 0.000665(\gamma_d) - 0.0269(w_i)$	Komornik, A. and D. David, (1969)
$P_s = (2.5 \times 10^{-1})(I_p)^{1.12} \times C^2/w_i^2 + 25$	Nayak N.V and Christensen R.W (1974)
$\text{Log } P_s = a_0 + a_1(w_L) + a_2(I_p) + a_3(\log \gamma_d) + a_4(m_c) + a_5(S_i)$ Where, the values of a_0, a_1, a_2, a_3, a_4 and a_5 were obtained from multiple regression analysis as -4.3341, 0.0071, 0.0006, 51.2802, 1.79 and 0.0037, respectively.	Rani S. and Rao K.M. (2009)
$\text{Log}(P_s) = -5.020 + 0.01383(I_p) + 2.356(\gamma_d)$	Erzin, Y. and Erol, O. (2004)

Where, P_s is swelling pressure; w_L is liquid limit; γ_d is dry density; w_i is initial water content; I_p is plasticity index; C is clay content; m_c is moisture content and S_i is initial surcharge pressure.

The author prepared three different clay samples from Sudan with varying water contents and dry densities and performed 34 tests to measure the swelling pressure using an oedometer cell. The author followed the same procedure as mentioned in above literature Zumrawi, M. M. E. (2012) and proposed the following equation after performing regression analysis on the experimental data-

$$\text{Swelling Pressure, } P_s = 263 \times (PI \times C)^{1.19} [F_i - 0.93 \times (PI \times C)^{-0.95}]$$

2.18

Where: F_i is the initial state factor, PI is the plasticity index, C is the clay content.

After comparing the measured and predicted swelling pressure values for all the data, the author found that there is a good agreement between the measured and predicted swelling pressure values.

Sridharan and Rao (1973) studied the mechanism controlling volume change of saturated clays and the role of the effective stress concept. The study deals with the mechanism controlling the one dimensional volume change behaviour of saturated kaolinite and montmorillonite clays. Eight organic pore fluids of different properties and water have been used to vary the interparticle forces in the one dimensional consolidation tests. To study the volume change mechanism existing pore fluid was replaced by another of different dielectric constant. From the results obtained from the tests it had been concluded that the volume change behaviour of clays is controlled basically by two mechanisms which are governed by effective stress concept. In first mechanism the volume change is controlled by the shearing resistance at interparticle level and in second mechanism volume change is controlled by the long range diffuse double layer repulsive forces.

Bharat et al. (2019) explored how chemicals move through compacted clays, affecting the materials porosity. They discovered that different methods of determining chemical diffusion yield varied concentration data. When comparing effective diffusion coefficients in reactive and non-reactive situations for the same clay, it becomes meaningless. The provided porous space plays a crucial role in calculating the effective diffusion coefficient in reactive scenarios. The choice of a laboratory diffusion technique depends on the required model parameters. No single technique can fully replace another. For instance, the half-cell technique is great for estimating porous space but not effective diffusion coefficient. On the other hand, In-Diffusion and through-Diffusion approaches are useful for measuring effective and apparent diffusion coefficients independently.

Tian¹ and Benson² (2017) conducted experiments to understand how an aggressive bauxite solution affects the performance of geosynthetic clay liners (GCLs) used in aluminum refining waste disposal sites. They tested two types of GCLs: one with sodium-bentonite (Na-B) and another with a combination of bentonite and polymer (B-P). The sodium-bentonite GCL with powdered bentonite had low hydraulic conductivity, while the one with granular bentonite showed higher conductivity in the presence of bauxite liquor. The B-P GCL initially had low conductivity but increased over time due to polymer elution. The study highlights that GCLs' hydraulic conductivity varies based on bentonite properties. The choice of GCL, especially those with a bentonite-polymer combination, should consider chemical compatibility with the liquid being contained in construction specifications.

Chen et al. (2018) tested the hydraulic conductivity of geosynthetic clay liners (GCLs) with granular sodium bentonite, exposed to coal combustion product (CCP) leachates. They selected five synthetic leachates based on a nationwide survey of CCP disposal facilities. The study used common GCLs from two American manufacturers and found that the hydraulic conductivity of GCLs varied with leachate type. GCLs permeated directly with trona leachate showed high conductivity, while others had moderate to high conductivity with different CCP leachates at 20 kPa. Results indicated that hydraulic conductivity was linked to leachate ionic strength and inversely related to bentonite swell index when hydrated in leachate. Increasing effective stress from 20 to 450 kPa substantially decreased hydraulic conductivity. Pre hydration on a subgrade had minimal impact, but pre hydration with DI water before trona leachate permeation significantly lowered hydraulic conductivity, suggesting potential chemical resistance strategies for CCP leachates.

Bouazza A. (2002) conducted a study on Geosynthetic Clay Liners (GCLs), which have become widely accepted as replacements for compacted clay liners in various applications such as cover systems, composite bottom liners, and environmental barriers. They are used in transportation facilities, storage tanks, canals, ponds, and impoundments. The study focused on researching the hydraulic and diffusion properties, chemical compatibility, mechanical behavior, durability, and gas migration of GCLs. The paper provides a review of key findings, emphasizing critical aspects that impact the service life of GCLs. This work aims to offer a comprehensive understanding of the design considerations for systems incorporating GCLs.

Sarabadani¹ and Rayhani² (2014) studied Geosynthetic Clay Liners (GCLs) commonly used in modern landfills to prevent leachate from escaping. They focused on how GCL hydraulic performance is influenced by the degree of hydration of the underlying subsoil. The research involved two GCL products placed on different subsoils under various normal stresses (0 to 8 kPa). Increasing normal stress significantly accelerated the rate of GCL hydration. For instance, under 8 kPa on sand subsoil, the GCL reached its final moisture content in about 8 weeks, compared to 24 weeks with no normal stress. Normal stress had a minimal impact on the final moisture content. A normal stress of 2 kPa slightly increased moisture uptake for most GCLs, but beyond that, changes were minor. The study highlighted that GCL manufacturing processes and subsoil grain size distribution affect both the rate of hydration and the final moisture content achieved.

Tan 1 et al. (2021) proposed a method to enhance the compactness of bentonite powder, commonly used as a buffer in high-level radioactive waste disposal. Compacting bentonite powder to high density is challenging without increased energy. The proposed solution involves granulation by wetting and drying bentonite into plate shapes, followed by crushing into granules. Lab tests compared granular bentonite with original bentonite powder of similar sizes. Results showed that granular bentonite maintained properties like free swelling ratio, swelling pressure, permeability, and water retention capacity. After compaction, granular bentonite exhibited significantly improved density (1.72 g/cm³) compared to the original (1.64 g/cm³) with a 38% reduction in energy consumption and a decreased void ratio. Tests on pore size distributions revealed that granulation eliminated larger pores (10.0 μm) while favoring smaller pores (1.0 μm). The study confirmed the feasibility of the wetting-drying agglomeration method for granule preparation, indicating improved compactness and reduced energy consumption without major changes in hydromechanical properties.

Maubeugel et al. (2017) studied on Geosynthetic Clay Liners (GCLs), which started in 1998 and included a rebuild in 2010, utilized six lysimeters in Lemfoerde, Germany, to investigate the long-term sealing behavior of GCLs with granular and powder bentonite fillings. The findings revealed that GCLs, being highly sensitive to changes in water content due to their thin thickness, are crucial structural elements in geoenvironmental applications such as landfill capping systems. Over the first 10 years, GCLs with granular bentonite cores showed a notable increase in permeation rates, indicating a degradation in sealing efficiency over time. This increase suggests that granular bentonite may be less effective for long-term sealing in certain conditions. Although specific performance details of powder bentonite GCLs are not provided in the excerpt, it is implied that they may have demonstrated better long-term sealing behavior compared to granular bentonite. Different cover systems were employed in the lysimeters to assess their impact on GCL performance, though the excerpt does not detail these effects. Additionally, laboratory studies focused on the rehydration and desiccation cycles of GCLs, examining the formation of desiccation cracks under multiple hydration and drying cycles, highlighting the importance of evaluating GCL resilience in varying environmental conditions. These findings underscore the necessity for long-term studies to ensure the durability and effectiveness of GCLs in real-world applications, emphasizing the need for careful selection and monitoring of GCL materials, especially in critical uses like landfill capping systems.

Siddiqua et al. (2011) This study presents the results of an experimental program designed to evaluate the impact of pore fluid salinity on the hydromechanical performance of light and dense backfill materials, which are engineered barrier materials considered in the Canadian concept for storing spent nuclear fuel in a deep geological repository. The research examines how pore fluid chemistry affects the swelling, compressibility, stiffness, and hydraulic conductivity of these backfills, essential parameters for analysis and design. Using pore fluid chemistry representative of groundwater in potential host rocks like granite and limestone, the findings reveal that light backfill performance is significantly influenced by changes in pore fluid chemistry. Specifically, the swell potential of light backfill decreases with increasing solution salinity, and hydraulic conductivity decreases with increasing effective montmorillonite dry density, with saline-saturated specimens showing higher hydraulic conductivity than those saturated with distilled water. Conversely, the behavior of dense backfill is primarily governed by its crushed granite component, rendering it relatively unaffected by changes in pore fluid chemistry. Tests confirm that dense backfill performs effectively as a sealing material, maintaining consistent performance regardless of pore fluid salinity.

Jadda and Bag (2020) This study investigates the impact of various electrolyte concentrations on the swelling pressure, consolidation characteristics, and hydraulic conductivity of two different Indian bentonites. Experiments included constant volume swelling pressure tests on compacted bentonite specimens and consolidation tests on saturated specimens, using 0, 0.1, 0.5, and 1.0 N NaCl and CaCl₂ solutions. Scanning Electron Microscope (SEM) and XRD analyses were employed to examine changes in the morphology and microstructure of the bentonite specimens. Hydraulic conductivity was derived from consolidation test results. At a dry density of 1.4 Mg/m³, the swelling pressure and hydraulic conductivity of divalent bentonite were found to be approximately 2.9 and 7.3 times higher, respectively, than those of monovalent bentonite when saturated with deionized water. Electrolyte solutions significantly altered the morphology, microstructure, and hydro-mechanical properties of monovalent bentonite, while the effect was negligible for divalent bentonite. An empirical equation was proposed to predict the hydraulic conductivity of the bentonites, showing good correlation with experimental results. The study concludes that divalent bentonite is more suitable as an engineered barrier material in electrolyte environments, whereas monovalent bentonite performs better in low salinity conditions.

CHAPTER 3

Materials and Methodology

3.1 General

In this chapter discussion is done on the materials and experimental methods used to carry out this study. Different laboratory experiments to determine the index properties and engineering properties of the soil samples (Granulated bentonite) and the pore fluids (distilled water-ethanol/methanol mixtures) used in this study are discussed elaborately.

3.2 Material

3.2.1 Granulated Bentonite

As we know that Bentonite have been proposed and used as engineered barriers for the enhancement of impervious landfill liners, cores of zoned earth dams and radioactive waste repository systems because it has low hydraulic conductivity, high swelling property, good self sealing capacities etc. Granulated bentonite refers to bentonite clay that has been processed and formed into granules. Bentonite is a type of absorbent clay that is composed mainly of montmorillonite, a fine-grained mineral. It has a unique structure that gives it remarkable absorption and swelling capabilities. Bentonite is often used in various industries for its diverse range of properties.

3.2.2 Pore fluids

Distilled water, ethanol, methanol and their mixes at various proportions were used as the pore-fluids to study the behaviour of the granulated bentonite upon permeation with organic pore fluids. The ethanol and methanol were mixed at an increment of 20% by volume with distilled water to prepare organic pore fluid of different proportions. The various proportion of organic pore fluids obtained after mixing are 100% distilled water, 20% ethanol/methanol-80% distilled water, 40% ethanol/methanol-60% distilled water, 60% ethanol/methanol-40% distilled water, 80% ethanol/methanol -20% distilled water.

3.3 Testing Methods

3.3.1 Atterberg limits

Atterberg limits were determined as per IS 2720 (Part V): 1985. Liquid limits of the different soil samples were determined using Casagrande apparatus. Thread rolling method was used to determine plastic limits.

3.3.2 Free swelling test

Free swelling tests of the soil samples were performed as per IS 2720 (Part XL):1977. 10 gm dried soil specimen was poured in two glass graduated cylinders of 100 ml capacity. One cylinder was filled with the pore fluid(distilled water) and varying concentrations of organic pore fluid which was considered for study and other cylinder was filled with kerosene oil up to 100 ml mark. After removal of entrapped air by gently shaking and stirring with a glass rod, the soils were allowed to settle and attain equilibrium state of volume for sufficient time (< 24 hrs.). The final volumes of the soils in each of the cylinders were noted for further calculations.

3.3.3 Oedometric swell and Swelling pressure

The oedometric swell and swelling pressure tests were performed in a conventional one-dimensional consolidometer apparatus. The dimensions of the cutter were 20 mm in height and 60 mm in internal diameter. A dry sample of granulated bentonite (by weight) was placed in the consolidometer cutter at 1 gm/cm³ density up to 2/3rd height of the cutter. The oedometric swelling test was performed as per IS 2720 (Part XV)-1965. The consolidometer was assembled by placing filter papers at the top and bottom of the soil specimen. The porous stones were placed at the top and bottom after boiling for 15 minutes. A seating load of 5 kN/m² was applied on the loading hanger and horizontal inclination was corrected, then the initial reading of the dial gauge was noted. The saturation of the dry soil samples was done by applying pore fluids (distilled water and different ethanol-distilled water and methanol-distilled water mixtures). After saturation, the samples started swelling and dial gauges started showing swelling. Dial gauge readings were taken at different time intervals till the swelling ceases. For the determination of swelling pressure, small amounts of load were applied gradually till the height of swollen soil sample came back to its original height.

3.3.4 Consolidation test

The consolidation tests were performed on the same conventional one-dimensional consolidometer apparatus use to determine the oedometric swelling and swell pressures explained earlier. The consolidation tests were performed as per IS 2720 (Part XV)-1965. The consolidation tests continued on the same soil samples tested for oedometric swelling determination. After the soil samples attained full swelling in oedometric swelling tests, consolidation tests had been started. Double incremental loading starting from 10 kN/m² upto

640 kN/m² was applied. For each increment of loading the compression dial readings were recorded till the dial reading attain a steady state.

The apparatus used in the study is given below:



Fig3.1: Consolidation setup

3.3.5 Permeability test

The permeability of the soil samples with different pore fluids were calculated theoretically from the coefficient of consolidation, C_v , values obtained after each stress increment from Equation [1].

$$k = C_v \cdot m_v \cdot \gamma_w \quad [1]$$

In the above equation, k is the coefficient of permeability, m_v is the coefficient of volume compressibility and γ_w is the unit weight of water. The coefficient of consolidation was determined by the Taylor's square root of time fitting method.

CHAPTER 4

Analysis of Swelling behaviour of Granulated bentonite

4.1 Introduction

Soils that undergo significant volume changes in response to moisture levels are known as swelling or expansive soils. These soils, particularly those rich in montmorillonite clays, have a distinctive structure with an alumina layer sandwiched between two silica layers. This configuration allows water to easily penetrate between the layers, causing an increase in soil volume. The moisture sensitivity of these soils often presents stability challenges for buildings constructed on them. However, expansive clays like bentonite are highly valued for use as landfill liners or barriers because they effectively prevent toxins from migrating into deeper soils and groundwater. With the rapid growth of populations and urban areas, the generation of pollutants has increased. These pollutants often contain compounds that can mix with water to produce leachate, potentially altering the properties of soils. Expansive soils are particularly vulnerable to such chemical changes. This chapter studied the swelling behavior of granulated bentonite when exposed to different organic pore fluids.

4.2 Analysis of Free swelling behaviour of Granulated bentonite

4.2.1 Effect of Granulated bentonite on free swelling

Ten samples of soils were prepared by mixing organic pore fluid at different proportion by volume. The proportions consist of 100% distilled water, 100% ethanol, 100% methanol, 80% ethanol/methanol-20% distilled water, 60% ethanol/methanol-40% distilled water, 40% ethanol/methanol-60% distilled water and 20% ethanol/methanol-80% distilled water. To obtain pore fluid of different proportions of ethanol/methanol concentration, ethanol/methanol are mixed with distilled water at an increment of 20% by volume for each trial of experiments. The free swell tests were done in the laboratory as per IS: 2720 Part (XL)-1977. 10 gm granulated bentonite soil specimen was taken & poured in two glass graduated cylinders of 100 ml capacity. One cylinder was filled with the pore fluid which was considered for study and other cylinder was filled with kerosene oil up to 100 ml mark. After removal of entrapped air by gently shaking and stirring with a glass rod, the soils were allowed to settle and attain equilibrium state of volume for sufficient time (< 24 hrs.). The final volumes of the soils in each of the cylinders were noted for further calculations.

The free swell index (FSI) was determined as per the equation given in IS: 2720 Part (XL)-1977.

$$FSI = (V_d - V_k) / V_k \times 100$$

Where V_d = Sediment volume of 10 gm soil in a 100 ml cylinder containing pore fluid V_k = Sediment volume of 10 gm soil in a 100 ml cylinder containing kerosene. The method based on FSI has a shortcoming in that it gives negative free swell indices for kaolinite rich soils. To counter this problem Sridharan et.al. (1985) proposed a criterion based on modified free swell index (MFSI) The modified free swell index (MFSI) was determined as per the equation proposed by Sridharana et.al. (1985)

$$\text{MFSI} = V_d/10$$

Where V_d = Sediment volume of 10 gm soil in a 100 ml cylinder containing pore fluid. It has been observed that the equilibrium sediment volume of kaolinite rich soils in non polar liquids like carbon tetra chloride and kerosene can be even greater than the equilibrium sediment volume of the same soils in water (Sridharan et.al. 1985). This observation had lead Sridharan and Prakash (1999) to propose the free swell ratio (FSR) The free swell ratio (FSR) was also determined as per the equation proposed by Sridharana et.al.(1985).

$$\text{FSR} = V_d/ V_k$$

Where V_d = Sediment volume of 10 gm soil in a 100 ml cylinder containing pore fluid

V_k = Sediment volume of 10 gm soil in a 100 ml cylinder containing kerosene/carbon tetra chloride.

Table 4.1 Swelling Index of Granulated Bentonite

Ethanol: Distilled water	Proportion	FSI	MSFI	FSR
	0:100	160%	2.6	2.6
	20:100	145%	2.45	2.45
	40:100	115%	2.15	2.15
	60:100	60%	1.6	1.6
	80:100	45%	1.45	1.45
	100:0	25%	1.25	1.25
Methanol: Distilled water	0:100	160%	2.6	2.6
	20:100	130%	2.3	2.3
	40:100	100%	2.0	2.0
	60:100	60%	1.6	1.6
	80:100	35%	1.35	1.35
	100:0	25%	1.1	1.1

Free swelling of all ten soil samples has been observed from the above table 4.1 by comparing the sediment volumes in case of distilled water, different mixtures of ethanol-water and methanol-water solutions as pore fluid with the sediment volumes in case of kerosene. It has been observed from the tests that the sediment volume of the granulated bentonite sample gets reduced as the pore fluid changes from distilled water to the ethanol-water and methanol-water mixtures. After particularly 100% ethanol and 100% methanol proportion there were no further swelling observed in any of the soil samples. It has also been observed that the sediment volume gets decreased in case of non polar fluids (kerosene).

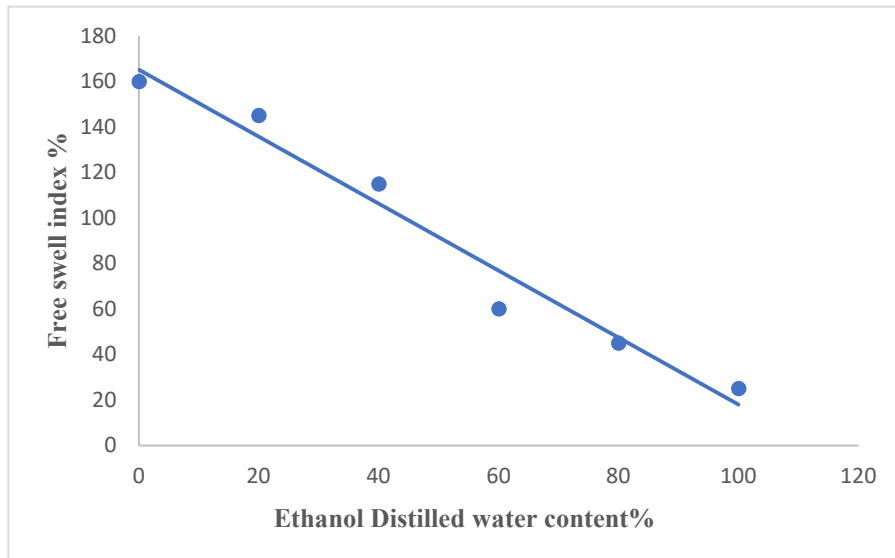


Fig 4.1: Free Swell Index of Ethanol Distilled water content

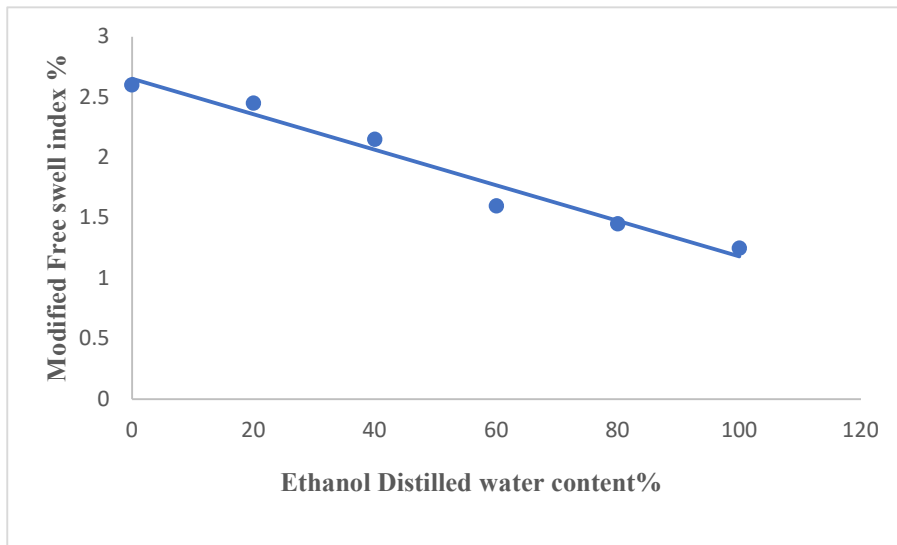


Fig 4.2: Modified Free Swell Index of Ethanol Distilled water content

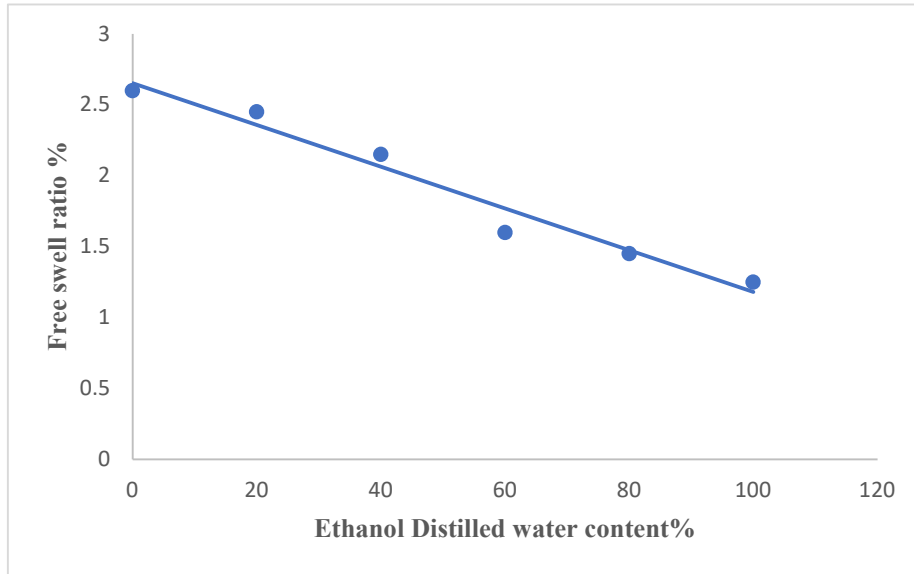


Fig 4.3: Free Swell Ratio of Ethanol Distilled water content

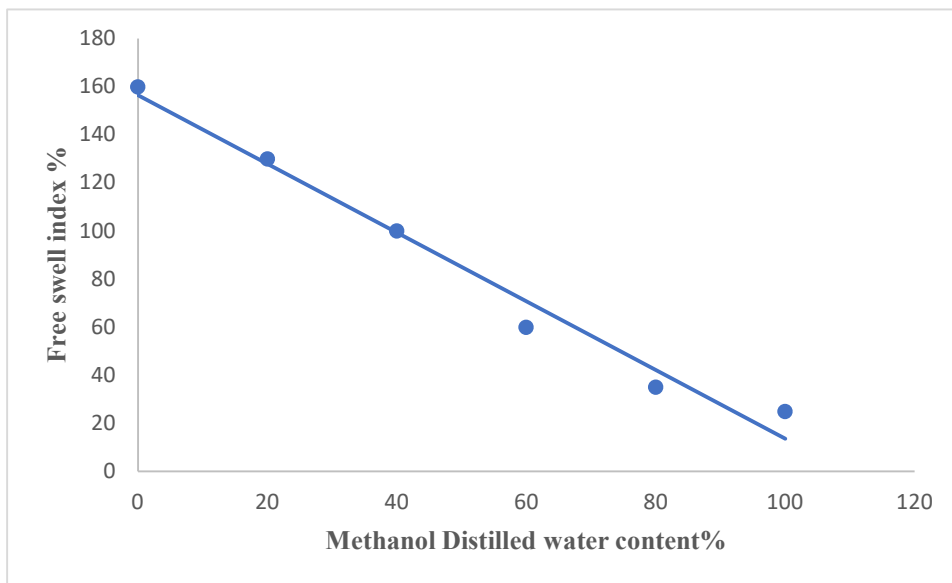


Fig 4.4: Free Swell Index of Methanol Distilled water content

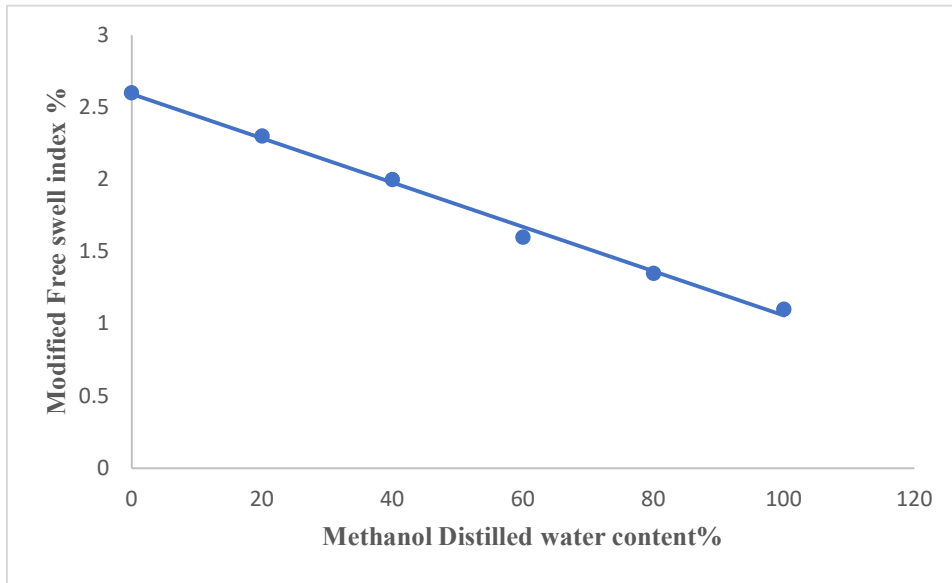


Fig 4.5: Modified Free Swell Index of Methanol Distilled water content

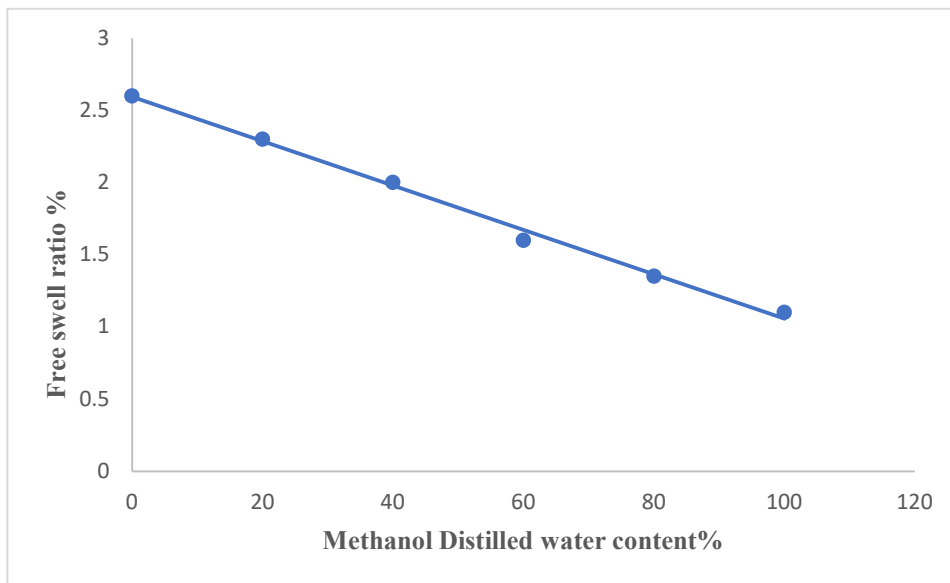


Fig 4.6: Free Swell Ratio of Methanol Distilled water content

The results from the tests done in the laboratory are plotted to study the behaviour of Granulated bentonite in presence of ethanol-water and methanol-water mixture. The plots between free swell ratios (FSR) vs ethanol water and methanol water solutions show exactly the same characteristics and same anomalies showed by the plots between free swell index (FSI) vs. ethanol water and methanol water. The above plots from fig (4.1-4.6) of free swell index (FSI), modified free swell index (MFSI) and free swell ratio (FSR) it is observed that swelling for pore fluid as distilled water is maximum, and then swelling reduces with the increase of methanol and ethanol content.

4.3 Analysis of Oedometric swelling and swelling pressure of Granulated bentonite

The laboratory experiments were performed in a conventional one-dimensional consolidometer apparatus. The dimensions of the cutter were 20 mm in height and 60 mm in internal diameter. A dry mixture of granulated bentonite (by weight) was placed in the consolidometer cutter at 1 gm/cm³ density up to 2/3rd height of the cutter. The swelling test was performed as per IS 2720 (Part XV)-1965. The consolidometer was assembled by placing filter papers at the top and bottom of the soil specimen. The porous stones were placed at the top and bottom after boiling for 15 minutes. A seating load of 5kN/m² was applied on the loading hanger and horizontal inclination was corrected, then the initial reading of the dial gauge was noted. The saturation of the dry soil samples was done by applying pore fluids (distilled water and different methanol-distilled water and ethanol-distilled water mixtures). After saturation, the samples started swelling and dial gauges started showing swelling. Dial gauge readings were taken at different time intervals till the swelling ceases. For the determination of swelling pressure, small amounts of load were applied gradually till the height of swollen soil sample came back to its original height.

$$\text{Swelling (\%)} = (\Delta H / H_0) \times 100\% \dots\dots\dots (4.3)$$

Where $\Delta H = H_f - H_0$; H_f = Final height after swelling after every 24 hrs.

H_0 = Initial height before swelling (13.33 mm)

4.3.1 Effect of Granulated bentonite on oedometric swelling: The time vs. swell percentage relationship for granulated bentonite at an initial dry density of 1 gm/cm³ for nine different pore fluids of 100% distilled water, 80% distilled water-20% ethanol/methanol, 60% distilled water-40% ethanol/ methanol mixture, 40% distilled water-60% ethanol/ methanol, 20% distilled water-80% ethanol/ methanol mixtures respectively are obtained. The plots of the experimental results are shown from Figure 4.9 to Figure 4.14

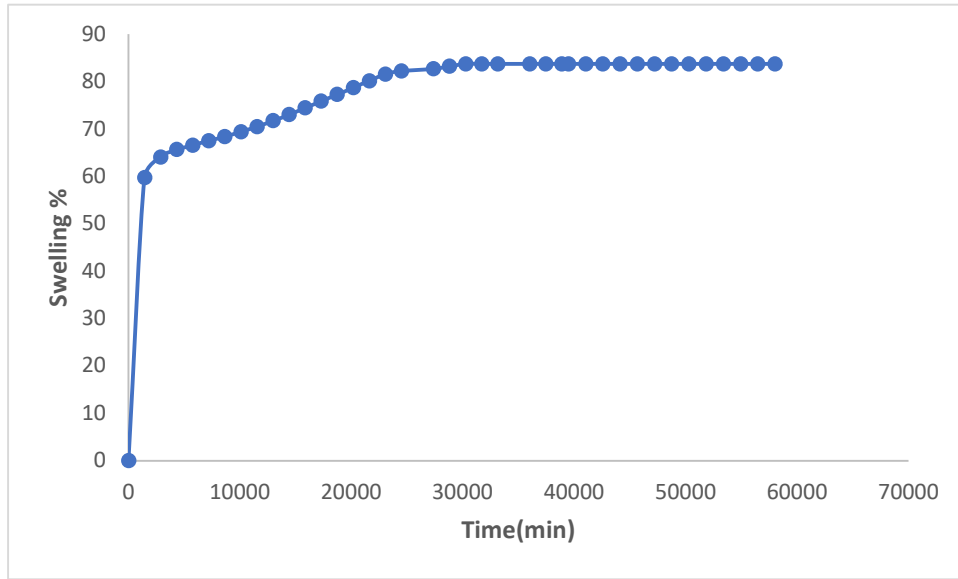


Fig4.7: Time vs. swell % relationship of Granulated bentonite for 100% distilled water mixture as pore fluid

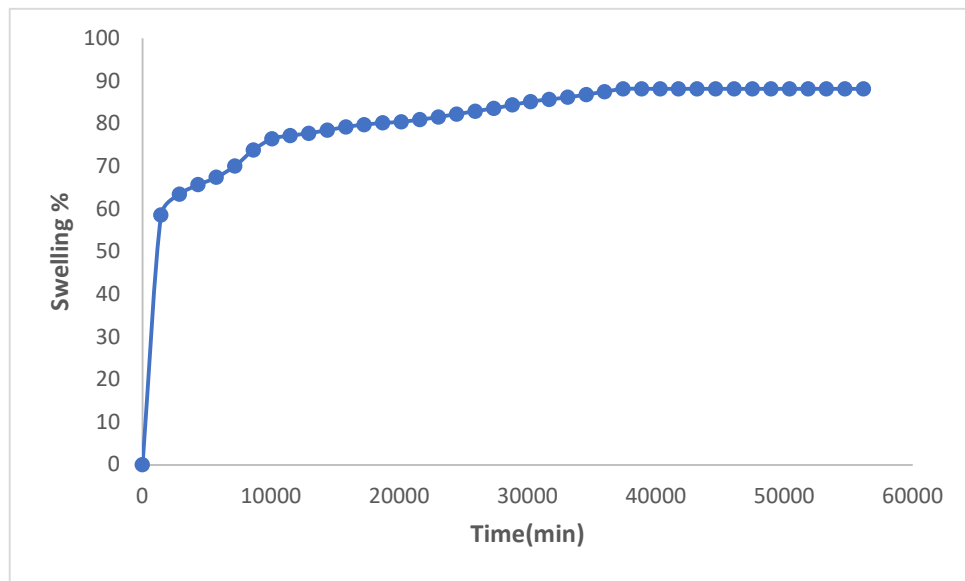


Fig 4.8: Time vs. swell % relationship of Granulated bentonite for 20% Ethanol+80% distilled water mixture as pore fluid

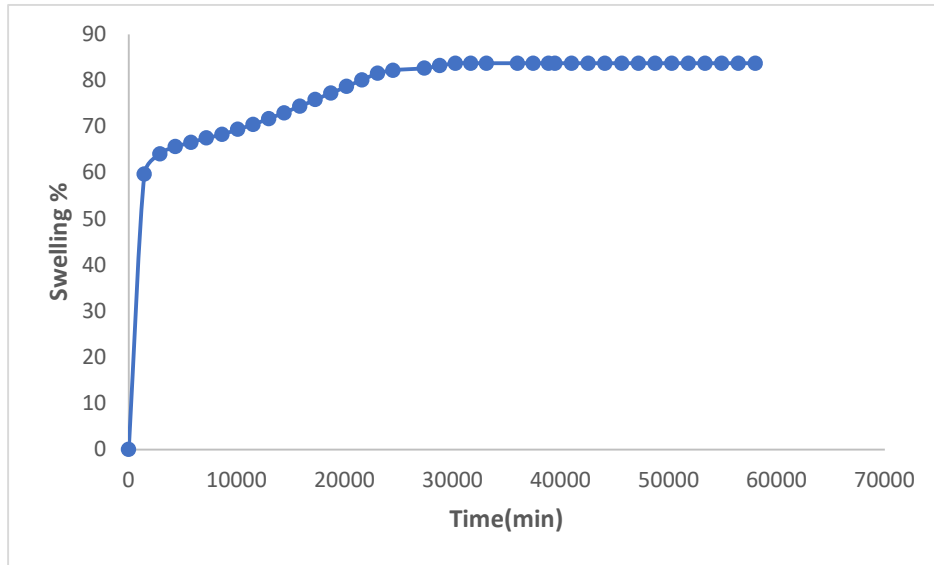


Fig 4.9: Time vs. swell % relationship of Granulated bentonite for 40% Ethanol+60% distilled water mixture as pore fluid

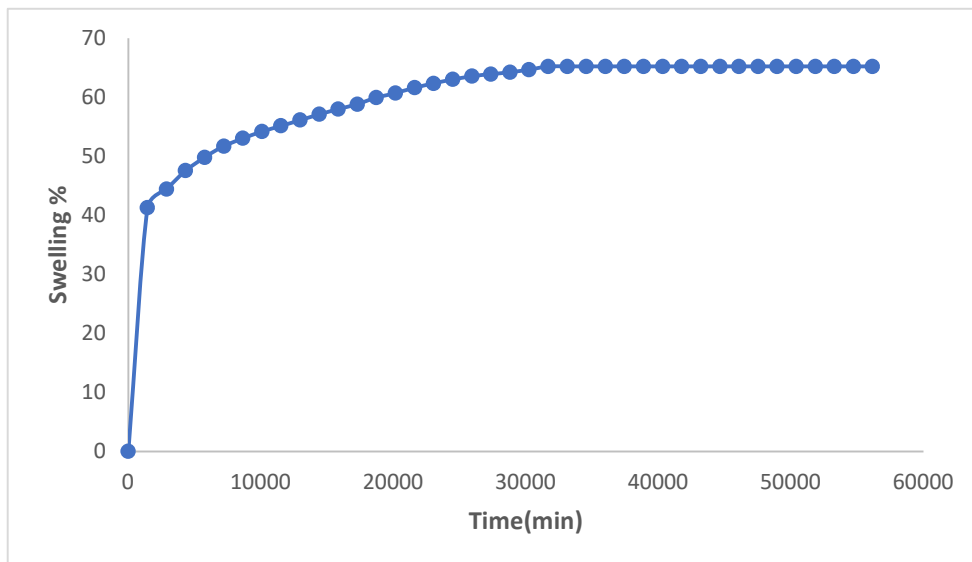


Fig 4.10: Time vs. swell % relationship of Granulated bentonite for 60% Ethanol+ 40% distilled water mixture as pore fluid

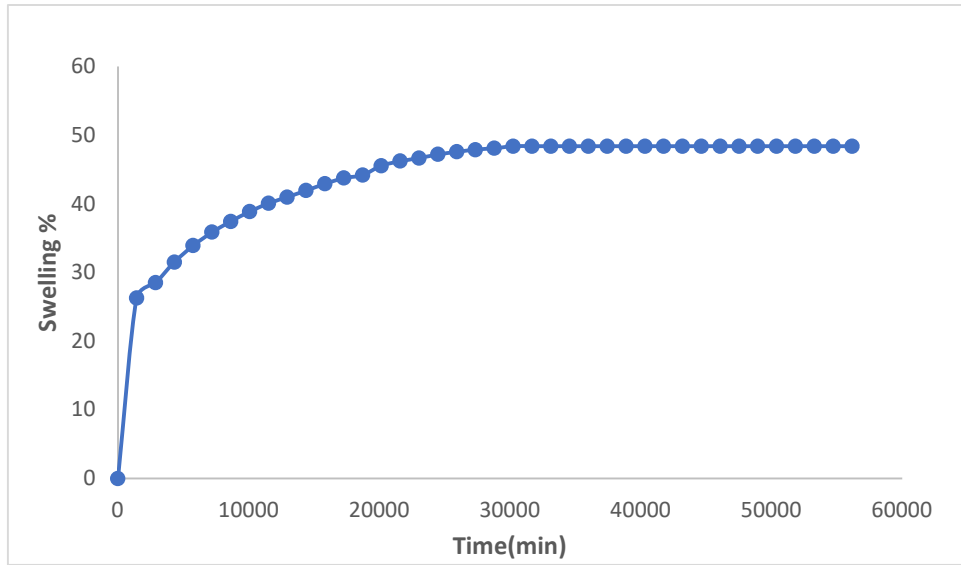


Fig 4.11: Time vs. swell % relationship of Granulated bentonite for 80% Ethanol+ 20% distilled water mixture as pore fluid

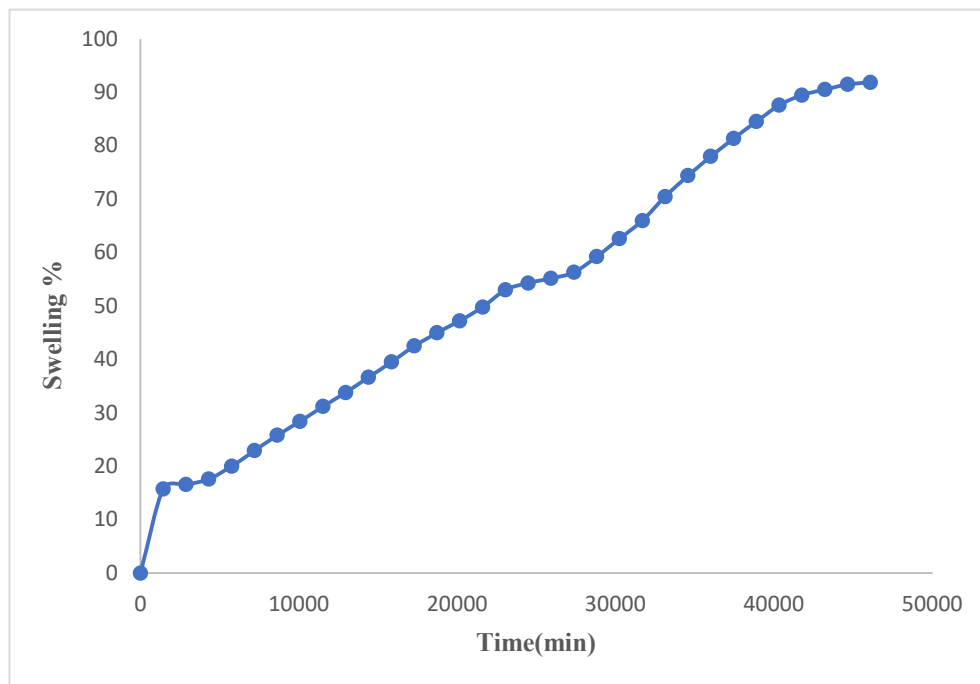


Fig 4.12: Time vs. swell % relationship of Granulated bentonite for 20% Methanol+ 80% distilled water mixture as pore fluid

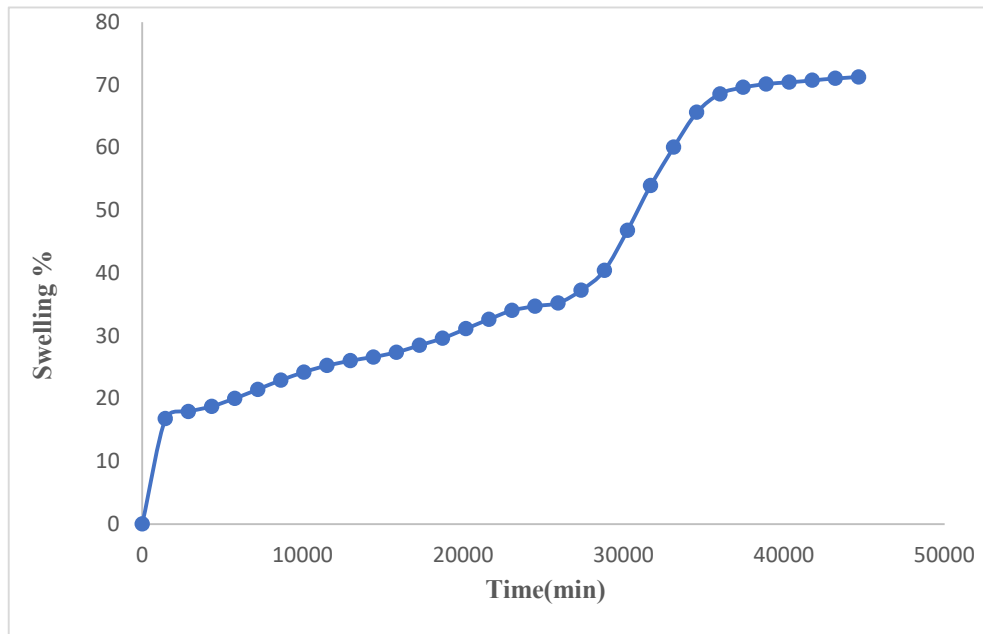


Fig 4.13: Time vs. swell % relationship of Granulated bentonite for 40% Methanol+ 60% distilled water mixture as pore fluid

4.3.2 Comparison of the swelling curves with distilled water and ethanol solution:

The swelling versus time with pore fluid as 100% distilled water, 20% ethanol-distilled water, 40% ethanol- distilled water, 60% ethanol- distilled water, 80% ethanol- distilled water for each sample mix have been plotted. Comparison curves with respect to distilled water and ethanol-water solution can be seen in Fig 4.14

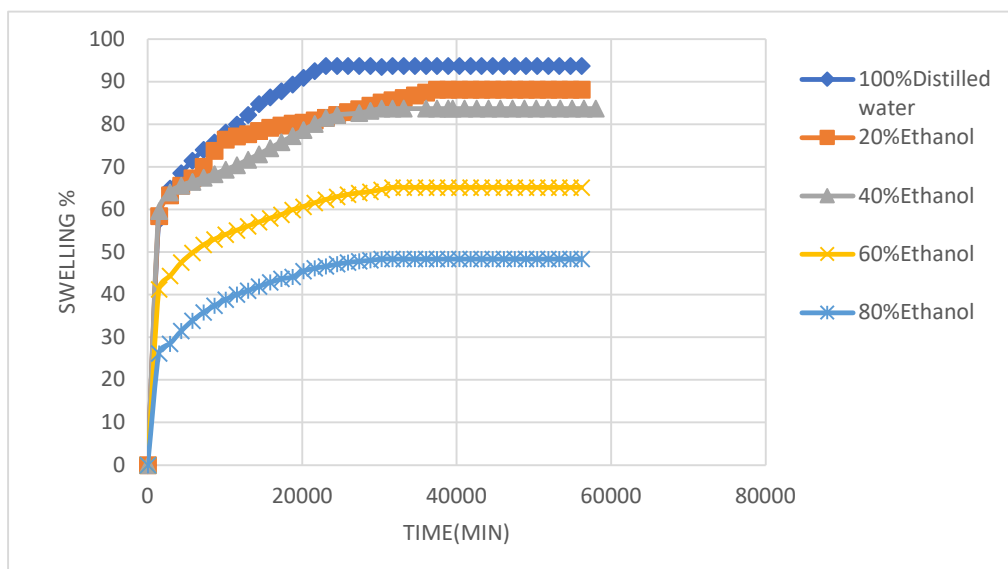


Fig4.14: Combine graph for the Time vs. swell % relationship of Granulated bentonite with Ethanol distilled water content

The above plots show that as we increases the concentration of the pore fluids the percentage of swelling is decreased. For 100% distilled water swelling is highest. The plots for the rest of the samples showed similar trends. The swelling of the samples can be attributed to the interaction between the pore fluids and clay surfaces. The pore fluids having higher dielectric constants interact with the clay surfaces forming thicker diffuse double layers which in turn results in higher swelling. Tables 4.2 and 4.3 show the swell percentage and swelling pressures of granulated bentonite for ethanol-water and methanol-water mixtures at different proportions as pore fluids respectively.

Table 4.2: Swell Percentage and swelling pressures of Granulated bentonite for distilled water and ethanol as pore fluids

Ethanol-water content	Swell (%)	Swelling Pressure (KN/m ²)
100 %Distilled water	93	600
20%Ethanol- 80%Distilled water	87	560
40%Ethanol- 60%Distilled water	83	540
60%Ethanol- 40%Distilled water	65	520
80%Ethanol- 20%Distilled water	48	320

Table 4.3: Swell Percentage and swelling pressures of Granulated Bentonite for distilled water and methanol as pore fluids

Methanol-water content	Swell (%)	Swelling Pressure (KN/m ²)
100 %Distilled water	93	600
20%Methanol-80%Distilled water	91	560
40%Methanol-60%Distilled water	71	520

4.3.3Relation between free swell and oedometric swelling of Granulated bentonite

The free swell indices and oedometric swelling of granulated bentonite in case of distilled water, mixtures of ethanol-water and methanol-water solutions as pore fluids. To explore the existence of any relation between the free swell indices with the oedometric swell for granulated bentonite with different proportions of pore fluids, they are plotted against each other in Fig 4.15 & Fig 4.16. In case of 100% distilled water, the free swelling index and oedometric swelling in presence of distilled water were 160% and 93% respectively. Both the free swell index and oedometric swelling reduces consistently as the pore fluid changes to 20% methanol-80% distilled water, 20% ethanol-80% distilled water, 40% methanol-60% distilled water, 40% ethanol-60% distilled water, 60% methanol-40% distilled water and 60% ethanol-40% distilled water, 80% methanol-20% distilled water and 80% ethanol-20% distilled water respectively. Similarly free swell index and oedometric swelling reduced consistently as the concentration of organic pore fluid increases.

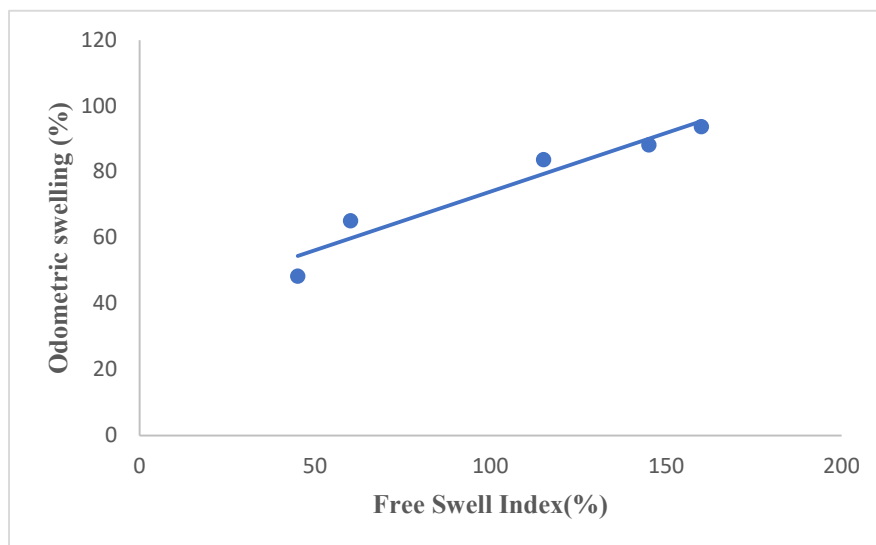


Fig. 4.15: Plot between Oedometric swell vs Free swell index for ethanol-distilled water solution

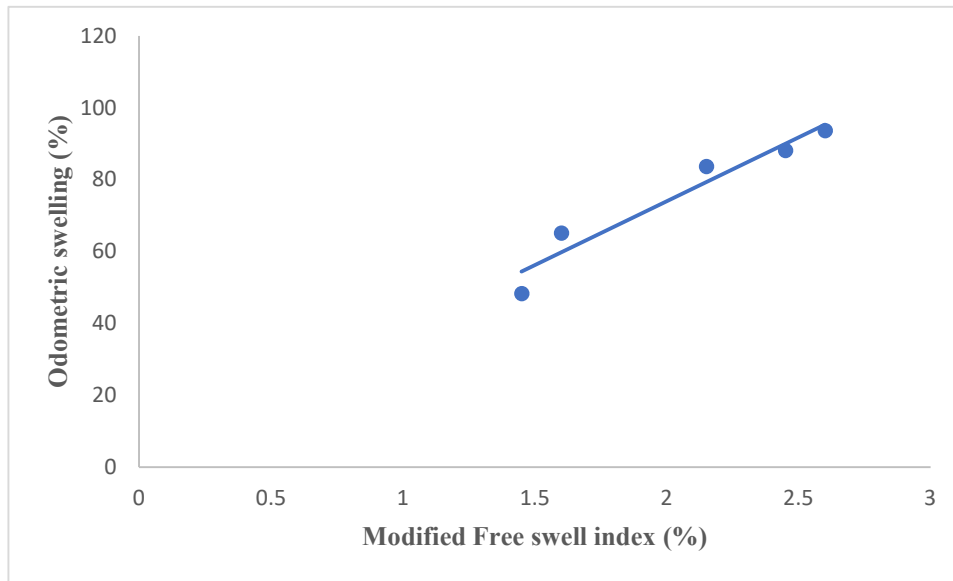


Fig.4.16: Plot between oedometric swell vs. modified free swell index for ethanol-distilled water solution

4.4 Representation of oedometric swelling in the form of a rectangular hyperbola

Kondner (1963) approximated that the nonlinear stress-strain curves of soils could be represented by rectangular hyperbola to a high degree of accuracy.

The hyperbola equation proposed by Kondner is $(\sigma_1 - \sigma_3) = \varepsilon / (a + b\varepsilon)$ (4.4)

Where σ_1 and σ_3 are the major and minor principal stresses respectively, ε is axial strain, a and b are constants that can be determined experimentally. The hyperbolic equation given in (4.4) could be represented as a straight line with “ a ” as intercept and “ b ” as slope, when $\varepsilon / (\sigma_1 - \sigma_3)$ is plotted as a function of axial strain ε . According to Kondner, the peak value of deviator stress $(\sigma_1 - \sigma_3)$ could be predicted by taking the limit of the equation (4.4) as ε becomes very large. Thus the inverse of the slope, which is the asymptotic value of the hyperbola, determines the peak value. This concept is used by Dakshinamurthy (1978) to predict maximum swelling. Most of the swelling vs. time plot in the swelling test can be represented by rectangular hyperbola and the equation for rectangular hyperbola would be

$$\% \text{ Swell} = t / (a + bt) \dots\dots (4.6)$$

Where t = time a and b are intercept and slope of the linear curve of time per percentage swell vs. time plots respectively. $1/b$ gives the maximum swell percentage. This equation would validate if the $t/\%$ swell vs. t plot resulted in a straight line.

Sridharan and Gurtug (2004) used this concept to predict the maximum swelling for soil samples compacted in different compaction energies. An almost perfect linear relationship is

obtained for all the soil samples, justifying that the shape of the time–swelling percentage curve can be treated as a rectangular hyperbola.

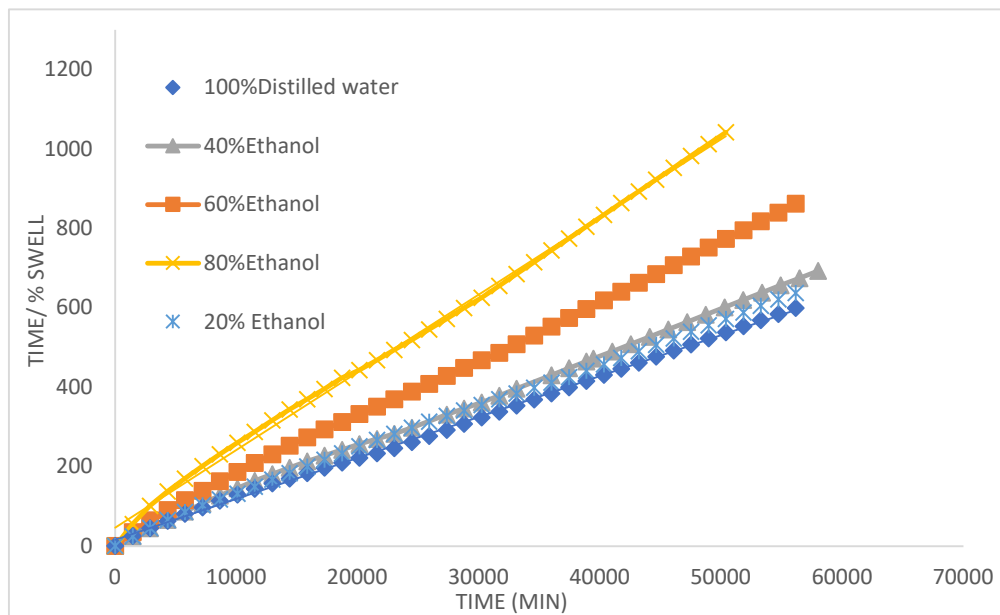


Fig.4.17: Combine graph of Time vs. time/% swell relationship for Ethanol distilled water

The above Figure 4.19 is showing the time /% swell vs. time plots for 100% distilled water, 20% ethanol-80% distilled water, 40% ethanol-60% distilled water, 60% ethanol-40% distilled and 80% ethanol- 20% distilled water respectively. Irrespective of the different percentage of distilled water and ethanol content, the plots for granulated bentonite show an almost linear relationship, justifying that the shape of time vs. swell percentage curve can be treated as a rectangular hyperbola.

CHAPTER 5

Analysis of Compressibility behaviour of Granulated bentonite

5.1 Introduction

Compressibility is an engineering property of soil by virtue of which soil undergoes volume change due to application of external loads. The process of compressibility where a saturated soil changes its volume by expelling the water present inside due to application of external load is called consolidation. In the laboratory this volume change behaviour of soil due to application of external load is measured by a one dimensional consolidation test or oedometer test devised by Terzaghi. The main objectives of performing consolidation test is to determine the total settlement of laterally confined saturated soil under external loading and the rate of settlement due to application of gradual loading. The total settlement of a soil is defined in terms of compression index (C_c) and the rate of settlement of a soil is defined by the co-efficient of consolidation (C_v). In this chapter the compressibility behaviour of Granulated bentonite with Ethanol distilled water mixture and Methanol water mixture permeated with different organic pore fluids are tested.

5.2 Analysis of Compressibility behaviour of Granulated bentonite in presence of organic pore fluid

The consolidation tests were performed in a conventional one-dimensional consolidometer apparatus. The dimensions of the cutter were 20 mm in height and 60 mm in internal diameter. A dry mixture of granulated bentonite (by weight) was placed in the consolidometer cutter at 1 gm/cm³ density up to 2/3rd height of the cutter. The tests were performed as per IS 2720 (Part XV)-1965. The consolidometer was assembled by placing filter papers at the top and bottom of the soil specimen. The porous stones were placed at the top and bottom after boiling for 15 minutes. A seating load of 5 kN/m² was applied on the loading hanger and horizontal inclination was corrected, then the initial reading of the dial gauge was noted. The saturation of the dry soil samples was done by applying pore fluids (distilled water and different methanol-distilled water and ethanol-distilled water mixtures). After saturation, the samples started swelling and dial gauges started showing swelling. Dial gauge readings were taken at different time intervals till the swelling ceases. For the determination of swelling pressure, small amounts of load were applied gradually till the height of swollen soil sample came back

to its original height. After the soil samples attained full swelling in oedometric swelling tests, consolidation tests had been started. Double incremental loading starting from 10 kN/m² upto 640kN/m² was applied. For each increment of loading the compression dial readings were recorded till the dial reading attain a steady state. The change in void ratio corresponding to the increase in overburden pressures were determined as follows

$$\Delta e = \frac{\Delta H}{H} (1 + e_0)$$

where ΔH is the change in sample thickness due to increase in overburden pressure H is the initial thickness of the sample, e_0 is the initial void ratio of the sample

After the consolidation process was over the sample was dismantled and dry weight of the specimen was carefully noted down by not allowing a single grain to escape. Then the void ratio have been calculated by the height of solids method. On the basis of experimental studies done on granulated bentonite variation of void ratio along with effective stress have been plotted graphically as given below:

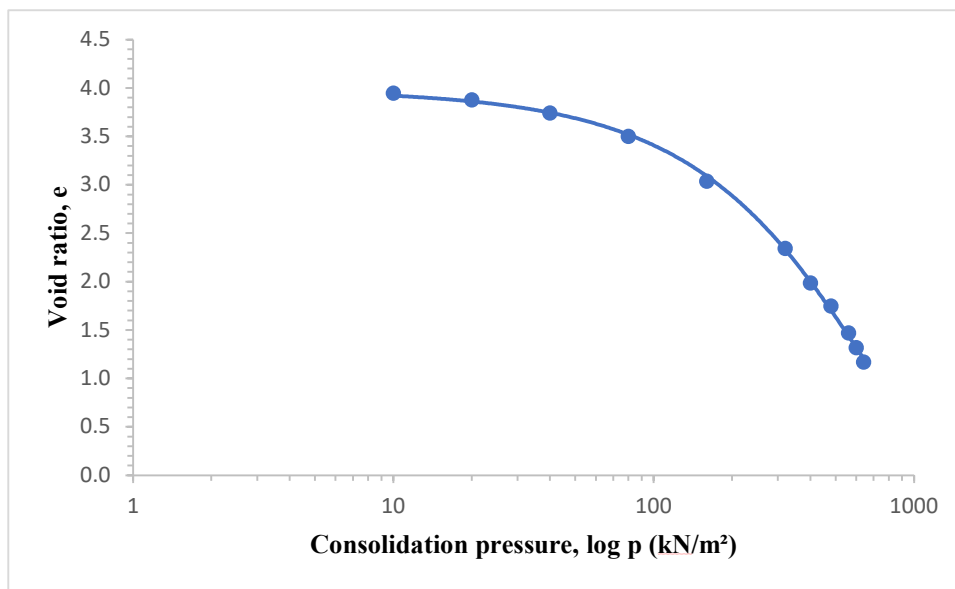


Fig 5.1: Relationship between void ratio vs effective stress of Granulated bentonite for 100% distilled water as pore fluid

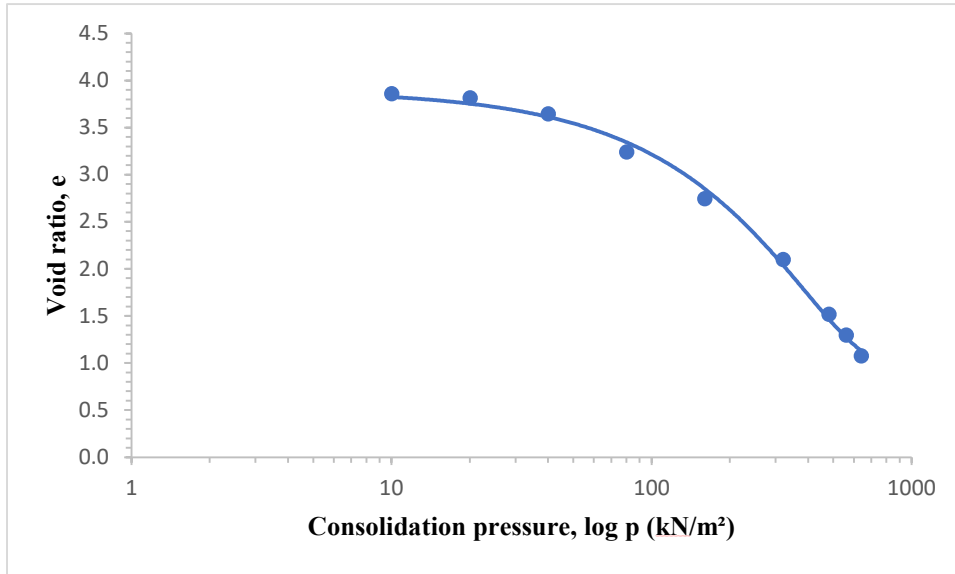


Fig5.2: Relationship between void ratio vs effective stress of Granulated bentonite for 20%Ethanol+ 80% Distilled water as pore fluid

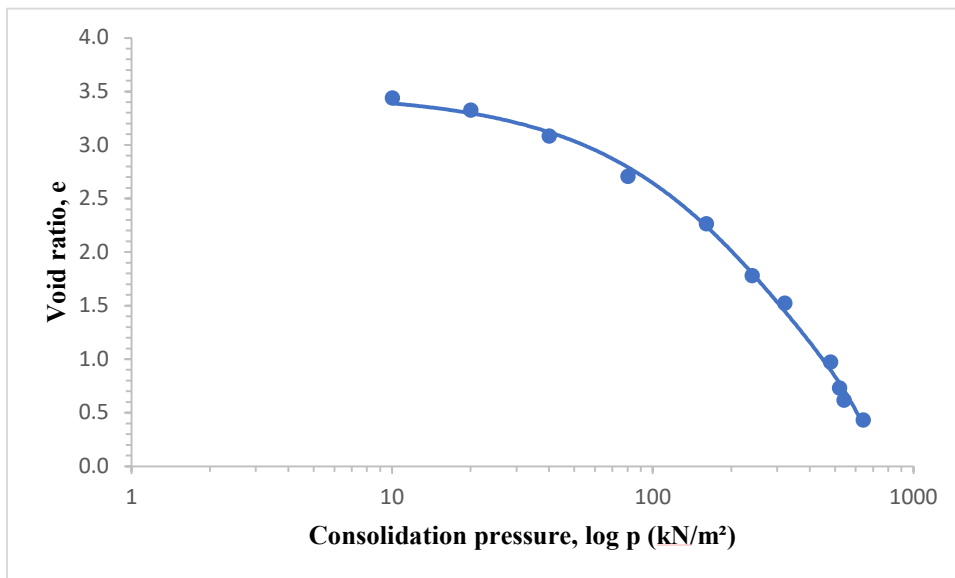


Fig5.3: Relationship between void ratio vs effective stress of Granulated bentonite for 40%Ethanol+ 60% Distilled water as pore fluid

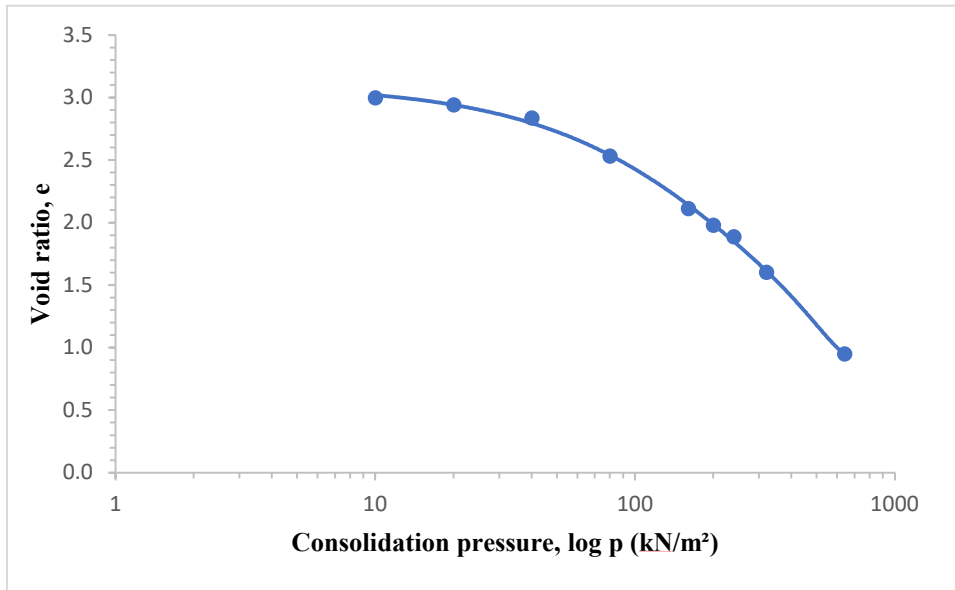


Fig5.4: Relationship between void ratio vs effective stress of Granulated bentonite for 60%Ethanol+ 40% Distilled water as pore fluid

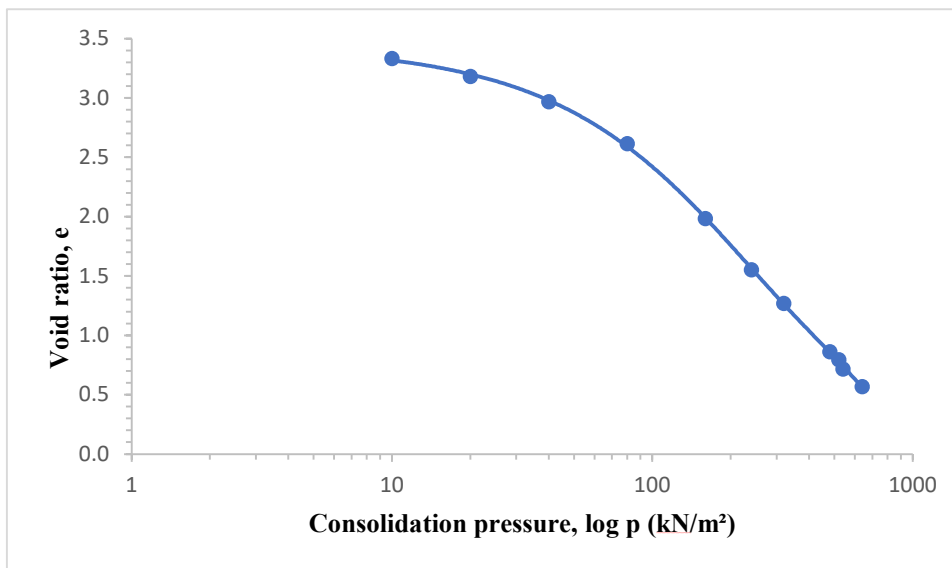


Fig5.5: Relationship between void ratio vs effective stress of Granulated bentonite for 80%Ethanol+ 20% Distilled water as pore fluid

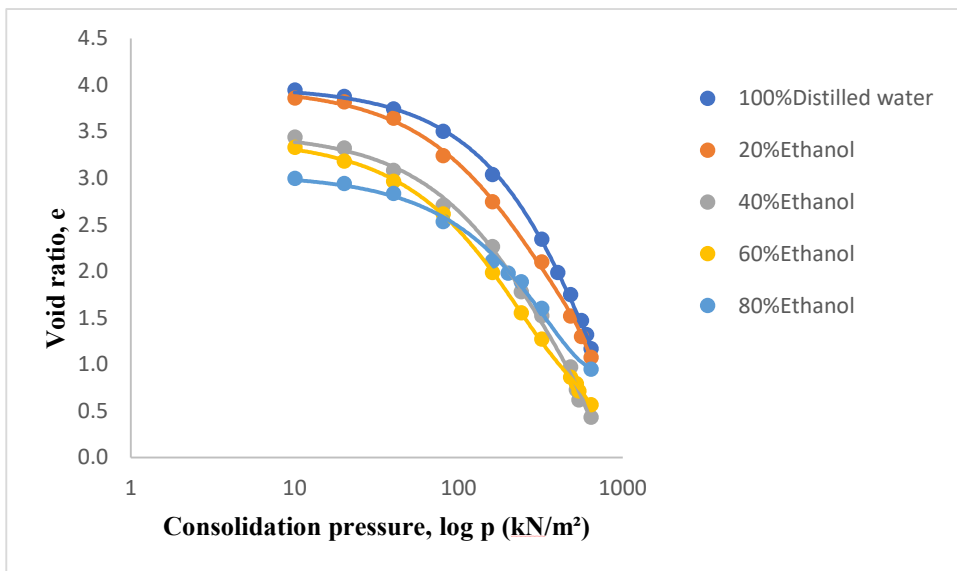


Fig5.6: Combination of Relationship between void ratio vs effective stress of Granulated bentonite

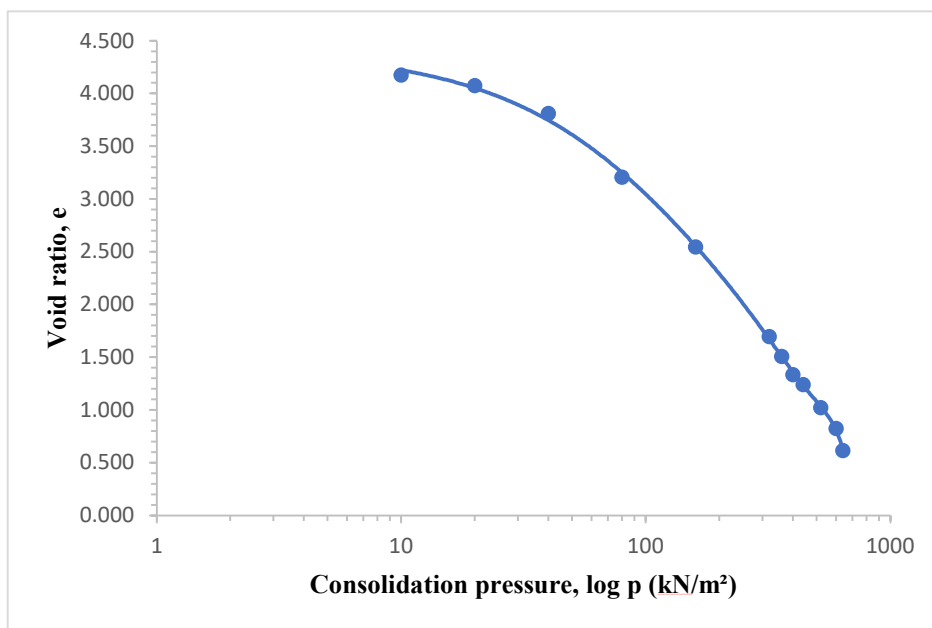


Fig5.7: Relationship between void ratio vs effective stress of Granulated bentonite for 20%Methanol+ 80% Distilled water as pore fluid

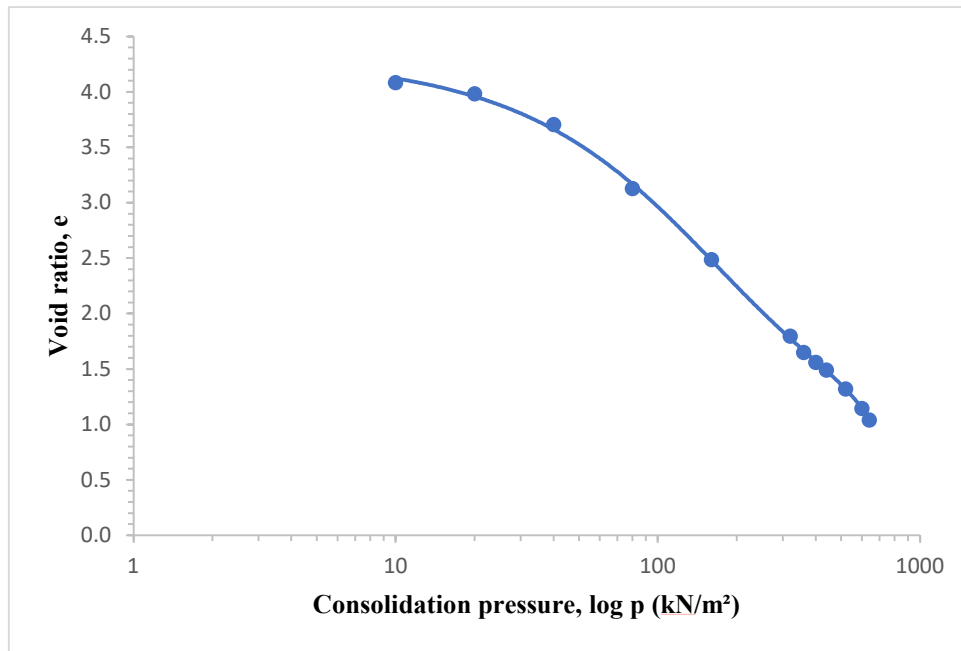


Fig5.8: Relationship between void ratio vs effective stress of Granulated bentonite for 40%Methanol+ 60% Distilled water as pore fluid

From the above $e - \log \sigma_v'$ plot it had been observed that for the different pore fluid content, void ratio decreased as the applied vertical pressure had increased. It had also been observed that with the increase in concentration of organic pore fluid, the void ratio had decreased. The $e - \log \sigma_v'$ curve for 100% distilled water lies at the top, $e - \log \sigma_v'$ curve for 80%Ethanol+20% Distilled water at the bottom. The effective stress-void ratio plots of granulated bentonite in presence of pore fluids showed that the sample having 100% distilled water contents had higher void ratio. The void ratios reduced with the increase of organic fluid content in the granulated bentonite. This can be attributed to the lower value of dielectric constant of ethanol than water which hinders the expansion of the diffused double layer of the clay resulting in less swelling.

5.3 Determination of Compression index (C_c):

The Compression index C_c is defined as the slope of the straight line portion of the void ratio versus log of effective stress for a normally consolidated clay.

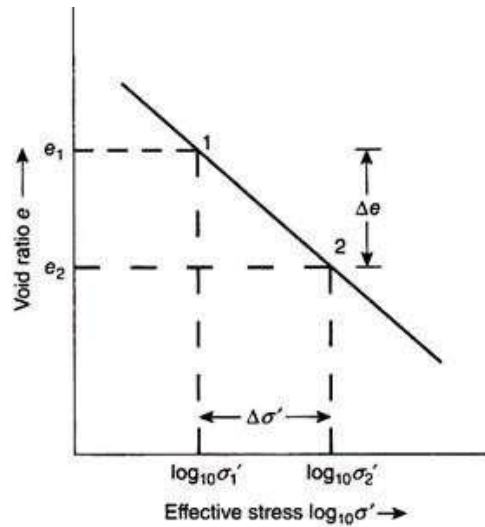


Fig 5.9 Void ratio versus log effective stress

The expression to find the compression index 'C_c' is given below-

$$C_c = \frac{(e_1 - e_2)}{\log_{10} \sigma'_2 - \log_{10} \sigma'_1} = \frac{\Delta e}{\log_{10}(\sigma'_2 / \sigma'_1)}$$

Where, Δe = Change in void ratio

$\log_{10} (\sigma'_2 / \sigma'_1)$ = Change in effective stress taken in log scale

From the test results from Fig (5.1-5.8) it was found that with increase in the proportion of organic pore fluids the Compression Index (C_c) of the soil decreases in general from that of distilled water of granulated bentonite. The values of compression index of the granulated bentonite with ethanol, methanol mixture with distilled water has been given below in the tabular form.

Table5.1: Compression Index of the granulated bentonite with ethanol distilled water

Sample	Compression Index (C _c)
100% Distilled water	3.975
20% Ethanol-80%Distilled water	3.407
40%Ethanol-60%Distilled water	2.657
60%Ethanol-40%Distilled water	2.271
80%Ethanol-20%Distilled water	1.959

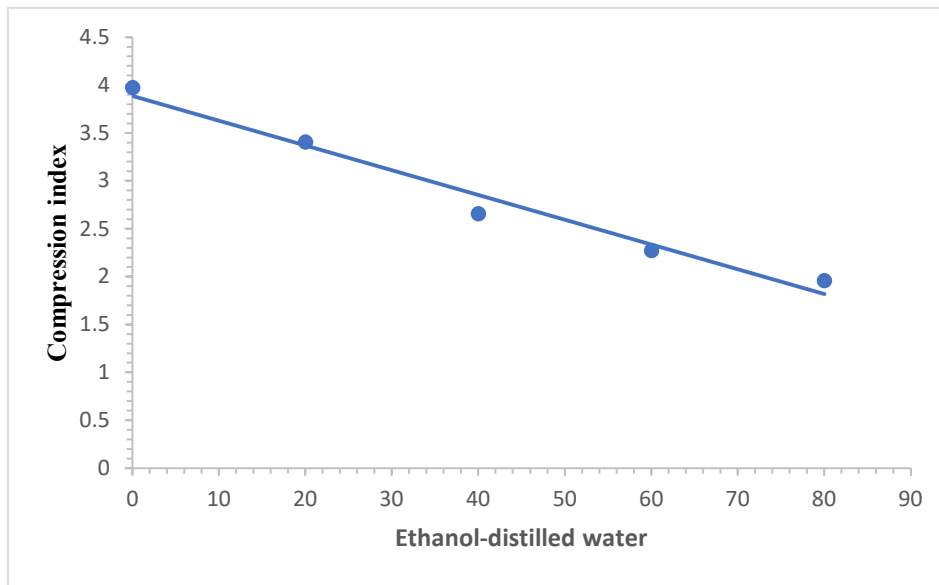


Fig 5.10: Relationship between Ethanol-distilled water and compression index.

From Fig 5.10 it can be seen that the compression index reduces with the addition of ethanol-distilled water. Compression index is decreasing linearly with the increase of percentage of ethanol in the ethanol water solution. This is because the ethanol water solution is acting like an organic compound in the granulated bentonite and with the increase in the percentage of the organic content in the organic solution, compressibility is decreasing.

The tables of specimen height and void ratio calculation are shown in Appendix I.

5.4 Determination of Coefficient of consolidation (C_v):

Coefficient of Consolidation ' C_v ' is defined as the parameter used to measure the rate at which the saturated clay or soil undergoes compaction or consolidation, when they subjected to an increase in the pressure. They are usually measured in square inch per second or square centimetre per second. The procedure involves measuring the change in height of soil sample as it is loaded in augmentation. By plotting the change in height against the square root of time or logarithm, coefficient of consolidation is being determined.

In this project the coefficient of consolidation is determined by the Taylor's square root of time fitting method. The method consists of plotting the dial gauge readings against the square root of time for any pressure increment. A straight line has to be drawn passing through

the primary consolidation zone. Another straight line is drawn with a slope 1.15 times of the previous line. This line meets the curve at a point and the x-coordinate of that point gives the value of $\sqrt{t_{90}}$. The coefficient of consolidation ' C_v ' can be calculated by the following equation-

$$C_v = \frac{(T_v \times d^2)}{t_{90}}$$

where, $\sqrt{t_{90}}$ is obtained from the curves.

$(T_v)_{90}$ = Time factor corresponding to 90% degree of consolidation = 0.848 (from table)

d = Average drainage path for the pressure increment = $(H_i + H_f) / 4$

H_i = Initial height

H_f = Final height obtained by height of solid method for a given pressure increment.

5.4.1 Comparison of the C_v values: The coefficient of consolidation ' C_v ' curves for all the samples using 100% distilled water , 20%,40% , 60% ,80% (ethanol methanol solution) have been plotted from Fig 5.11 to Fig 5.38 respectively.

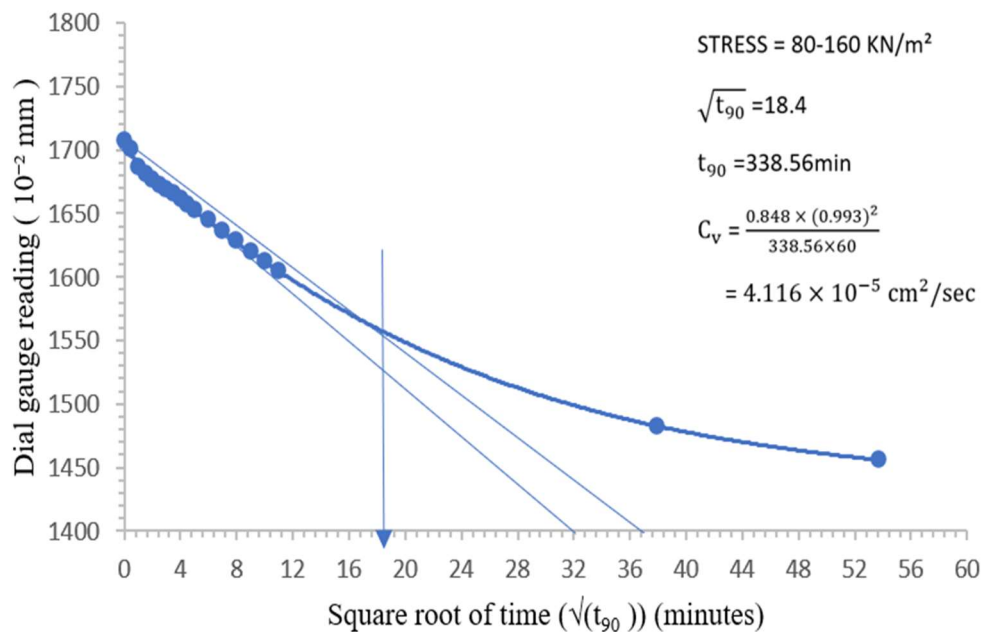


Fig 5.11: Time-consolidation curve of sample 1 for 100% Distilled water as pore fluid at 80- 160kPa

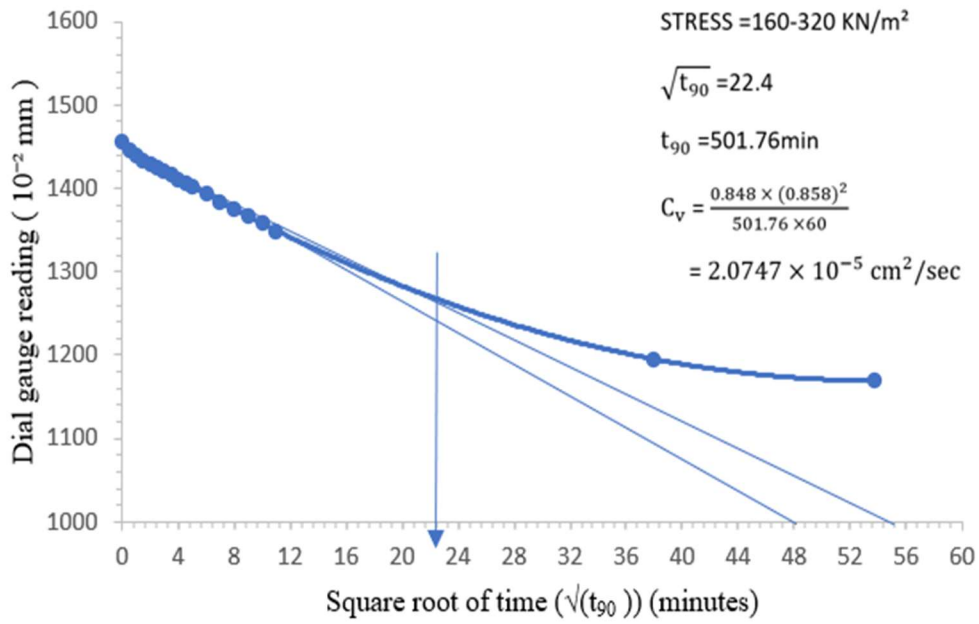


Fig5.12: Time-consolidation curve of sample 1 for 100% Distilled water as pore fluid at 160- 320kPa

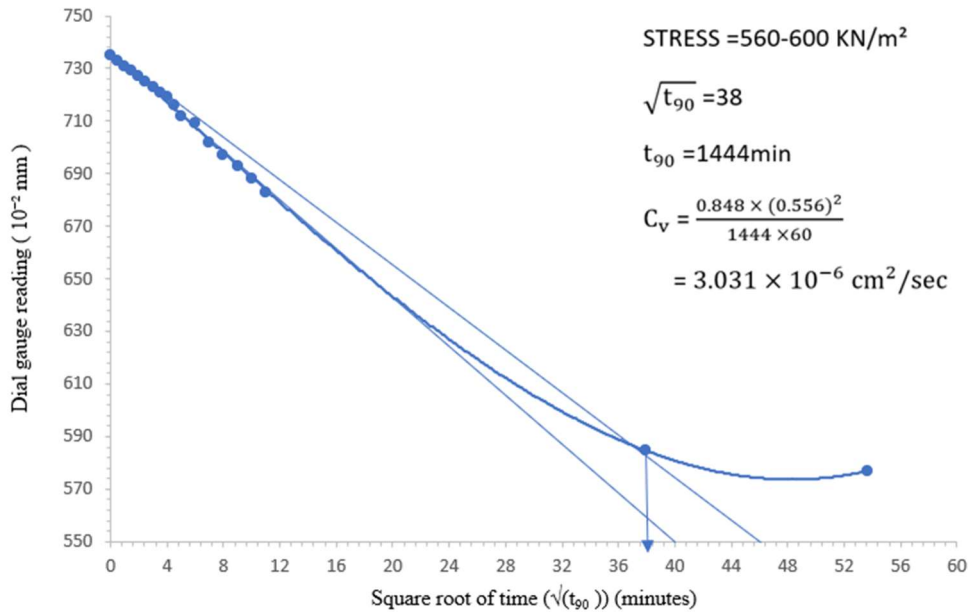


Fig 5.13: Time-consolidation curve of sample 1 for 100% Distilled water as pore fluid at 560- 600kPa

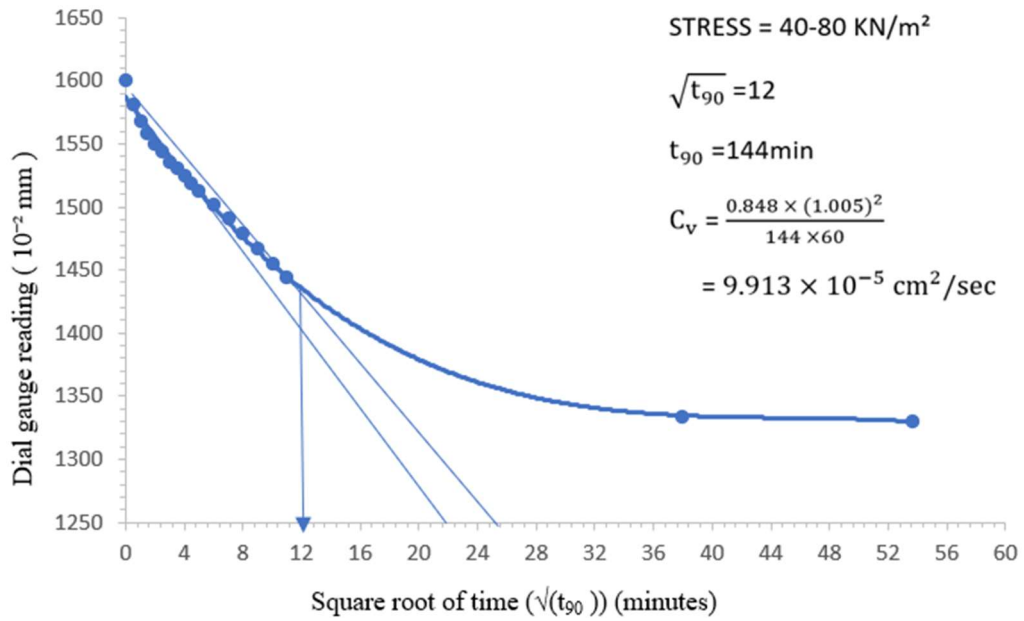


Fig5.14: Time-consolidation curve of sample 2 for 20% Ethanol as pore fluid at 40-80kPa

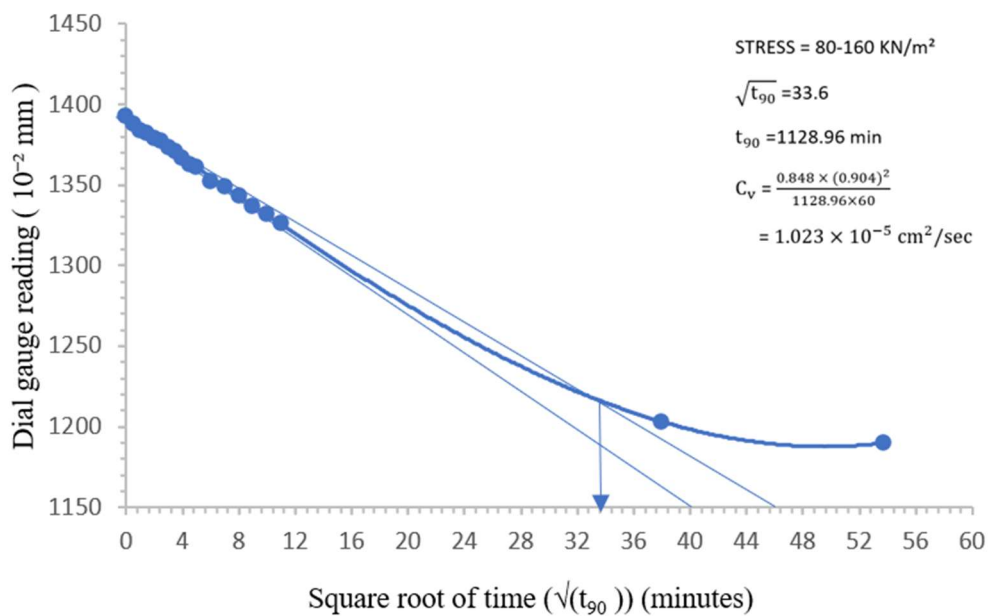


Fig 5.15: Time-consolidation curve of sample 2 for 20% Ethanol as pore fluid at 80-160kPa

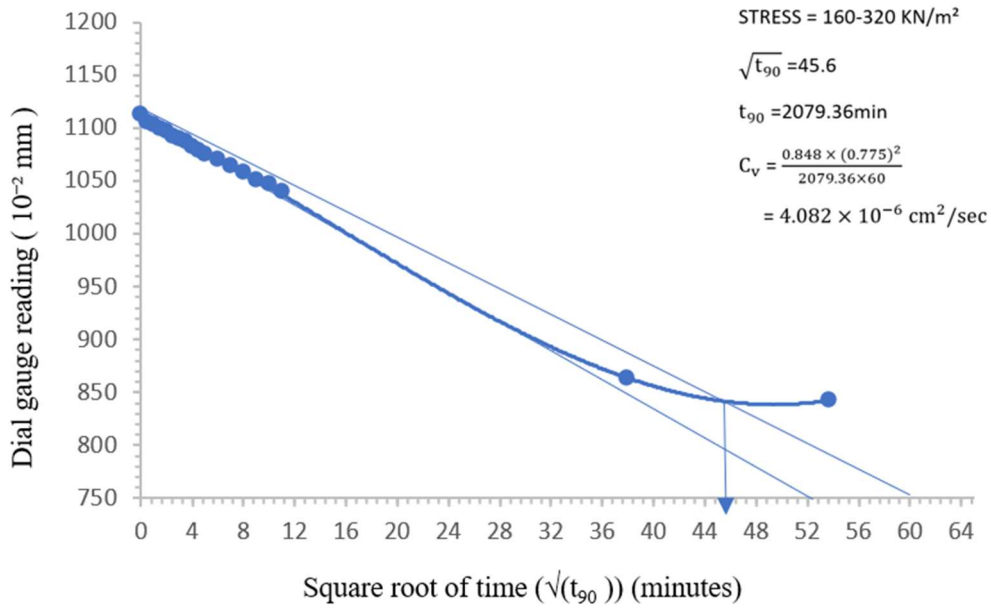


Fig 5.16: Time-consolidation curve of sample 1 for 20% Ethanol as pore fluid at 160-320kPa

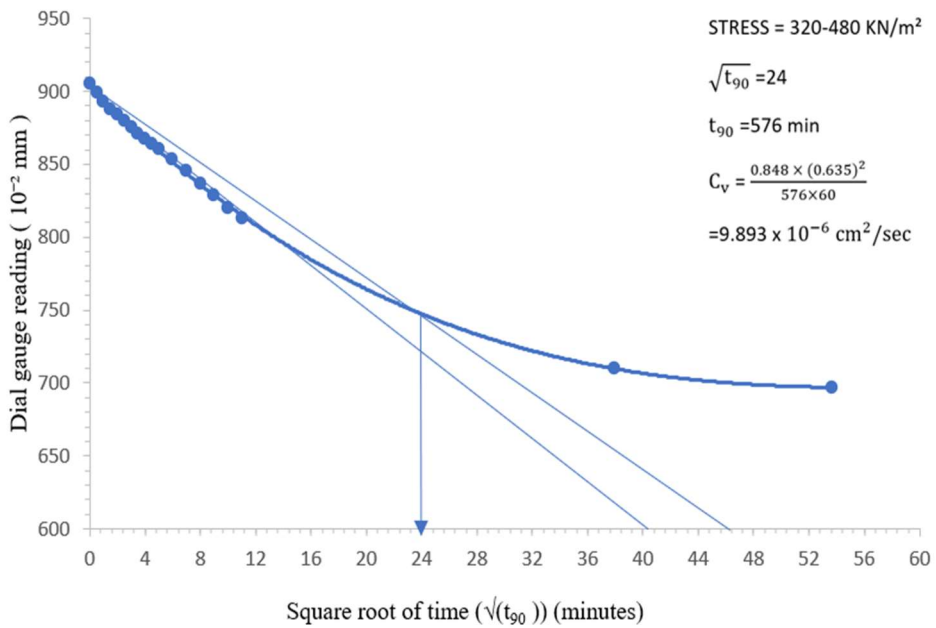


Fig5.17: Time-consolidation curve of sample 2 for 20% Ethanol as pore fluid at 320-480kPa

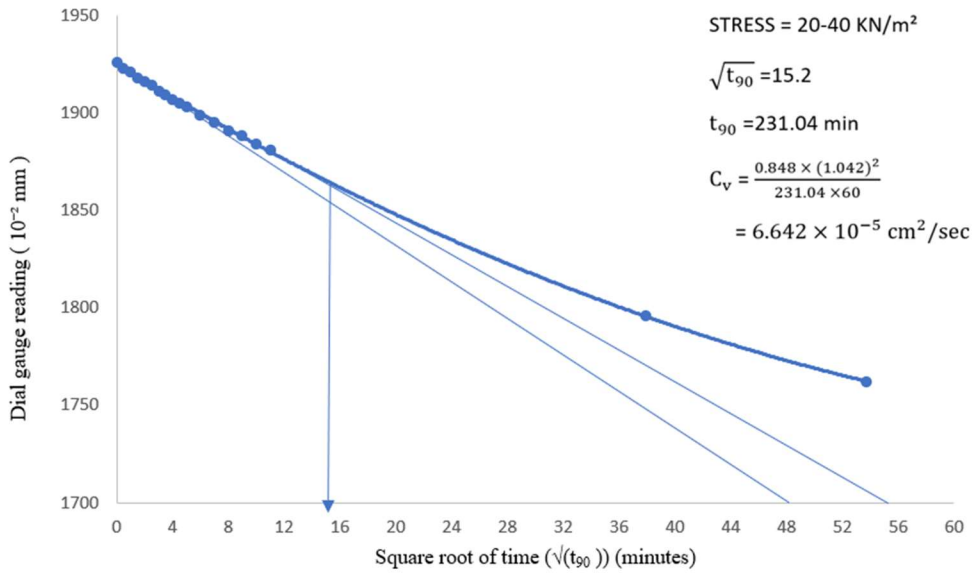


Fig5.18: Time-consolidation curve of sample 3 for 40%Ethanol+60% Distilled water as pore fluid at 20- 40kPa

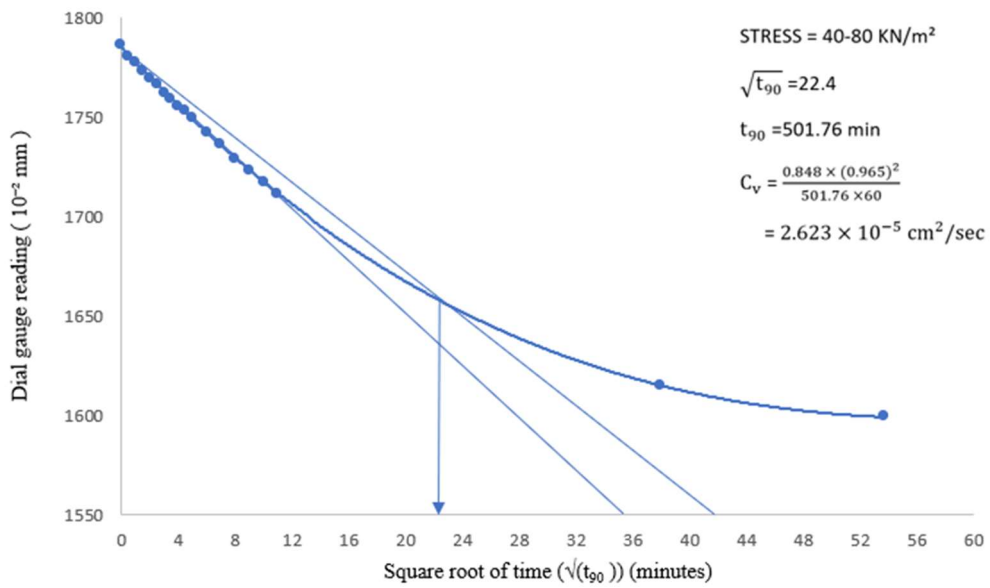


Fig5.19 : Time-consolidation curve of sample 3 for 40%Ethanol+60% Distilled water as pore fluid at 40- 80kPa

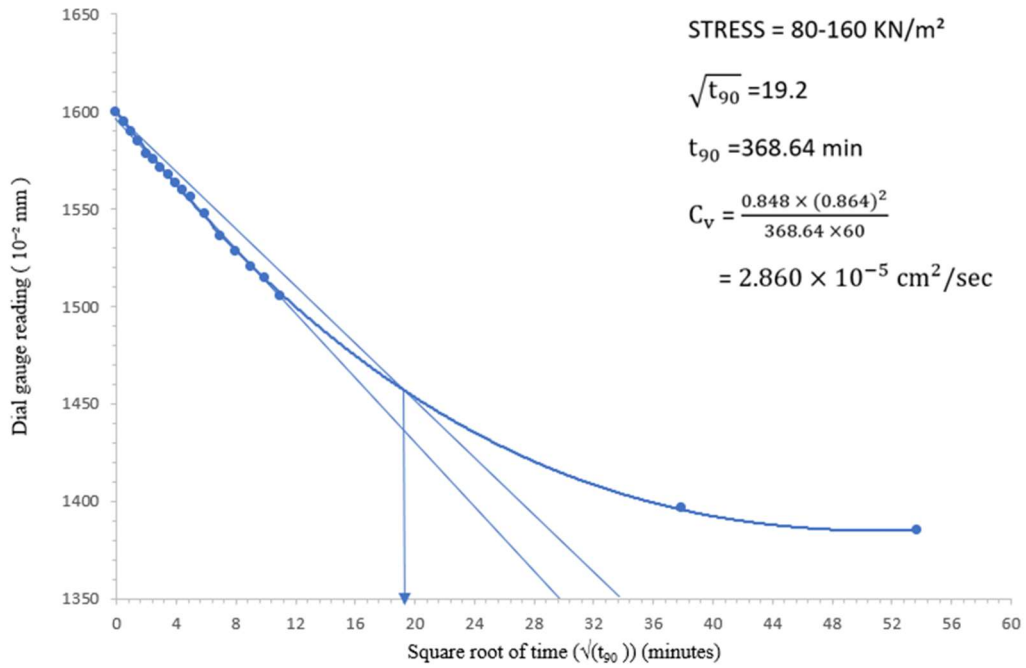


Fig5.20: Time-consolidation curve of sample 3 for 40%Ethanol+60% Distilled water as pore fluid at 80- 160kPa

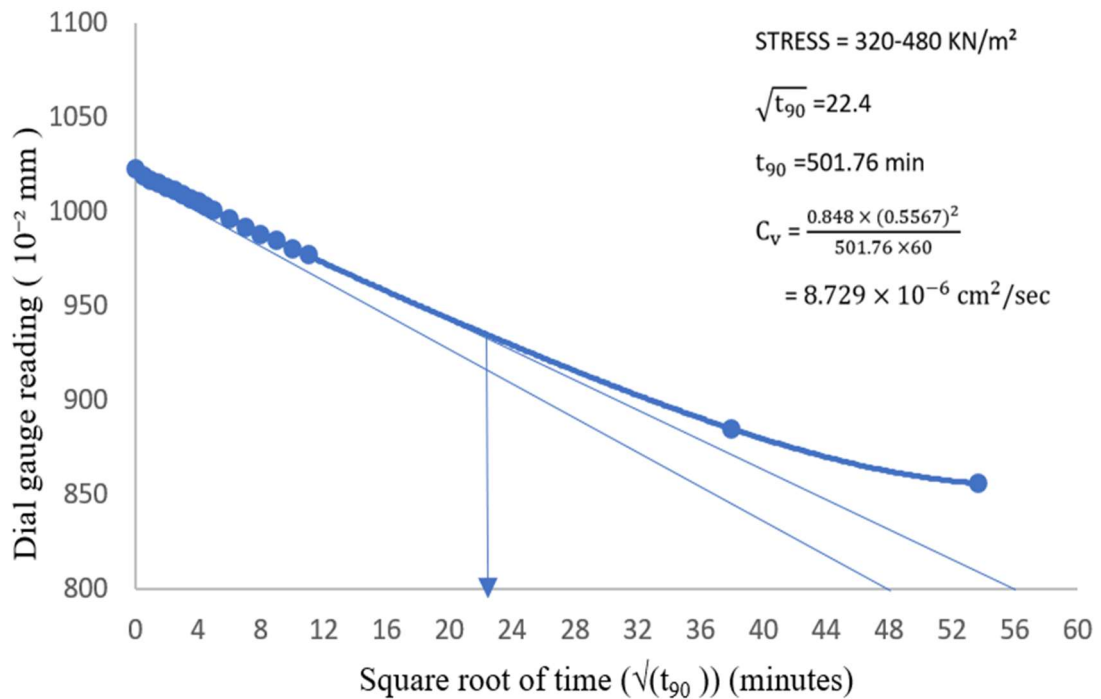


Fig5.21: Time-consolidation curve of sample 3 for 40%Ethanol+60% Distilled water as pore fluid at 320- 480kPa

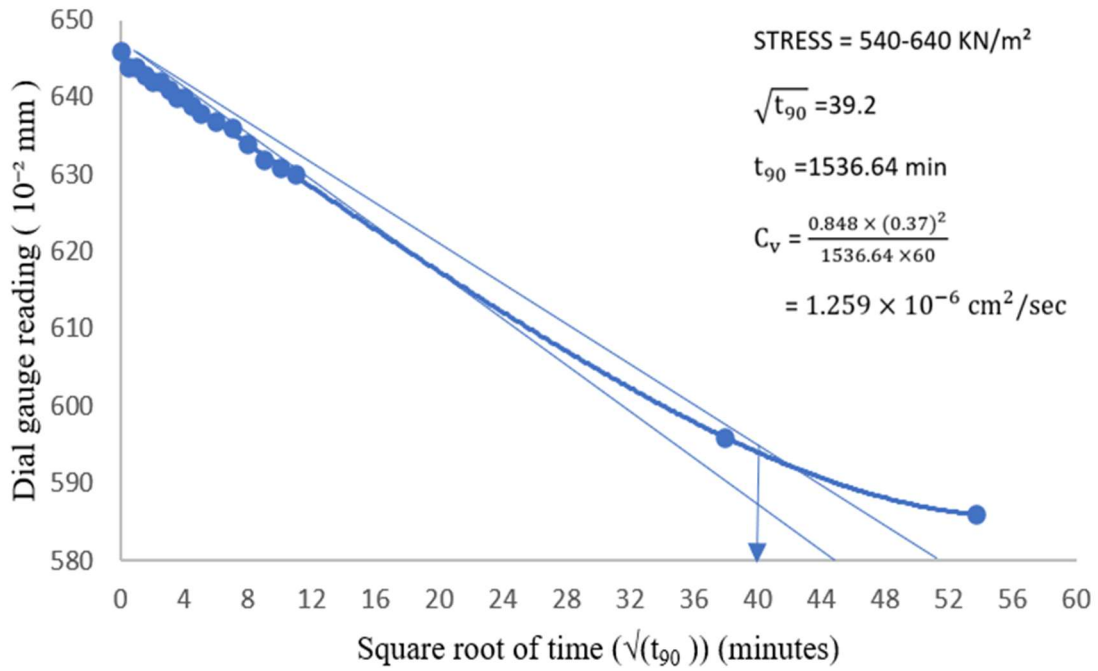


Fig5.22: Time-consolidation curve of sample 3 for 40%Ethanol+60% Distilled water as pore fluid at 540- 640kPa

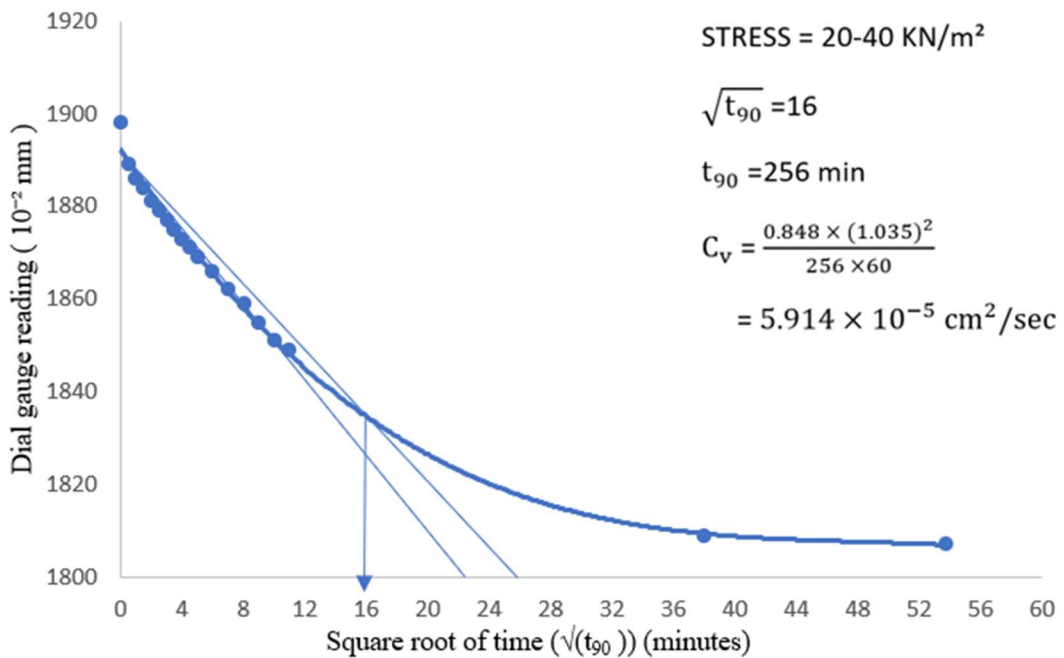


Fig5.23: Time-consolidation curve of sample 4 for 60%Ethanol+40% Distilled water as pore fluid at 20- 40kPa

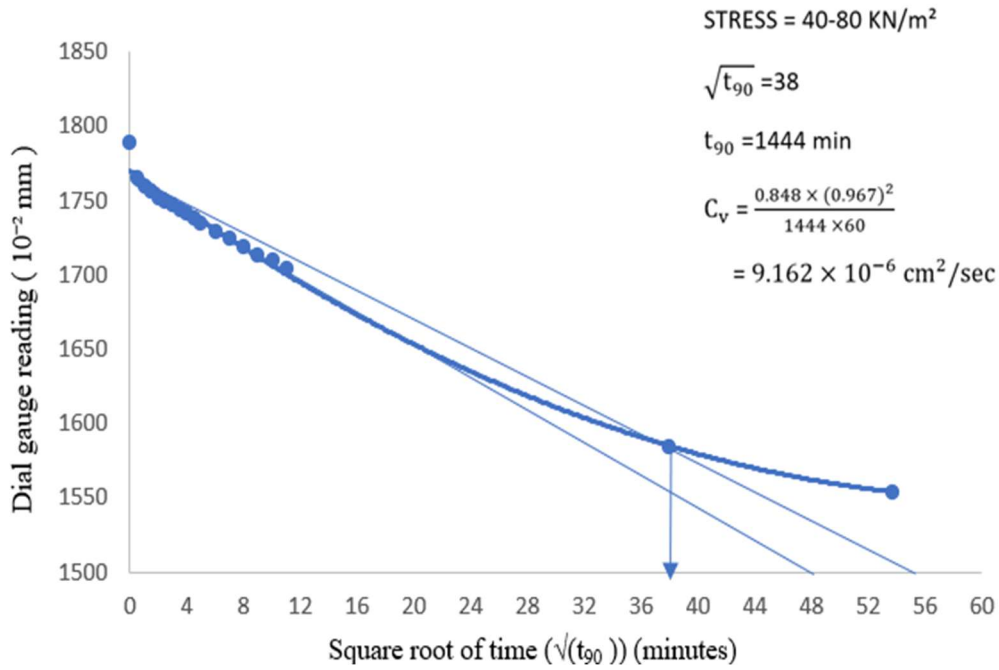


Fig5.24: Time-consolidation curve of sample 4 for 60%Ethanol+40% Distilled water as pore fluid at 40- 80kPa

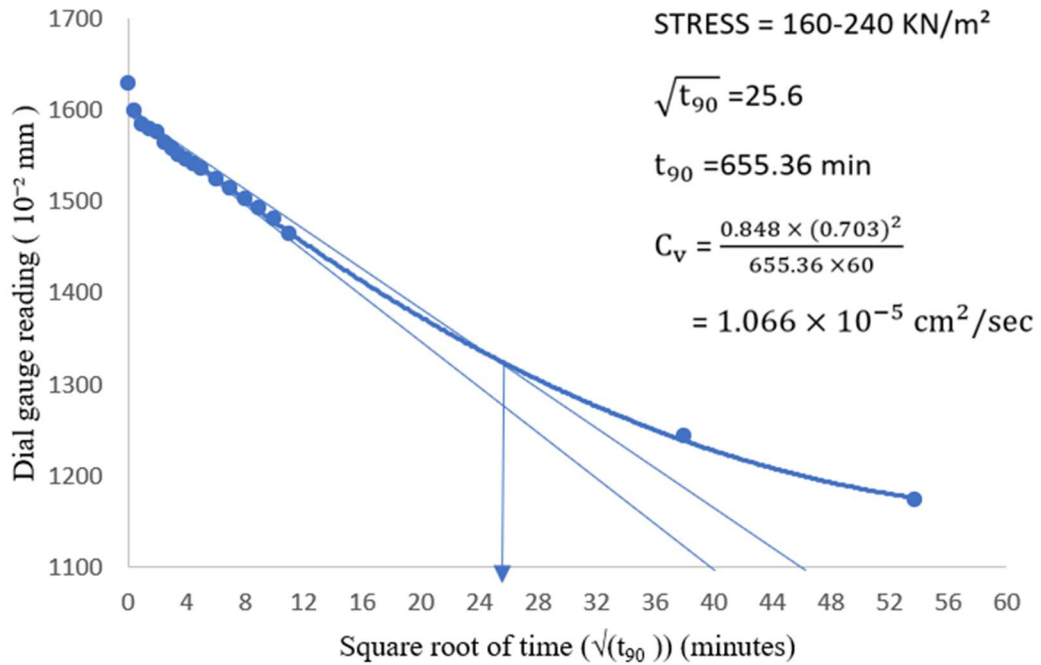


Fig5.25: Time-consolidation curve of sample 4 for 60%Ethanol+40% Distilled water as pore fluid at 160- 240kPa

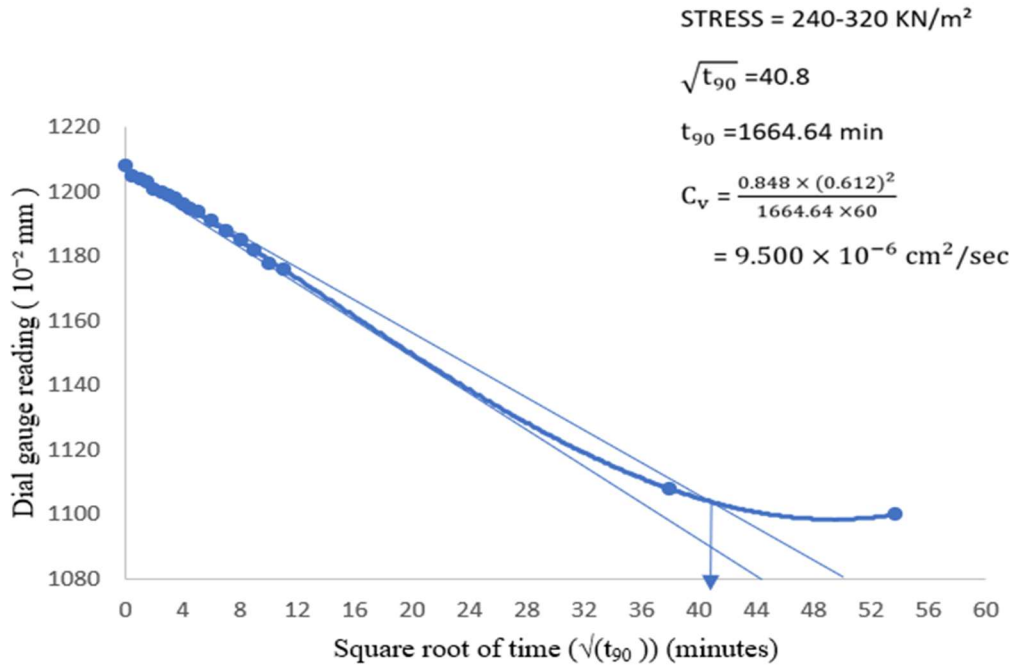


Fig5.26: Time-consolidation curve of sample 4 for 60%Ethanol+40% Distilled water as pore fluid at 240- 320kPa

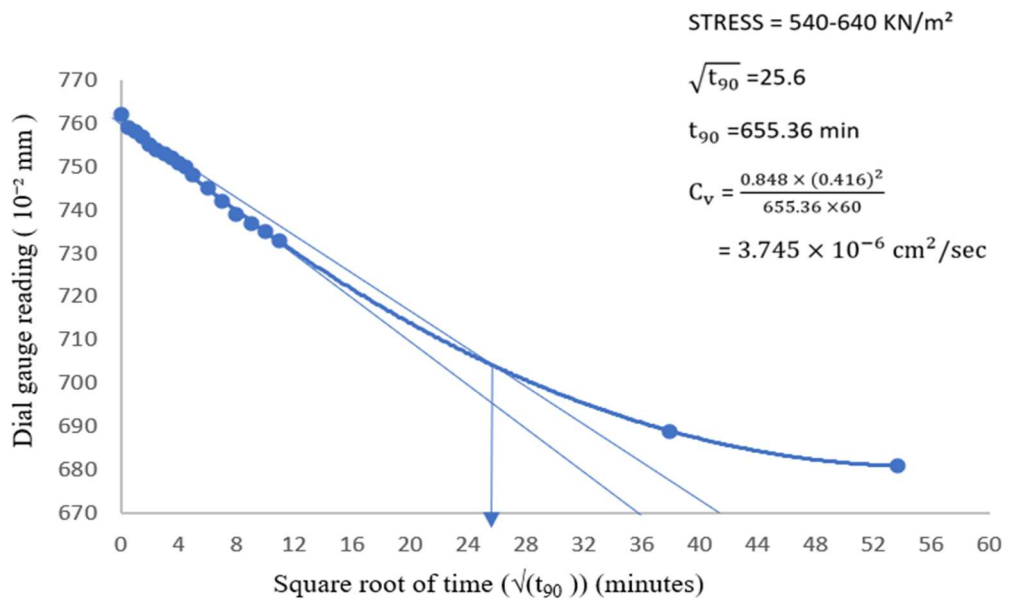


Fig5.27: Time-consolidation curve of sample 4 for 60%Ethanol+40% Distilled water as pore fluid at 540- 640kPa

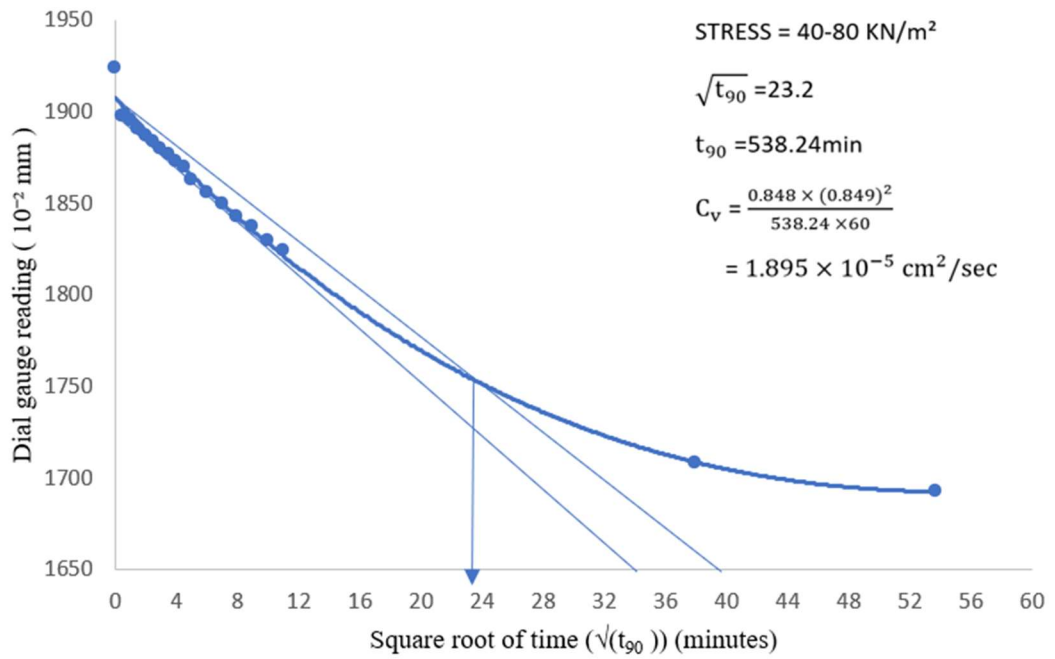


Fig5.28: Time-consolidation curve of sample 5 for 80%Ethanol+20% Distilled water as pore fluid at 40- 80kPa

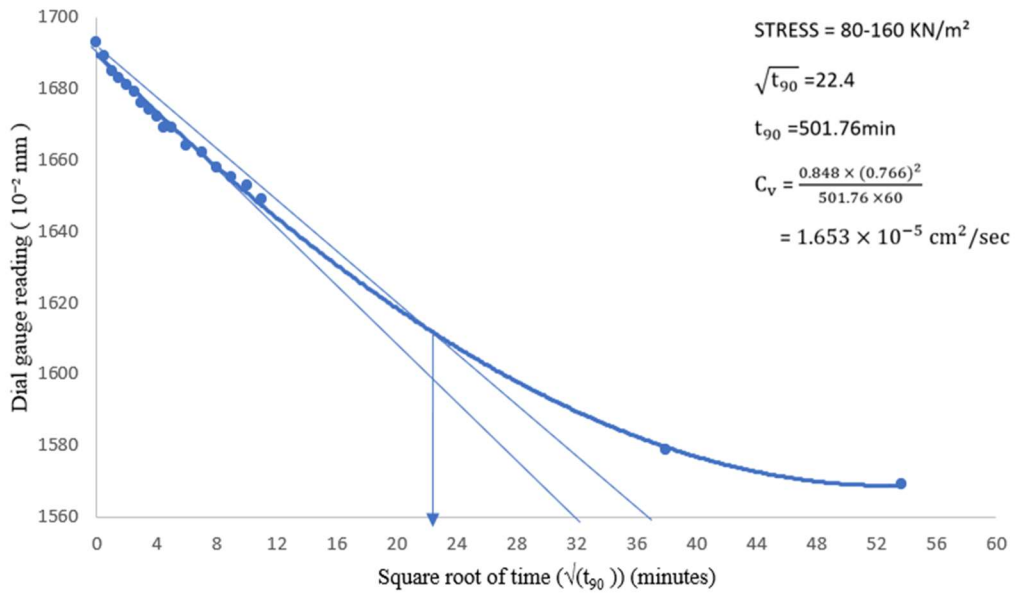


Fig5.29: Time-consolidation curve of sample 5 for 80%Ethanol+20% Distilled water as pore fluid at 80- 160kPa

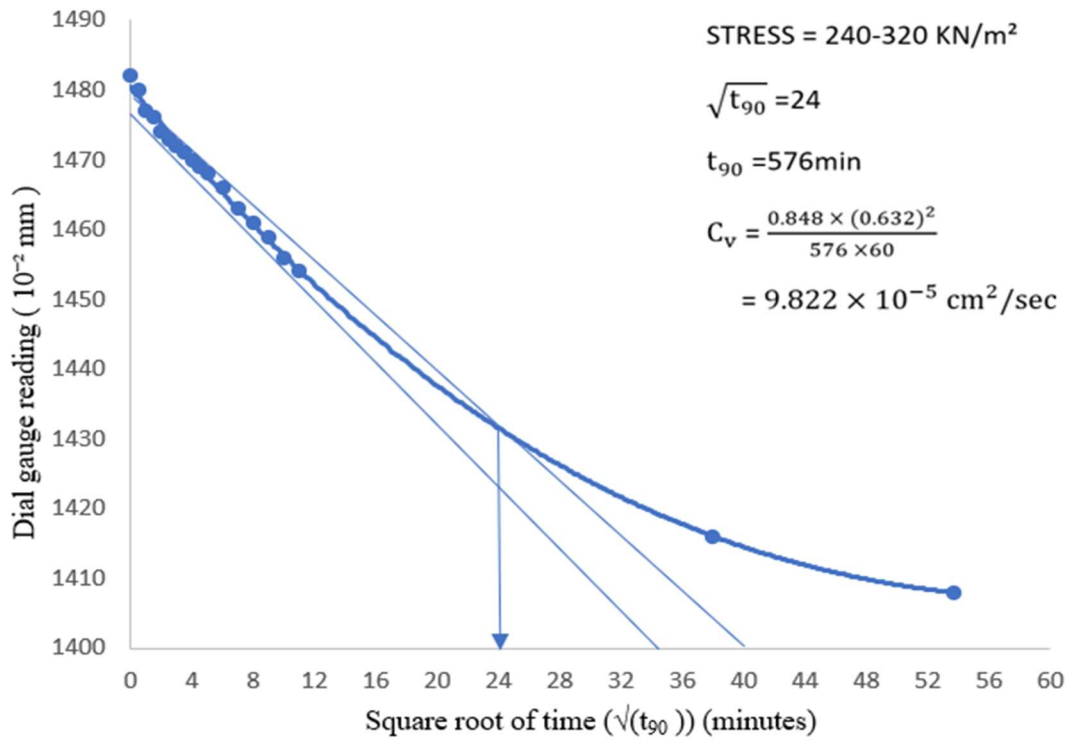


Fig5.30: Time-consolidation curve of sample 5 for 80%Ethanol+20% Distilled water as pore fluid at 240- 320kPa

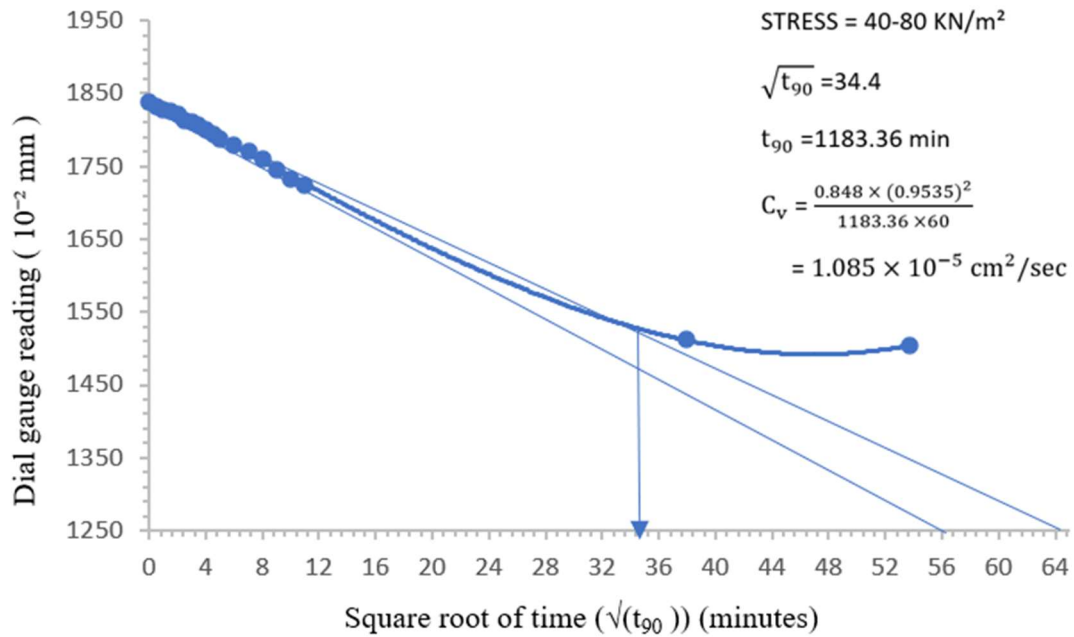


Fig5.31: Time-consolidation curve of sample 6 for 20%Methanol+80% Distilled water as pore fluid at 40- 80kPa

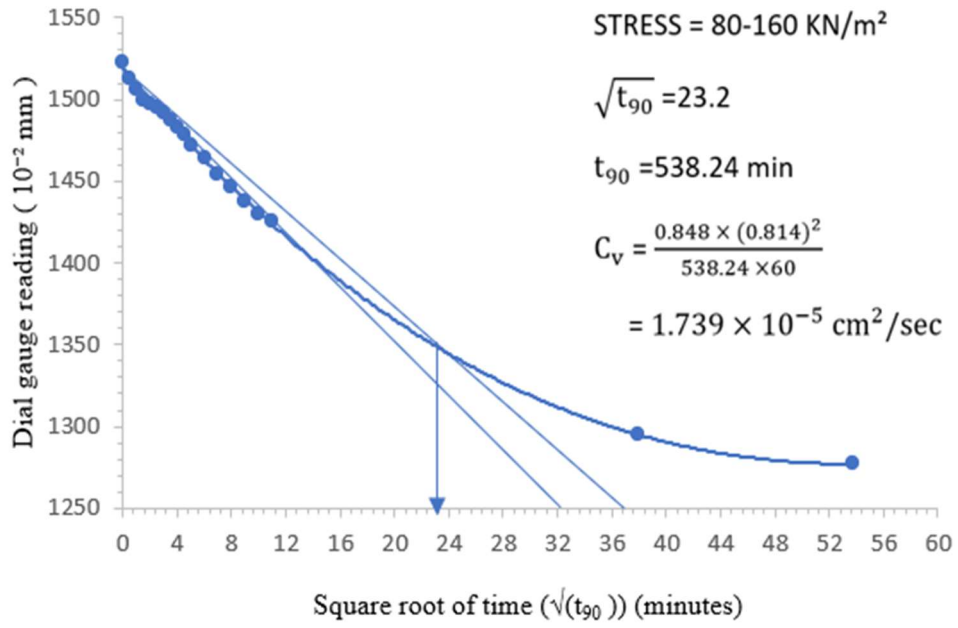


Fig5.32: Time-consolidation curve of sample 6 for 20%Methanol+80% Distilled water as pore fluid at 80- 160kPa

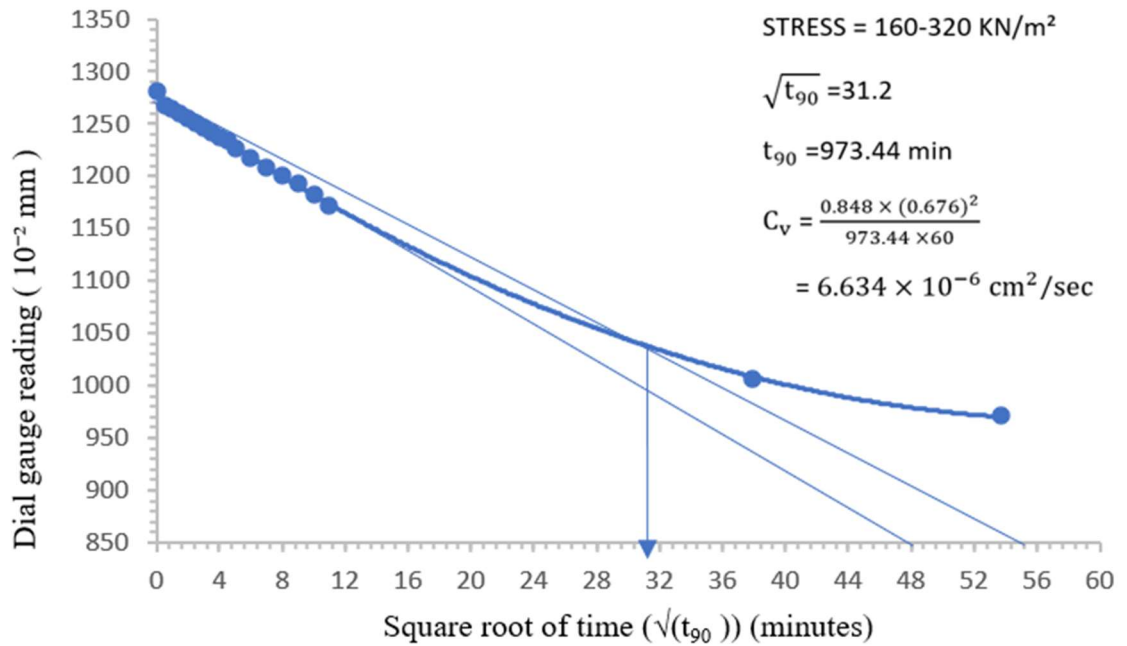


Fig5.33: Time-consolidation curve of sample 6 for 20%Methanol+80% Distilled water as pore fluid at 160- 320kPa

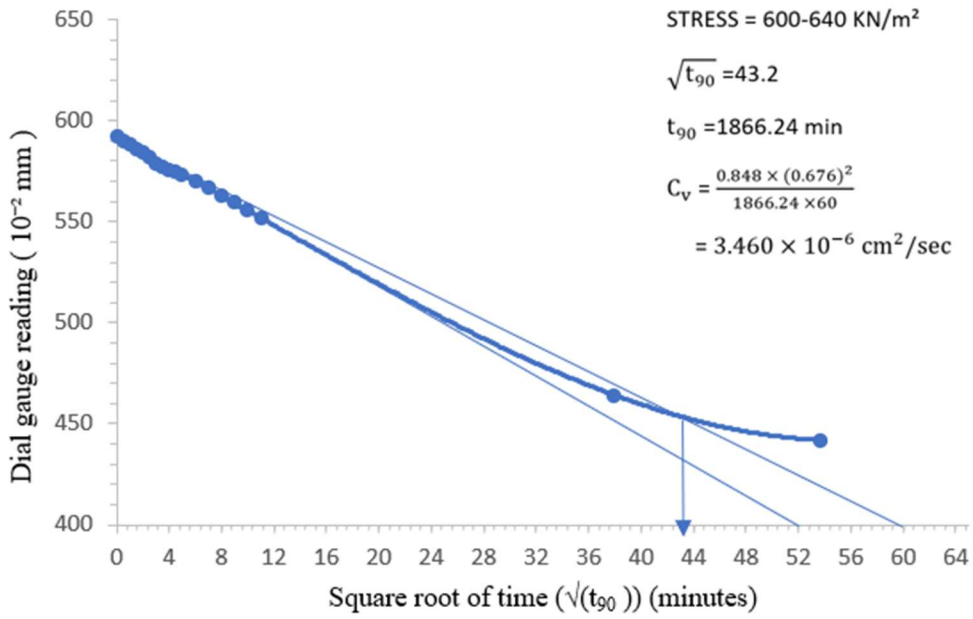


Fig5.34: Time-consolidation curve of sample 6 for 20%Methanol+80% Distilled water as pore fluid at 600- 640kPa

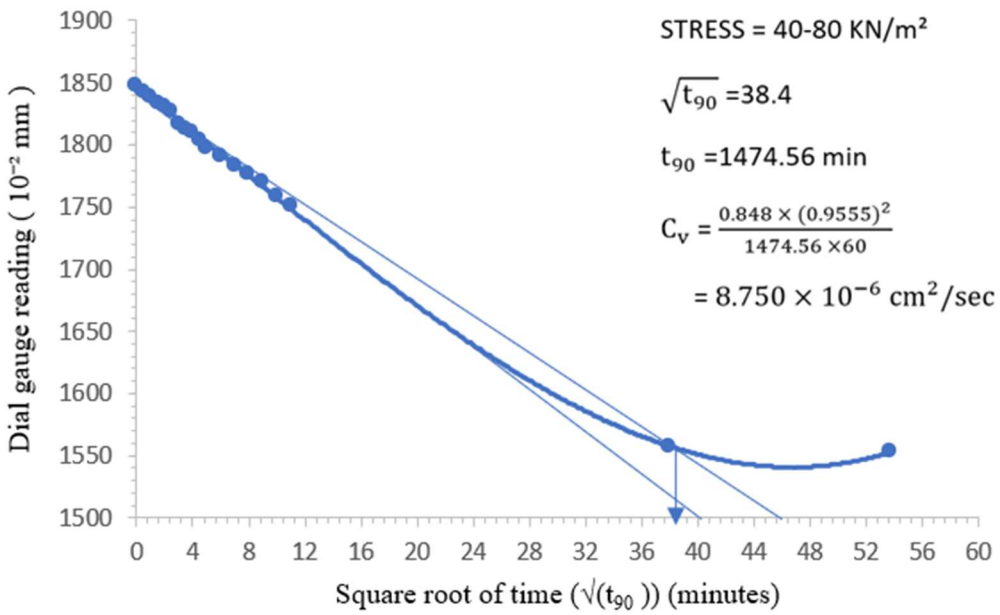


Fig5.35: Time-consolidation curve of sample 7 for 40%Methanol+60% Distilled water as pore fluid at 40- 80kPa

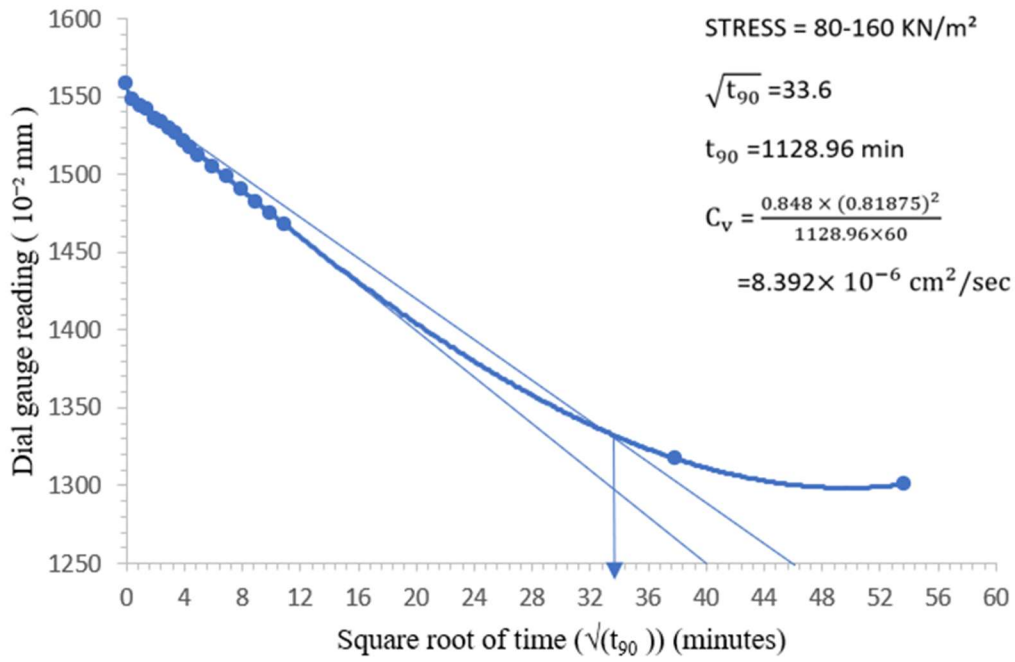


Fig5.36: Time-consolidation curve of sample 7 for 40%Methanol+60% Distilled water as pore fluid at 80- 160kPa

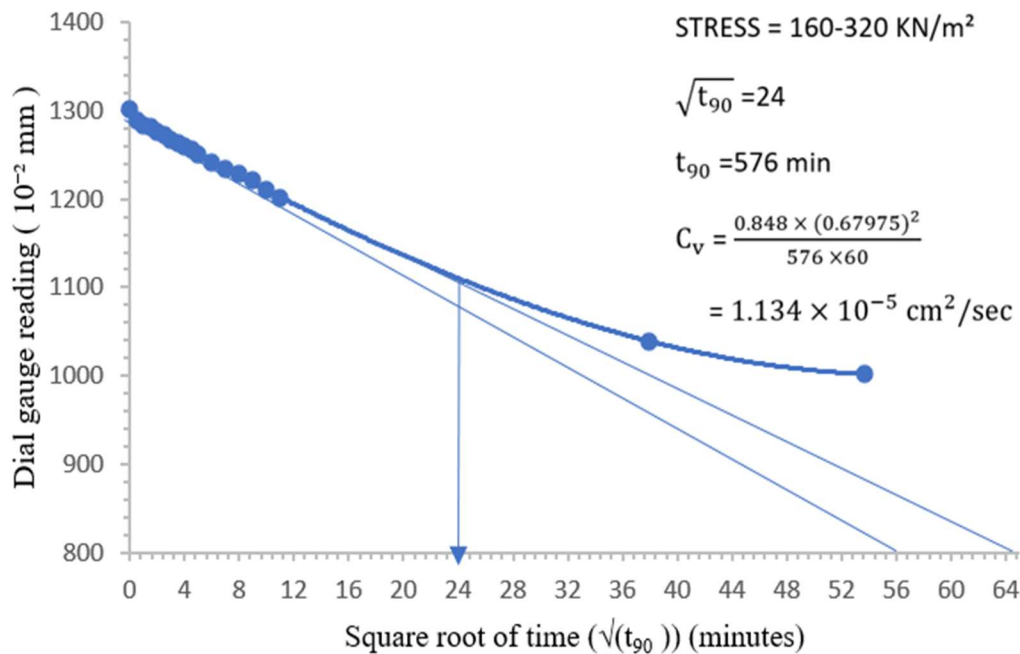


Fig5.37: Time-consolidation curve of sample 7 for 40%Methanol+60% Distilled water as pore fluid at 160- 320kPa

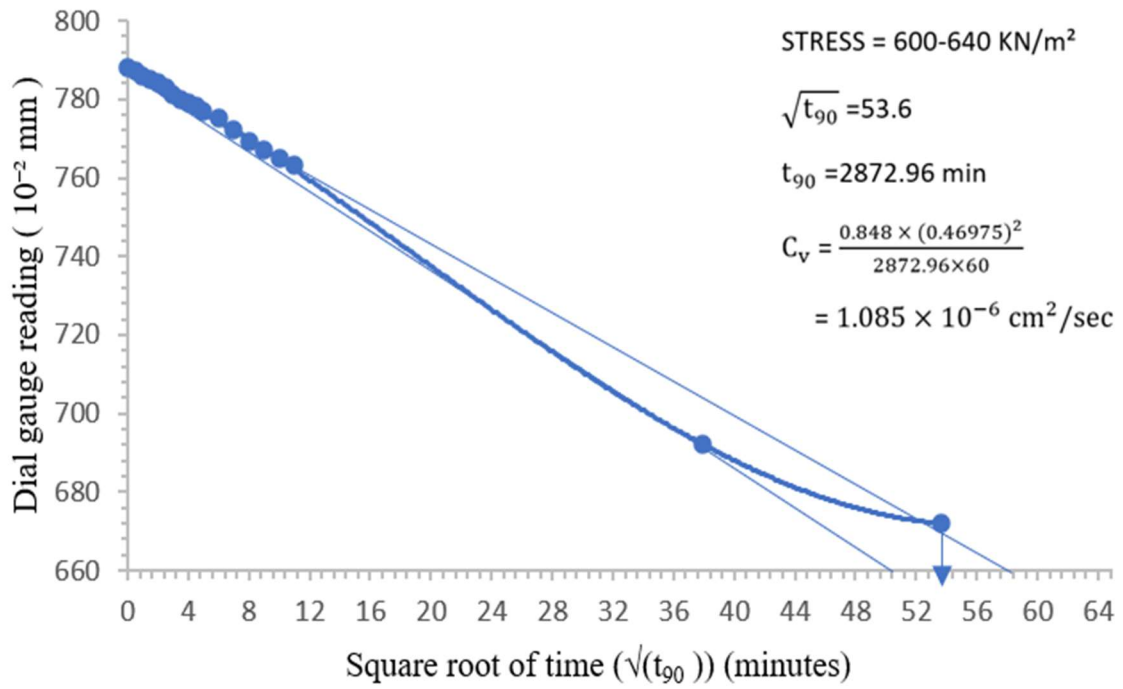


Fig5.38: Time-consolidation curve of sample 7 for 40%Methanol+60% Distilled water as pore fluid at 600- 640kPa

Table 5.2: Consolidation and permeability properties of granulated bentonite mixed with 100% Distilled water & ethanol solution

Applied pressure	Void Ratio	Coefficient of compressibility a_v (m ² /kN)	Coefficient of volume change, m_v (m ² /kN)	Coefficient of consolidation, C_v (sqcm/sec)	Coefficient of permeability, k (cm/sec)	
kPa	e					
10	3.946					
20	3.877	6.9×10^{-3}	1.40×10^{-3}			
40	3.724	7.65×10^{-3}	1.57×10^{-3}			
80	3.501	5.58×10^{-3}	1.18×10^{-3}			
160	3.039	5.78×10^{-3}	1.28×10^{-3}	4.116×10^{-5}	5.166×10^{-9}	5.1658E-09
320	2.344	4.34×10^{-3}	1.08×10^{-3}	2.074×10^{-5}	2.198×10^{-9}	2.1981E-09
400	1.985	4.49×10^{-3}	1.34×10^{-3}			
480	1.748	2.96×10^{-3}	0.99×10^{-3}			
560	1.469	3.49×10^{-3}	1.27×10^{-3}			
600	1.318	3.78×10^{-3}	1.53×10^{-3}	0.303×10^{-5}	0.4549×10^{-9}	4.549E-10
640	1.168	3.75×10^{-3}	1.62×10^{-3}			

Table 5.3: Consolidation and permeability properties of granulated bentonite mixed with 20%Ethanol & 80%Distilled water

Applied pressure	Void Ratio	Coefficient of compressibility a_v (m ² /kN)	Coefficient of volume change, m_v (m ² /kN)	Coefficient of consolidation, C_v (sqcm/sec)	Coefficient of permeability, k (cm/sec)	
kPa	e					
10	3.861					
20	3.839	2.20×10^{-3}	0.45×10^{-3}			
40	3.666	8.65×10^{-3}	1.79×10^{-3}			
80	3.205	1.15×10^{-3}	2.47×10^{-3}	9.913×10^{-5}	24.044×10^{-9}	2.40441E-08
160	2.745	5.75×10^{-3}	1.37×10^{-3}	1.023×10^{-5}	1.374×10^{-9}	1.3742E-09
320	2.126	3.87×10^{-3}	1.03×10^{-3}	0.408×10^{-5}	0.412×10^{-9}	4.119E-10
480	1.667	2.87×10^{-3}	0.92×10^{-3}	0.989×10^{-5}	0.895×10^{-9}	8.9505E-10
560	1.501	2.08×10^{-3}	0.78×10^{-3}			
640	1.329	2.15×10^{-3}	0.86×10^{-3}			

Table 5.4: Consolidation and permeability properties of granulated bentonite mixed with 40%Ethanol & 60%Distilled water

Applied pressure	Void Ratio	Coefficient of compressibility a_v (m ² /kN)	Coefficient of volume change, m_v (m ² /kN)	Coefficient of consolidation, C_v (sqcm/sec)	Coefficient of permeability, k (cm/sec)	
kPa	e					
10	3.440					
20	3.325	1.150×10^{-3}	2.59×10^{-3}			
40	3.083	1.210×10^{-3}	2.80×10^{-3}	6.642×10^{-5}	20.83×10^{-9}	2.08302E-08
80	2.707	9.40×10^{-3}	2.30×10^{-3}	2.623×10^{-5}	5.995×10^{-9}	5.9954E-09
160	2.265	5.53×10^{-3}	1.49×10^{-3}	2.860×10^{-5}	4.180×10^{-9}	4.18044E-09
240	1.781	6.05×10^{-3}	1.85×10^{-3}			
320	1.523	3.23×10^{-3}	1.16×10^{-3}			
480	0.972	3.44×10^{-3}	1.36×10^{-3}	0.873×10^{-5}	1.165×10^{-9}	1.1645E-09
520	0.730	6.05×10^{-3}	3.07×10^{-3}			
540	0.619	5.55×10^{-3}	3.21×10^{-3}			
640	0.433	1.86×10^{-3}	1.15×10^{-3}	0.126×10^{-5}	0.142×10^{-9}	1.4204E-10

Table 5.5: Consolidation and permeability properties of granulated bentonite mixed with 60%Ethanol & 40%Distilled water

Applied pressure	Void Ratio	Coefficient of compressibility a_v (m ² /kN)	Coefficient of volume change, m_v (m ² /kN)	Coefficient of consolidation, C_v (sqcm/sec)	Coefficient of permeability, k (cm/sec)	
kPa	e					
10	3.332					
20	3.182	15×10^{-3}	3.46×10^{-3}			
40	2.967	10.75×10^{-3}	2.57×10^{-3}	5.914×10^{-5}	17.396×10^{-9}	1.7396E-08
80	2.615	8.80×10^{-3}	2.22×10^{-3}	0.916×10^{-5}	1.798×10^{-9}	1.7975E-09
160	1.985	7.88×10^{-3}	2.18×10^{-3}			
240	1.552	5.41×10^{-3}	1.81×10^{-3}	1.066×10^{-5}	1.892×10^{-9}	1.89226E-09
320	1.27	3.53×10^{-3}	1.38×10^{-3}	0.950×10^{-5}	0.9319×10^{-9}	9.319E-10
480	0.863	2.54×10^{-3}	1.12×10^{-3}			
520	0.794	1.73×10^{-3}	0.93×10^{-3}			
540	0.715	3.95×10^{-3}	2.20×10^{-3}			
640	0.567	1.48×10^{-3}	0.86×10^{-3}	0.374×10^{-5}	0.32021×10^{-9}	3.2021E-10

Table 5.6: Consolidation and permeability properties of granulated bentonite mixed with 80%Ethanol & 20%Distilled water

Applied pressure	Void Ratio	Coefficient of compressibility a_v (m ² /kN)	Coefficient of volume change, m_v (m ² /kN)	Coefficient of consolidation, C_v (sqcm/sec)	Coefficient of permeability, k (cm/sec)	
kPa	e					
10	2.996					
20	2.942	5.40×10^{-3}	1.351×10^{-3}			
40	2.836	5.30×10^{-3}	1.344×10^{-3}			
80	2.532	7.60×10^{-3}	1.981×10^{-3}	1.895×10^{-5}	3.682×10^{-5}	3.6824E-09
160	2.111	5.26×10^{-3}	1.490×10^{-3}	1.653×10^{-5}	2.415×10^{-5}	2.4157E-09
200	1.979	3.30×10^{-3}	1.061×10^{-3}			
240	1.886	2.33×10^{-3}	0.780×10^{-3}			
320	1.602	3.55×10^{-3}	1.230×10^{-3}			
640	0.949	2.04×10^{-3}	0.784×10^{-3}	9.822×10^{-5}	1.139×10^{-5}	1.1386E-09

Table 5.7: Consolidation and permeability properties of granulated bentonite mixed with 20%Methanol & 80%Distilled water

Applied pressure	Void Ratio	Coefficient of compressibility a_v (m ² /kN)	Coefficient of volume change, m_v (m ² /kN)	Coefficient of consolidation, C_v (sqcm/sec)	Coefficient of permeability, k (cm/sec)	
kPa	e					
10	4.174					
20	4.073	10.10×10^{-3}	1.952×10^{-3}			
40	3.857	10.80×10^{-3}	2.129×10^{-3}			
80	3.189	16.70×10^{-3}	3.438×10^{-3}	1.085×10^{-5}	3.196×10^{-9}	3.1956E-09
160	2.544	8.06×10^{-3}	1.925×10^{-3}	1.739×10^{-5}	3.413×10^{-9}	3.4134E-09
320	1.705	5.24×10^{-3}	1.480×10^{-3}	0.663×10^{-5}	0.651×10^{-9}	6.508E-10
360	1.602	2.58×10^{-3}	0.952×10^{-3}			
400	1.42	4.55×10^{-3}	1.749×10^{-3}			
440	1.28	3.50×10^{-3}	1.446×10^{-3}			
520	1.023	3.21×10^{-3}	1.409×10^{-3}			
600	0.85	2.16×10^{-3}	1.069×10^{-3}			
640	0.715	3.38×10^{-3}	1.824×10^{-3}	0.346×10^{-5}	0.678×10^{-9}	6.7898E-10

Table 5.8: Consolidation and permeability properties of granulated bentonite mixed with 40%Methanol & 60%Distilled water

Applied pressure kPa	Void Ratio e	Coefficient of compressibility a_v (m ² /kN)	Coefficient of volume change, m_v (m ² /kN)	Coefficient of consolidation, C_v (sqcm/sec)	Coefficient of permeability, k (cm/sec)	
10	4.048					
20	3.983	6.54×10^{-3}	1.295×10^{-3}			
40	3.705	13.9×10^{-3}	2.789×10^{-3}			
80	3.128	14.43×10^{-3}	3.066×10^{-3}	0.875×10^{-5}	2.575×10^{-9}	2.575E-09
160	2.487	8.01×10^{-3}	1.941×10^{-3}	0.839×10^{-5}	1.646×10^{-9}	1.646E-09
320	1.796	4.32×10^{-3}	1.239×10^{-3}	0.113×10^{-5}	0.181×10^{-9}	1.805E-10
360	1.648	3.70×10^{-3}	1.323×10^{-3}			
400	1.561	2.18×10^{-3}	0.821×10^{-3}			
440	1.491	1.75×10^{-3}	0.683×10^{-3}			
520	1.320	2.14×10^{-3}	0.858×10^{-3}			
600	1.145	2.19×10^{-3}	0.943×10^{-3}			
640	1.041	2.60×10^{-3}	1.212×10^{-3}	0.108×10^{-5}	0.106×10^{-9}	1.0649E-10

From the above C_v graphs and the tables as we increase the organic pore fluids , the coefficient of consolidation (C_v) tends to increase with an increase in organic fluids. This indicates a faster rate of consolidation. This might be due to changes in the soil’s permeability or compressibility caused by the organic fluids, allowing the soil to adjust more quickly to load changes. The increase in C_v suggests that the organic fluids are having a beneficial effect on the rate at which the soil consolidates.

These findings emphasize the influence of organic pore fluids on the compressibility and consolidation characteristics of granulated bentonite, highlighting the need to consider fluid composition in applications involving bentonite under varying environmental conditions.

CHAPTER 6

Analysis of Permeability behaviour of Granulated bentonite

6.1 Introduction

The property by virtue of which a porous medium conduct fluid is known as the permeability of the medium and it is a function of both the medium and permeated fluid (Lambe and Whitman, 1969). Permeability has been considered as one of the most important property of soil in geotechnical engineering. Permeability of soil depends on many factors like shape and size of the grain size of soils, properties of pore fluids, structural arrangements of soil particles, degree of saturation of soils etc. The exponential increase in human population simultaneously increases the municipal solid waste generation. Due to this enormous growth of waste production around the world, designing and construction of landfill becomes a very important issue in present day scenario. Clay, especially bentonite is considered as very effective material to construct the landfill liners to obstruct the migration of leachate to sub soils due to its excellent adsorption and swelling characteristics. Landfill liners are generally designed keeping water as pore fluid in the mind. When water is mixed with the organic pollutants present in the landfill, it becomes fluids having properties different than water, due to which the liner materials may behave differently upon coming in contact of such organic fluids. Permeability of the liner is a very important mechanical property and it plays a very crucial role in effective functioning of the landfill. In this chapter discussions are done on the permeability properties of Granulated bentonite at different effective stresses in dry loose condition by permeating ethanol-distilled water and methanol-distilled water mixtures. Though initial conditions of the soil will effect the permeability behaviour to some extent, however void ratio, soil characteristics, soil structure and nature of organic pore fluids are some primary factors effecting the permeability of soils.

6.2 Determination of coefficient of permeability (k):

The coefficient of permeability of a soil describes how easily a liquid will move through a soil. It is also commonly referred to as the hydraulic conductivity of a soil.

Once we have the values for m_v and C_v , we can use the following equation to determine the value of k :

$$k = C_v m_v \gamma_w$$

Where k = Hydraulic conductivity

C_v = coefficient of consolidation

m_v = coefficient of volume compressibility

γ_w = unit weight of water.

6.3 Analysis of Permeability behaviour of granulated bentonite in presence of organic pore fluid

Commercially available highly expansive bentonite including granulated bentonite were used for the study. Market available distilled water, ethanol and methanol was used for the study. The ethanol and methanol are mixed at an increment of 20% by volume with distilled water to prepare organic pore fluid of different proportion. One dimensional consolidometer apparatus was used for the study of permeability. The height and internal diameter of the cutter of the consolidometer were 20 mm and 60 mm respectively. Dry sample of granulated bentonite (by weight) was placed at an initial density of 1 gm/cm³ up to 2/3rd (13.33 mm) height of the cutter. Filter papers were placed at the top and bottom of the samples and porous stones were placed above and below the filter papers after boiling for 15 minutes. An initial seating load of 5 kN/m² was applied on the loading hanger at the start of the test. The saturation of the dry soil sample was done by applying the organic pore fluids in the consolidometer (distilled water and various methanol-distilled water and ethanol-distilled water mixtures). Since the soil sample is highly expansive in nature; then it is allowed to swell completely. At the start of the test the pore fluid is applied to the consolidometer to fully saturate the soil sample at full height and overburden stress (10 kN/m²) is applied. After full settlement occurred for that respective stress (10 kN/m²), the dial gauge reading is measured to determine permeability for that particular stress (10 kN/m²). After determination of the compressibility and permeability of the sample for that stress (10 kN/m²), next loading (20 kN/m²) is applied and same process is repeated. The test is done by applying consecutive overburden stresses of 10, 20, 40, 80, 160, 320 and 640 respectively.

6.3.1 Variation of the permeability with void ratio

The variation of permeability for the studied Granulated bentonite with ethanol and methanol water mixtures, viz., 100% Distilled water; 80% ethanol/methanol -20% Distilled water; 60% ethanol/methanol -40% Distilled water; 40% ethanol/methanol -60% Distilled water; 20% ethanol/methanol -80% Distilled water; in presence of the various organic pore fluids are presented from figures 6.1 to 6.8.



Fig.6.1: Coefficient of permeability vs. void ratio relationship for 100% Distilled water

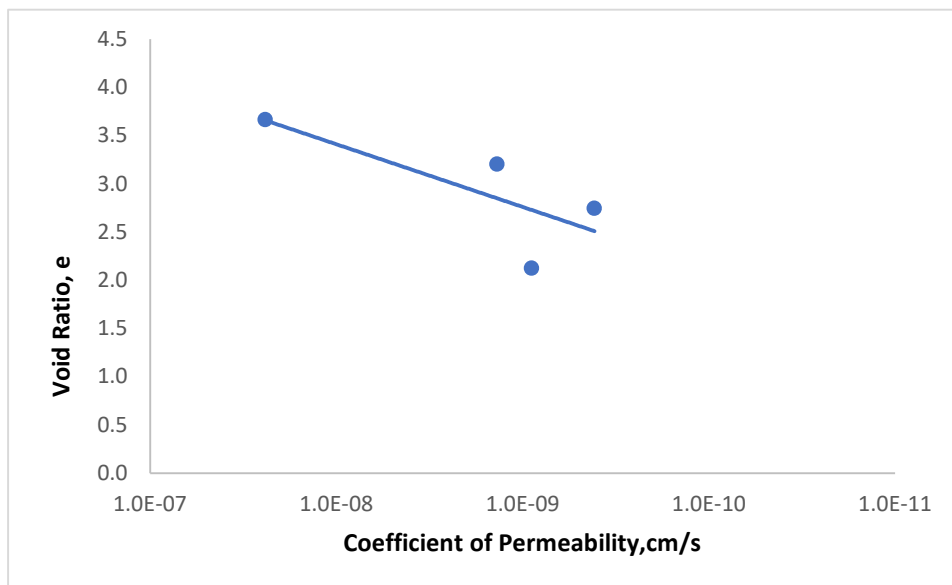


Fig6.2: Coefficient of permeability vs. void ratio relationship for 20% Ethanol + 80% Distilled water

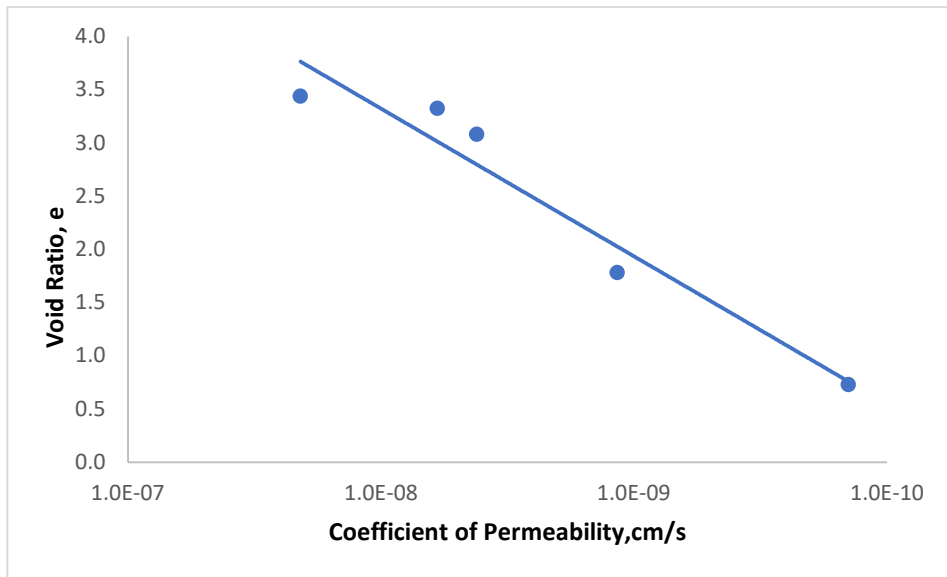


Fig6.3: Coefficient of permeability vs. void ratio relationship for 40%Ethanol+ 60% Distilled water

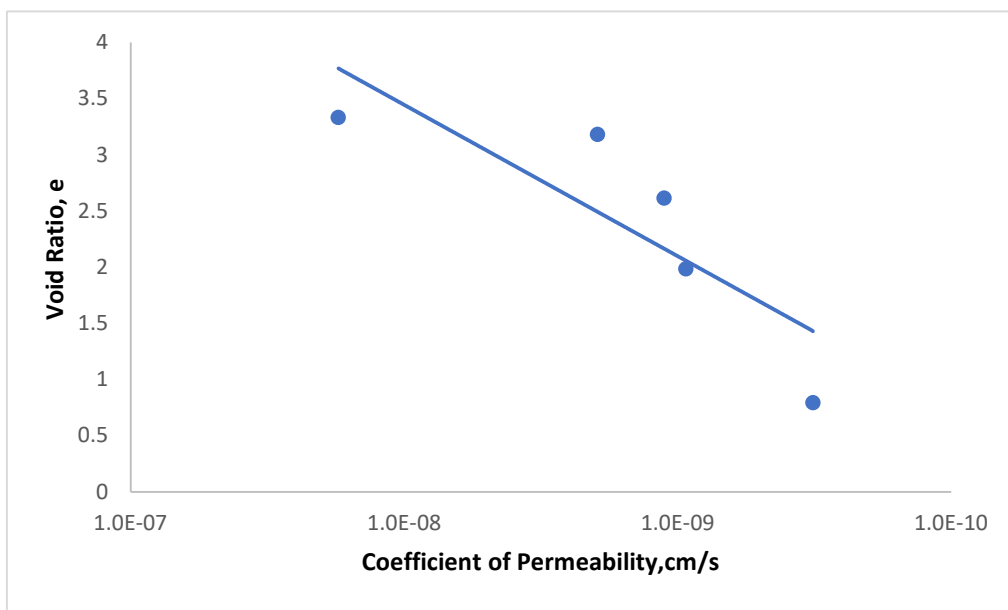


Fig6.4: Coefficient of permeability vs. void ratio relationship for 60%Ethanol+ 40% Distilled water



Fig6.5: Coefficient of permeability vs. void ratio relationship for 80%Ethanol+ 20% Distilled water

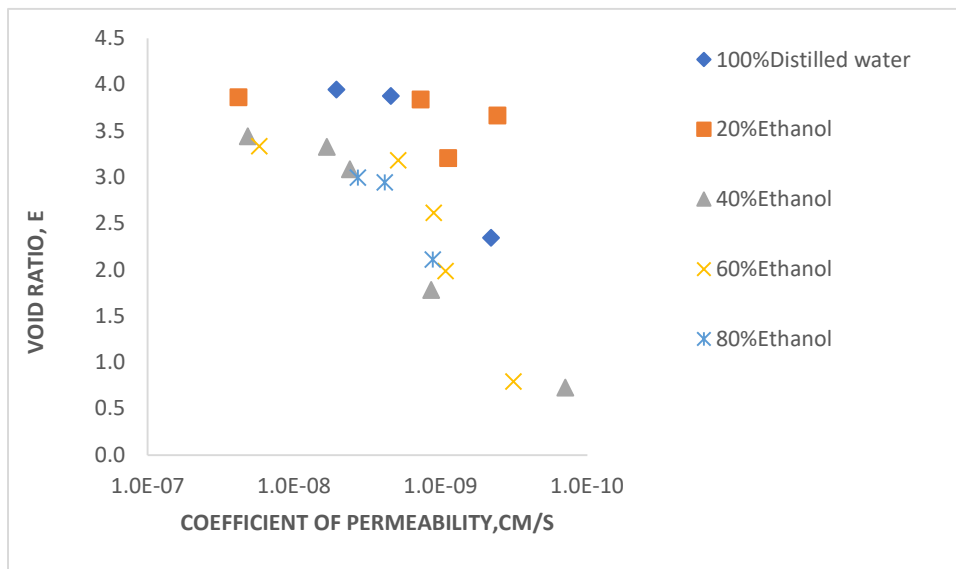


Fig6.6: Combination of Relationship between Coefficient of permeability vs. void ratio of Granulated bentonite for Ethanol-distilled water

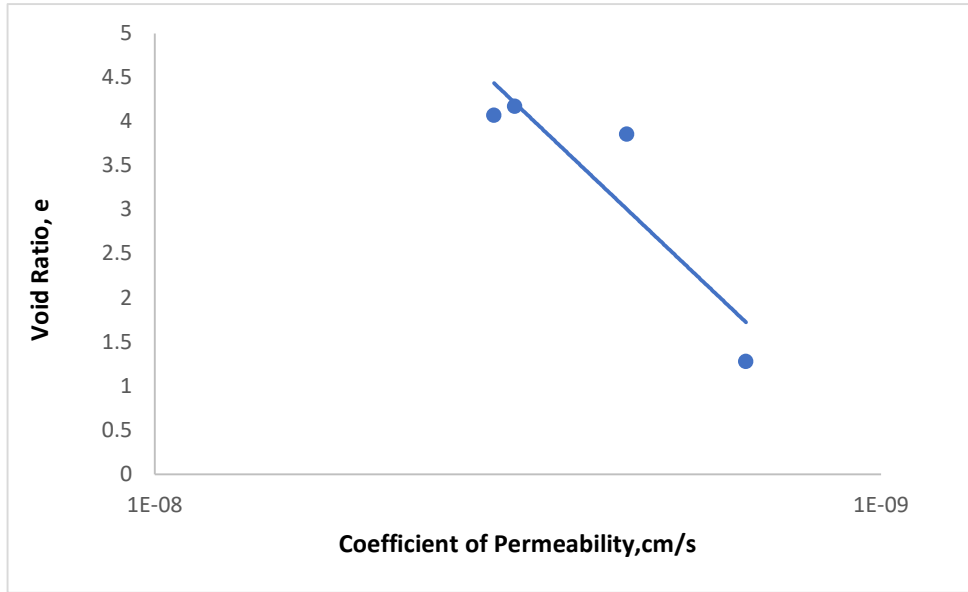


Fig6.7: Coefficient of permeability vs. void ratio relationship for 20%Methanol+ 80% Distilled water

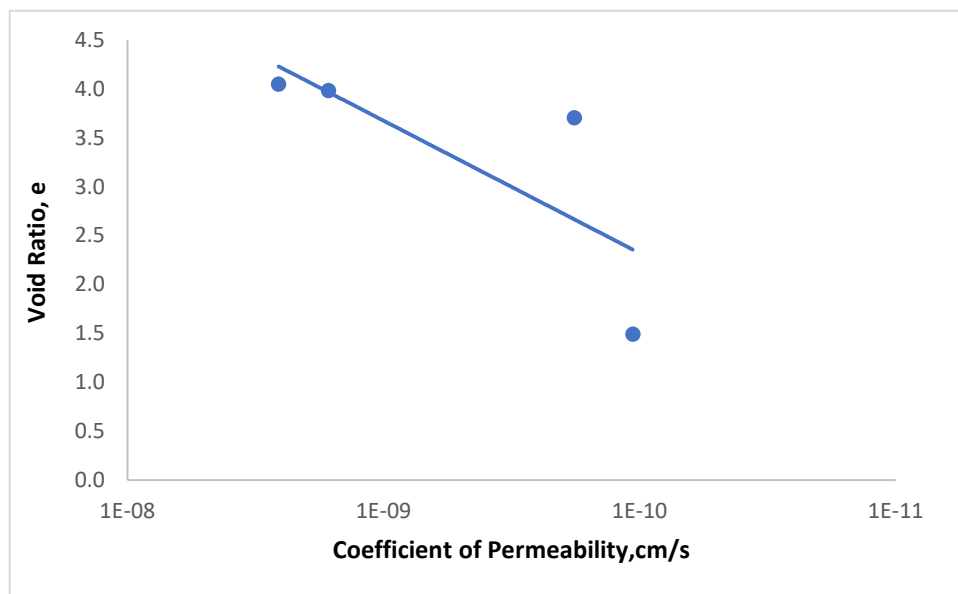


Fig6.8: Coefficient of permeability vs. void ratio relationship for 40%Methanol+ 60% Distilled water

The variation of the permeability of granulated bentonite in the presence of the organic fluids is presented in Figure (6.1-6.8). In the presence of distilled water and for a particular effective stress, the void ratio and permeability was found to be more as comparison with increase in the concentration of organic pore fluids. The experimental results indicated that for the similar effective stress and with the increase in the organic content of the permeant, the void ratio decreased but the permeability of the studied sample increased considerably. In the presence of water, the clay fabric is in the dispersed state exhibits a higher void ratio with increased swelling potential. On the other hand, when the granulated bentonite is inundated with organic pore fluid, the clay particles undergo rearrangement and assume a flocculated structure thereby a lesser void ratio is exhibited. In other words, the macro pores within the soil matrix is reduced. However, permeability is a flow phenomenon which is dependent on the micro pores or the effective void ratio. As the organic content in the pore fluid is increased the micro pores or the available pore spaces in the soil increase which results in increased permeability.

6.4 Variation of the permeability with %ethanol distilled water content of pore fluids

It was found that the dielectric constant of the organic pore fluid influences the effective pore spaces available for the flow. Therefore, in order to understand the underlying mechanism, the variation of the permeability with ethanol concentration at different void ratios is presented in Figure 6.9

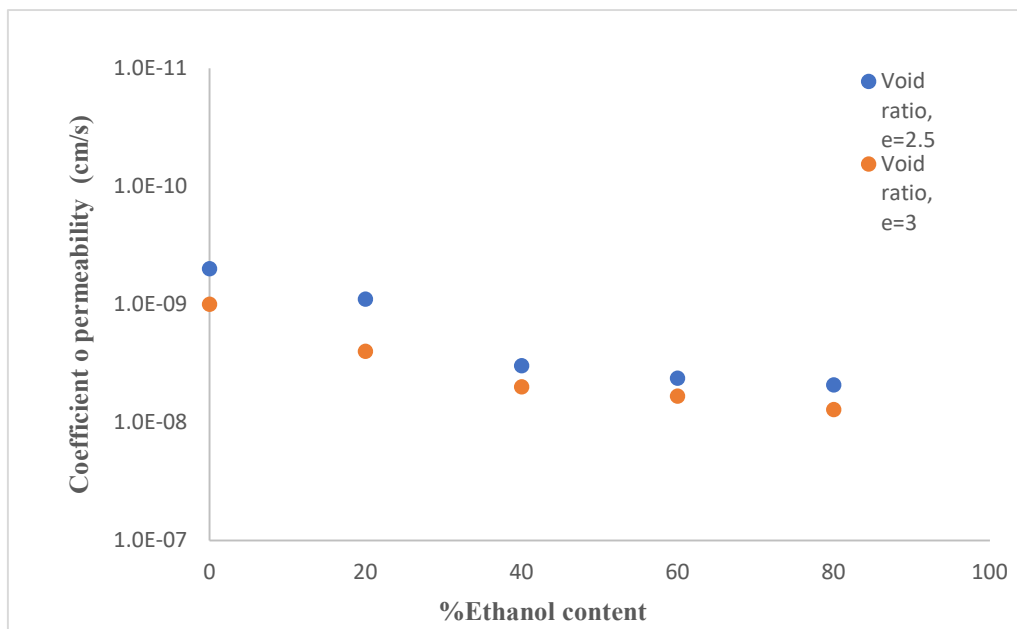


Fig.6.9: Coefficient of permeability vs %ethanol distilled water content of pore fluid relationship at void ratio, e=2.5 & e=3

From the Fig 6.9 it can be seen that the permeability increases with the increase of ethanol proportion in pore fluid. The permeability of granulated bentonite for distilled water is lowest as compared to the pore fluid as ethanol-distilled water mixtures. The variation of permeability can be explained by the dielectric property of the pore fluid. When distilled water is used as pore fluid which has high dielectric constant, there is formation of thicker diffused double layer which hinder the permeability. When distilled water is replaced by ethanol gradually the dielectric constant gets reduced and the diffused double layer formation also gets thinner and thus permitting more permeability.

CHAPTER- 7

CONCLUSION AND SCOPE FOR FURTHER STUDY

7.1 Conclusion:

In this work, the swelling, compressibility and permeability characteristics of nine granulated bentonite sample with different mixture of organic pore fluids and distilled water were studied using one- dimensional consolidation test.

From this work, following conclusions can be derived

- i. In Free Swelling test maximum swelling occurs in granulated bentonite for 100% distilled water and subsequently swelling decreases with the increase of organic pore fluids percentage. Of the three methods FSI, MFSI and FSR to study free swell, MFSI is considered to be more suitable for comparison of free swell of granulated bentonite.
- ii. For Oedometric Swelling test maximum swelling occurs in granulated bentonite in case of 100% distilled water solution subsequently swelling decreases with the increase of organic pore fluids percentage.
- iii. Good linear relationship exists between both free swelling and oedometric swelling of granulated bentonite with the different organic pore fluids.
- iv. Swelling pressure for granulated bentonite is higher for distilled water solution, which reduces linearly with the reduction of distilled water portion.
- v. The coefficient of consolidation increased with increase of organic pore fluid and distilled water concentration but decreased with the increase in applied stress.
- vi. The compression index decreased with the increase of organic pore fluid and higher values were obtained with 100% distilled water as compared with organic pore fluid.
- vii. The coefficient of permeability increased with increase of organic pore fluid

7.2 Scope for further study:

From this study, further research can explore the following areas to deepen the understanding and practical applications of granulated bentonite with organic pore fluids:

- i. To conduct consolidation tests to assess the stability and durability of granulated bentonite swelling and compressibility over time.
- ii. Investigate chemical interactions between granulated bentonite and a range of organic fluids, and assess the impact of additives or stabilizers on performance.
- iii. To study the effect of granulated bentonite mixed it with sand or having different particle sizes to be mixed with organic fluids to analyse the behaviour of microstructural changes.
- iv. Develop and validate numerical models to predict granulated bentonite behaviour with organic fluids under various conditions and simulate field conditions for long-term performance.
- v. Examine the effects of combining multiple organic fluids with distilled water on granulated bentonite properties and explore the benefits of hybrid systems.

By addressing these areas, future research can provide a comprehensive understanding of the interactions between granulated bentonite and organic pore fluids, leading to improved material design and application in various engineering and environmental contexts.

REFERENCES

- Arasan, S. (2010). Effect of chemicals on geotechnical properties of clay liners: a review. *Research Journal of Applied Sciences, Engineering and Technology*, 2(8), 765-775.
- Baille, W., Tripathy, S., & Schanz, T. (2010). Swelling pressures and one-dimensional compressibility behaviour of bentonite at large pressures. *Applied Clay Science*, 48(3), 324-333.
- Bharat, T. V., Das, P., & Srivastava, A. (2019). Insights into Contaminant Transport Modeling Through Compacted Bentonites. *Frontiers in Geotechnical Engineering*, 101-120.
- Bouazza, A. (2002). Geosynthetic clay liners. *Geotextiles and Geomembranes*, 20(1), 3-17.
- Bureau of Indian Standards (1985) Methods of test for soils: Determination of liquid limit and plastic limit, IS 2720-5, New Delhi, India.
- Bureau of Indian Standards (1986) Methods of test for soils: Determination of Consolidation properties, IS 2720-15, New Delhi, India.
- Cantillo, V., Mercado, V., & Pájaro, C. (2017). Empirical correlations for the swelling pressure of expansive clays in the city of Barranquilla, Colombia. *Earth Sciences Research Journal*, 21(1), 45-49.
- Chen, J. N., Benson, C. H., & Edil, T. B. (2018). Hydraulic conductivity of geosynthetic clay liners with sodium bentonite to coal combustion product leachates. *Journal of Geotechnical and Geoenvironmental Engineering*, 144(3), 04018008.
- Deka D. (2020). Prediction of Swelling Pressure of Different Bentonite–Sand Mixtures. M.Tech, thesis submitted to Assam Engineering College, Jalukbari, Guwahati-13, Assam
- Estabragh, A. R., Beytollahpour, I., Moradi, M., & Javadi, A. A. (2014). Consolidation behavior of two fine-grained soils contaminated by glycerol and ethanol. *Engineering geology*, 178, 102-108.
- Estabragh, A. R., Beytollahpour, I., Moradi, M., & Javadi, A. A. (2016). Mechanical behavior of a clay soil contaminated with glycerol and ethanol. *European Journal of Environmental and Civil Engineering*, 20(5), 503-519.
- Evangelina, Y. S., & John, R. A. (2010, December). Effect of leachate on the engineering properties of different bentonites. In *Proc., of Indian Geotechnical Conf.-2010, GEOTrendz* (pp. 377-380).
- Jadda, K., & Bag, R. (2020). Variation of swelling pressure, consolidation characteristics and hydraulic conductivity of two Indian bentonites due to electrolyte concentration. *Engineering Geology*, 272, 105637.
- Maubeuge, K. V., Müller-Kirchenbauer, A., & Schlötzer, C. (2017). Comparing the Testing of Geosynthetic Clay Liners (GCLs) with Bentonite Powder and Granular Cores. In *Geotechnical Frontiers 2017* (pp. 117-126).
- Mowafy, M. Y., & Bauer, G. E. (1985). Prediction of swelling pressure and factors affecting the swell behaviour of an expansive soils. *Transportation research record*, 1032, 23-28.
- ME Zumrawi, M. (2012). Prediction of swelling characteristics of expansive soils.
- Rahman S. K. (2023) Effects of pore fluid on Swelling, Compressibility and Permeability Characteristics of Bentonite–Sand Mixtures. PhD, thesis submitted to Assam Engineering College, Jalukbari, Guwahati-13, Assam.

- Saikia, T., Sharma, B., & Rahman, S. K. (2021). Effect of Ethanol on Compressibility Swelling and Permeability Characteristics of Bentonite–Sand Mixtures. In *Problematic Soils and Geoenvironmental Concerns: Proceedings of IGC 2018* (pp. 69-80). Springer Singapore.
- Sarabadani, H., & Rayhani, M. T. (2014). Influence of normal stress on hydration of GCLs from subsoil. *The Journal of Solid Waste Technology and Management*, 39(4), 292-303.
- Sharma, B., & Deka, P. (2019). A study on compressibility, swelling and permeability behaviour of bentonite–sand mixture. In *Geotechnical Characterisation and Geoenvironmental Engineering: IGC 2016 Volume 1* (pp. 43-50). Springer Singapore.
- Sharma, B., Sarma, S., & Sridhran, A. (2017). A study on compressibility, swelling and permeability characteristics of a bentonite-sand mixture. In *Indian Geotechnical Conference, Guwahati, India* (pp. 43-50).
- Siddiqua, S., Blatz, J., & Siemens, G. (2011). Evaluation of the impact of pore fluid chemistry on the hydromechanical behaviour of clay-based sealing materials. *Canadian Geotechnical Journal*, 48(2), 199-213.
- Singh, S., & Prasad, A. (2007). Effects of chemicals on compacted clay liner. *Electronic Journal of Geotechnical Engineering*, 12(D), 1-15.
- Sivapullaiah, P. V., Sridharan, A., & Stalin, V. K. (1996). Swelling behaviour of soil bentonite mixtures. *Canadian Geotechnical Journal*, 33(5), 808-814.
- Sridharan, A., & Rao, G. V. (1973). Mechanisms controlling volume change of saturated clays and the role of the effective stress concept. *Geotechnique*, 23(3), 359-382.
- Sridharan, A., & Gurtug, Y. (2004). Swelling behaviour of compacted fine-grained soils. *Engineering geology*, 72(1-2), 9-18.
- Sridharan, A. S. U. R. I., Rao, A. S., & Sivapullaiah, P. V. (1986). Swelling pressure of clays. *Geotechnical Testing Journal*, 9(1), 24-33.
- Tan, Y., Li, H., Sun, D. A., & Ming, H. (2020). Granular bentonite preparation and effect of granulation behavior on hydromechanical properties of bentonite. *Advances in Civil Engineering*, 2020(1), 8879792.
- Tan, Y. Z., Xie, Z. Y., Peng, F., Qian, F. H., & Ming, H. J. (2021). Optimal mixing scheme for graphite–bentonite mixtures used as buffer materials in high-level waste repositories. *Environmental Earth Sciences*, 80, 1-13.
- Vipulanandan, C., & Leung, M. (1991). Effect of methanol and seepage control in permeable kaolinite soil. *Journal of hazardous materials*, 27(2), 149-167.
- Zumrawi, M. (2013). Prediction of swelling pressure for compacted expansive soils. *University of Khartoum Engineering Journal*, 3(2), 35-39.

Appendix I

Table 5.9 Specimen height and void ratio calculation for 100% Distilled water sample

Applied Pressure (KN/m ²)	Final Dial Reading (mm)	No. of division	Dial change, $\Delta H = a \times \text{L.C.}$ (mm)	Specimen height, $H = H_1 - \Delta H$ (mm)	Height of voids, $H - H_s$ (mm)	Void ratio, $e = (H - H_s) / H_s$
		(a)				
10	1942			23	18.35	3.946
20	1910	32	0.32	22.68	18.03	3.877
40	1847	63	0.63	22.05	17.4	3.742
80	1735	112	1.12	20.93	16.28	3.501
160	1520	215	2.15	18.78	14.13	3.039
320	1197	323	3.23	15.55	10.9	2.344
400	1030	167	1.67	13.88	9.23	1.985
480	920	110	1.1	12.78	8.13	1.748
560	790	130	1.3	11.48	6.83	1.469
600	720	70	0.7	10.78	6.13	1.318
640	650	70	0.7	10.08	5.43	1.168

Table 5.10 Specimen height and void ratio calculation for 20% Ethanol & 80% Distilled water sample

Applied Pressure (KN/m ²)	Final Dial Reading (mm)	No. of division	Dial change, $\Delta H = a \times \text{L.C.}$ (mm)	Specimen height, $H = H_1 - \Delta H$ (mm)	Height of voids, $H - H_s$ (mm)	Void ratio, $e = (H - H_s) / H_s$
		(a)				
10	1910			22	17.474	3.861
20	1890	20	0.2	21.8	17.274	3.817
40	1812	78	0.78	21.02	16.494	3.644
80	1630	182	1.82	19.2	14.674	3.242
160	1405	225	2.25	16.95	12.424	2.745
320	1113	292	2.92	14.03	9.504	2.100
480	850	263	2.63	11.4	6.874	1.519
560	750	100	1	10.4	5.874	1.298
640	650	100	1	9.4	4.874	1.077

Table 5.11 Specimen height and void ratio calculation for 40% Ethanol & 60% Distilled water sample

Applied Pressure (KN/m ²)	Final Dial Reading (mm)	No. of division	Dial change, $\Delta H = a \times \text{L.C.}$ (mm)	Specimen height, $H = H_1 - \Delta H$ (mm)	Height of voids, $H - H_s$ (mm)	Void ratio, $e = (H - H_s)/H_s$
		(a)				
10	1973			22	17.045	3.440
20	1916	57	0.57	21.43	16.475	3.325
40	1796	120	1.2	20.23	15.275	3.083
80	1610	186	1.86	18.37	13.415	2.707
160	1391	219	2.19	16.18	11.225	2.265
240	1151	240	2.4	13.78	8.825	1.781
320	1023	128	1.28	12.5	7.545	1.523
480	750	273	2.73	9.77	4.815	0.972
520	630	120	1.2	8.57	3.615	0.730
540	575	55	0.55	8.02	3.065	0.619
640	483	92	0.92	7.1	2.145	0.433

Table 5.12 Specimen height and void ratio calculation for 60% Ethanol & 40% Distilled water sample

Applied Pressure (KN/m ²)	Final Dial Reading (mm)	No. of division	Dial change, $\Delta H = a \times \text{L.C.}$ (mm)	Specimen height, $H = H_1 - \Delta H$ (mm)	Height of voids, $H - H_s$ (mm)	Void ratio, $e = (H - H_s)/H_s$
		(a)				
10	1974			22	16.921	3.332
20	1898	76	0.76	21.24	16.161	3.182
40	1789	109	1.09	20.15	15.071	2.967
80	1610	179	1.79	18.36	13.281	2.615
160	1290	320	3.2	15.16	10.081	1.985
240	1070	220	2.2	12.96	7.881	1.552
320	927	143	1.43	11.53	6.451	1.270
480	720	207	2.07	9.46	4.381	0.863
520	685	35	0.35	9.11	4.031	0.794
540	645	40	0.4	8.71	3.631	0.715
640	570	75	0.75	7.96	2.881	0.567

Table 5.13 Specimen height and void ratio calculation for 80% Ethanol & 20% Distilled water sample

Applied Pressure (KN/m ²)	Final Dial Reading (mm)	No. of division	Dial change, $\Delta H = a \times \text{L.C.}$ (mm)	Specimen height, $H = H_1 - \Delta H$ (mm)	Height of voids, $H - H_s$ (mm)	Void ratio, $e = \frac{(H - H_s)}{H_s}$
		(a)				
10	1994			18.43	13.818	2.996
20	1969	25	0.25	18.18	13.568	2.942
40	1920	49	0.49	17.69	13.078	2.836
80	1780	140	1.4	16.29	11.678	2.532
160	1586	194	1.94	14.35	9.738	2.111
200	1525	61	0.61	13.74	9.128	1.979
240	1482	43	0.43	13.31	8.698	1.886
320	1351	131	1.31	12	7.388	1.602
640	1050	301	3.01	8.99	4.378	0.949

Table 5.14 Specimen height and void ratio calculation for 20% Methanol & 80% Distilled water sample

Applied Pressure (KN/m ²)	Final Dial Reading (mm)	No. of division	Dial change, $\Delta H = a \times \text{L.C.}$ (mm)	Specimen height, $H = H_1 - \Delta H$ (mm)	Height of voids, $H - H_s$ (mm)	Void ratio, $e = \frac{(H - H_s)}{H_s}$
		(a)				
10	1974			22	17.748	4.174
20	1931	43	0.43	21.57	17.318	4.073
40	1819	112	1.12	20.45	16.198	3.810
80	1563	256	2.56	17.89	13.638	3.207
160	1281	282	2.82	15.07	10.818	2.544
320	920	361	3.61	11.46	7.208	1.695
360	840	80	0.8	10.66	6.408	1.507
400	766	74	0.74	9.92	5.668	1.333
440	726	40	0.4	9.52	5.268	1.239
520	634	92	0.92	8.6	4.348	1.023
600	550	84	0.84	7.76	3.508	0.825
640	460	90	0.9	6.86	2.608	0.613

Table 5.15 Specimen height and void ratio calculation for 40% Methanol & 60% Distilled water sample

Applied Pressure (KN/m ²)	Final Dial Reading (mm)	No. of division	Dial change, $\Delta H = a \times \text{L.C.}$ (mm)	Specimen height, $H = H_1 - \Delta H$ (mm)	Height of voids, $H - H_s$ (mm)	Void ratio, $e = (H - H_s) / H_s$
		(a)				
10	1992			22	17.673	4.084
20	1948	44	0.44	21.56	17.233	3.983
40	1828	120	1.2	20.36	16.033	3.705
80	1578	250	2.5	17.86	13.533	3.128
160	1301	277	2.77	15.09	10.763	2.487
320	1002	299	2.99	12.1	7.773	1.796
360	938	64	0.64	11.46	7.133	1.648
400	900	38	0.38	11.08	6.753	1.561
440	870	30	0.3	10.78	6.453	1.491
520	796	74	0.74	10.04	5.713	1.320
600	720	76	0.76	9.28	4.953	1.145
640	675	45	0.45	8.83	4.503	1.041